UNIVERSIDADE FEDERAL DE CIÊNCIAS DA SAÚDE DE PORTO ALEGRE - UFCSPA
CURSO DE PÓS-GRADUAÇÃO EM CIÊNCIAS DA SAÚDE

Maurício Alves Altê

Estudo estrutural e planejamento de novos inibidores para a enzima prefenato desidratase de *Mycobacterium tuberculosis*

PORTO ALEGRE
2017

Maurício Alves Altê

Estudo estrutural e planejamento de novos inibidores para a enzima prefenato desidratase de *Mycobacterium tuberculosis.*

Dissertação submetida ao Programa de Pós-Graduação em Ciências da Saúde da Universidade Federal de Ciências da Saúde de Porto Alegre, como requisito para a obtenção do grau de Mestre.

Orientador: Dr. Rafael Andrade Caceres

Porto Alegre
2017

Catalogação na Publicação

Alves Alte, Mauricio
Estudo estrutural e planejamento de novos inibidores para a enzima prefenato desidratase de Mycobacterium tuberculosis / Mauricio Alves Alte. -- 2017.
96 p. : il., graf., tab. ; 30 cm.

Dissertação (mestrado) -- Universidade Federal de Ciências da Saúde de Porto Alegre, Programa de Pós-Graduação em Ciências da Saúde, 2017.

Orientador(a): Rafael Andrade Caceres.

1. Tuberculose. 2. Prefenato desidratase. 3. Desenho racional de fármacos. 4. Bioinformática estrutural. I. Título.

Sistema de Geração de Ficha Catalográfica da UFCSPA com os dados fornecidos pelo(a) autor(a).

AGRADECIMENTOS

Aos meus queridos pais, irmãs e irmão. Embora da recente distância de um ano que se completa, eu sei que vocês estão torcendo muito por mim e depositam muita fé, amor e carinho. Obrigado por tudo, por sempre estarem ao meu lado nos momentos mais difíceis da vida, eu jamais me esquecerei de cada um de vocês. Dedico este trabalho especialmente a vocês mãe e pai que me ensinaram a ter valores e princípios da vida.

Ao orientador e amigo pela oportunidade, paciência e por acreditar no meu potencial e na capacidade de aprender. Foi um grande desafio entrar em uma área desconhecida e nova de estudos *in silico*, que envolve estudos computacionais, embora também seja uma oportunidade única de entrar no meio acadêmico e científico, pelo qual tenho grande admiração e interesse.

Aos amigos, em geral, pelo carisma e conselhos, um grande abraço.

RESUMO

A tuberculose (TB) é considerada um grave problema de saúde pública por manter alta taxa de incidência, prevalência e mortalidade na população em nível mundial, sendo a segunda doença infecciosa mais letal da humanidade, seguindo o pelo vírus da imunodeficiência humana (HIV). A Organização Mundial da Saúde (OMS) estima que um terço da população, cerca de dois bilhões de pessoas, esteja infectada com a *Mycobacterium tuberculosis*. A dificuldade no tratamento e controle da tuberculose em razão do aumento de cepas resistentes a múltiplos fármacos e da complexidade da coinfecção HIV/TB tem conduzido à busca de agentes antimicrobianos mais eficientes. A enzima prefenato desidratase pertence à via do corismato, mecanismo essencial para a sobrevivência do microrganismo, demonstrando ser um interessante alvo no desenvolvimento de fármacos mais seletivos, seguros, menos tóxicos e com ação bactericida e bacteriostática. O objetivo deste estudo foi obter e investigar a estrutura 3D da prefenato desidratase de *Mycobacterium tuberculosis*, além de propor potenciais inibidores com uso de ferramentas de bioinformática. A estrutura terciária da enzima foi resolvida através de modelagem por homologia com base na estrutura cristalográfica 3MWB. Os resultados do nosso modelo demonstram que 93,7% dos resíduos de aminoácidos estão em regiões mais favoráveis e 5,4% em adicionalmente favoráveis no gráfico de Ramachandran. Já o perfil Verify-3 foi de 90,34% dos resíduos para valores escore 3D-1D ≥ 0,2. Na docagem molecular foram selecionados, da biblioteca de 30.908 compostos, 100 ligantes com maior afinidade de ligação, tendo variação no autodock de -12,45 a -10,52 kcal/mol em relação à fenilalanina (-7,8 kcal/mol). Dentre os dez melhores estão o ZINC69138131 e ZINC28047676 que são compostos derivados do benzomidazol, o que corrobora com os dados da literatura por ter uma ampla atividade inibitória como antioxidante, antimicrobiana e antiviral. Ademais, recentes pesquisas realçam a ação eficaz do benzomidazol contra a tuberculose. Os dados deste trabalho e das análises de predição farmacológica e toxicológica serão úteis na escolha de potenciais protótipos a serem testados *in vitro* e *in vivo*.

Palavras-chave: Tuberculose; Prefenato desidratase; Desenho racional de fármacos; Bioinformática estrutural.

ABSTRACT

Tuberculosis (TB) is considered a serious public health problem by keeping high rate of incidence, prevalence and mortality in the worldwide population, being the second most lethal infectious disease of humanity, following the human immunodeficiency virus (HIV). The World Health Organization estimates that a third of the population is infected with the *Mycobacterium tuberculosis.* The difficulty in treating and controlling tuberculosis is due to the increase of multidrug resistant strains and the complexity of HIV/TB coinfection, which has led to the search of more efficient antimicrobial agents. The enzyme prephenate dehydratase belongs to the pathway of chorismate, an essential mechanism to the survival of the microorganism, displaying to be an interesting target for the development of more selective, safe, less toxic, with bactericidal and bacteriostatic action drugs. The aim of this study was to obtain and investigate the 3D structure of prephenate dehydratase of *Mycobacterium tuberculosis,* beyond to propose potential inhibitors using bioinformatics tools. The tertiary structure of the enzyme was modelled by homology modeling method based on the 3MWB crystallographic structure. The 3D model showed 93.7% of the amino acid residues in more favorable regions and 5.4% in additionally favorable in the Ramachandran Plot. In turn, the Verify-3D profile exhibit 90.34% of residues with a 3D-1D value score ≥ 0.2. In relation to the molecular docking were selected, from a library of 30.908 compounds, 100 ligands with higher binding affinity ranging from -12.45 to -10.52 kcal/mol about the phenylalanine (-7.8 kcal/mol). Among the top ten compounds are ZINC69138131 and ZINC28047676, which are derived from benzomidazol. This corroborates the data available in the literature, showing a broad inhibitory activity as antioxidant, antimicrobial and antiviral. In addition, recent research highlights the effective action of benzomidazole against tuberculosis. The 3D model obtained in this work and the prediction of toxicity and pharmacological activity are useful for a better understanding of interactions of active sites of enzyme and in the selection of potential prototypes to be tested *in vitro* and *in vivo*.

Key words: Tuberculosis; Prephenate dehydratase; Rational design of drugs; Structural bioinformatics

LISTA DE FIGURAS

Introdução

Artigo

LISTA DE TABELAS

Introdução

Artigo

LISTA DE ABREVIATURAS

ADMETox: Absorção, distribuição, metabolismo, excreção e toxicidade
AIDS: Síndrome da Imunodeficiência Adquirida
BK: Bacilo de Koch
BLAST: Basic Local Alignment Search Tool
CM: Corismato mutase
HIV: Vírus da Imunodeficiência humana
IBGE: Instituto Brasileiro de Geografia e Estatística
MS: Ministério da Saúde
Mtb: *Mycobacterium tuberculosis*
NCBI: Centro Nacional de Informação Biotecnológica
OMS: Organização Mundial da Saúde
PDB: Banco de dados de proteínas (Protein Data Bank)
PDT: Prefenato desidratase
RMSD: Desvio médio quadrático (do inglês Root Mean Square Deviation)
RHZ: Rifampicina, Hidrazida e Pirazinamida
SINAN: Sistema de Informação de Agravos de Notificação
TB: Tuberculose
MDR: Tuberculose resistente a múltiplos fármacos
XDR: Tuberculose extensivamente resistente aos fármacos
TDR: Cepas totalmente resistentes a fármacos

SUMÁRIO

1. INTRODUÇÃO

1.1 Tuberculose

A tuberculose (TB) é uma doença infecto-contagiosa causada pelo microrganismo *Mycobacterium tuberculosis* (Mtb) que afeta principalmente os pulmões, mas pode se manifestar em outros órgãos como rins, ossos, gânglios linfáticos, pleura, laringe, intestino e cérebro (tuberculose extrapulmonar) (BRASIL, 2010, 2014; WHO, 2016; BARKER, 2008). A TB se destaca, dentre as patologias, como um sério problema de saúde pública e continua a ser um fator alarmante em vista da presente disseminação de pessoas infectadas e levadas a óbitos (RAPPUOLI & ADEREM, 2011; RAVIGLIONE et al., 2012; LEMOS, 2008; WHO, 2016). A coinfecção com o vírus da imunodeficiência humana (HIV) tem contribuído para a expansão da doença, evidenciando um alto risco de infecção primária, secundária, reinfecção ou reativação por TB (SANTOS & BECK, 2009; MUNIZ et al., 2006; CAMPOS, 2006). As limitações do tratamento e do diagnóstico em relação à interação bidirecional e sinérgica do HIV/TB conduzem à necessidade de adotar mudanças nas estratégias e intervenções (SANTOS & BECK, 2009; MUNIZ et al., 2006; RAVIGLIONE et al., 2012 ; LEMOS, 2008). A organização mundial da saúde (OMS) estima que um terço da população, cerca de dois bilhões de pessoas, esteja infectada com o bacilo da Mtb (WHO, 2016). Em 2015, houve 10,4 milhões de novos casos e 1,8 milhões de óbitos (1,4 milhão de HV-negativo e 0,4 milhão de HIV-positivo) pela TB no mundo (WHO, 2016). O Brasil está incluído neste cenário global, ocupando a 18° posição no ranking de países com maior número de casos de TB e a capital do estado do Rio Grande do Sul possui o segundo maior nível de incidência e primeira colocação no percentual de coinfecção TB-HIV no país (WHO, 2016; BRASIL, 2016). De acordo com os dados do Ministério da Saúde/Sinan e IBGE, a cidade de Porto Alegre possui índice de incidência de 88,8 casos para cada 100 mil habitantes e de mortalidade de 4,5 casos por 100 mil habitantes (BRASIL, 2016). Além disso, o surgimento frequente de cepas de Mtb resistentes a múltiplos fármacos agrava ainda mais o problema, embora outros fatores como condições socioeconômicas, abandono do tratamento e interações desfavoráveis entre os fármacos possa propiciar um aumento do número de infectados (WILDNER et al., 2011; DI PERRI et al., 2005; HIJJAR & PROCÓPIO, 2006; RAVIGLIONE et al.,

2012; SANTOS & BECK, 2009; AMER et al., 2008). O aparecimento de cepas multi-resistentes (MDR), extensivamente resistentes (XDR) e, mais recentemente, cepas totalmente resistentes a fármacos tem sido descrito na literatura (TDR) (CAFÉ OLIVEIRA et al., 2016; KIRBY, 2013).

1.2 *Mycobacterium tuberculosis*

Mycobacterium tuberculosis ou bacilo de Koch foi descoberto em 1882 por Robert Koch e é o principal agente etiológico causador da tuberculose em seres humanos (OTTENHOFF, 2009; KAUFMANN, HUSSEY e LAMBERT, 2010; HIJJAR & PROCÓPIO, 2006). Pertence à ordem das Actinomycetales, família Mycobacteriaceae e gênero *Mycobacterium* (WILDNER et al., 2011; CAMPOS, 2006; BRASIL, 2010). Há também outras espécies que pertencem ao complexo *Mycobacterium tuberculosis* e provocam subsequente patologia: *M. bovis, M. africanum, M. canetti, M. caprae, M. pinnipeddi e M. microti* (BRASIL, 2014; WILDNER et al., 2011; CAMPOS, 2006). O microrganismo, por ser uma micobactéria, apresenta-se como bacilo aeróbico, não formador de esporos e de toxinas, não encapsulado, não flagelado, fracamente gram-positivo, imóvel, pleomórfico, parasita intracelular facultativo e com notável desenvolvimento de resistência bacteriana a agentes químicos (FRIEDEN et al., 2003; CASTELO FILHO et al., 2004; LEMOS, 2008; VERONESI-FOCACCIA, 2009). Os bacilos têm uma taxa de crescimento lento, com intervalo de termpo de 20 horas ou mais, e se constitui, frequentemente, de estruturas de filamentos de cadeia reta ou ramificada no qual tendem a crescer em aglomerados (BRASIL, 2010, 2014). Inclusive dispõe da capacidade de permanecer em estado de dormência, porém viáveis para ativação e infecção (KNECHEL, 2009; AHMAD, 2011; BRASIL, 2014). Outro fator importante são os ácidos micólicos, ácidos graxos, principal componente da parede celular do bacilo que concede resistência e impermeabilidade em relação a aspectos do ambiente hostil como a dessecação, agentes químicos, antibióticos e substâncias hidrofóbicas (BRASIL, 2008; WILDNER et al., 2011). A denominação de bacilo álcool-ácido-resistente no Mtb é ocasionada por este aspecto estrutural lipídico, no qual dá resistência à descoloração da bactéria, uma vez já corada por fucsina fenicada, ao empregar ácidos fortes diluídos e álcool absoluto. Na prática este método é designado de Ziehl-Neelsen (MONROE et al., 2008; BRASIL, 2008, 2010).

Esta característica é muito empregada nos estudos de casos e isolamento de TB por ser um método sensível e específico para o diagnóstico da doença (MOÇAMBIQUE, 2012; BRASIL, 2008, 2010).

1.3 Transmissão e patogênese

A transmissão ocorre de pessoa-a-pessoa por meio da inalação dos bacilos, eliminados em gotículas de secreções respiratórias (gotículas de Flugge) que ficam suspensas no ar durante a tosse, fala ou espirro (MOÇAMBIQUE, 2012; BRASIL, 2014; FRIEDEN et al., 2003; TORTORA; FUNKE & CASE, 2000). As partículas maiores depositam-se no chão, enquanto as menores sofrem uma rápida evaporação, originando um aerossol, núcleo de wells, que contém de um a três bacilos (MOÇAMBIQUE, 2012; DUCATI et al., 2006; WILDNER et al., 2011). Os aerossóis podem permanecer por 6 horas no ambiente e ao infectar os alvéolos, nos pulmões, ativam os macrófagos do organismo que fagocitam a bactéria (MOÇAMBIQUE, 2012; SNIDER; RAVIGLIONE; KOCHI, 1994; KAUFMANN & MCMICHAEL, 2005; KNECHEL, 2009). Muitas vezes, a micobactéria pode sobreviver e replicar no interior do fagossomo do macrófago, um local ideal para o crescimento e proteção contra os anticorpos e outras defesas imunes (KORB; CHUTURGOON & MOODLEY, 2016; CASTELO FILHO et al., 2004). A multiplicação dos bacilos ocasiona uma resposta quimiotática pelos linfócitos T que ativam os outros macrófagos e o transformam em células epitelioides, formando uma lesão fechada denominada tubérculo ou granuloma caseoso (O'GARRA et al., 2013; KORB; CHUTURGOON & MOODLEY, 2016; URDAHL; SHAFIANI & ERNST, 2011). A morte das células traz, além da liberação dos bacilos, a liberação de enzimas e citocinas que ocasionam a inflamação no pulmão (RUSSELL, 2007; KUMAR et al., 2010). Após várias semanas, o interior do tubérculo torna-se caseoso e, assim, é caracterizado como uma necrose caseosa central (RUSSEL et al., 2009). Neste estágio os bacilos entram em estado de dormência devido à falta de oxigênio, nutrientes, condições ácidas de pH e produção de óxido nítrico, proporcionando um ambiente hostil, podendo a doença voltar a se manifestar (reativar) só ao longo dos anos (O'GARRA et al., 2013; RUSTAD et al., 2008; PATEL; 2JHAMB & SINGH, 2011; ELKS et al., 2013). Essas lesões caseosas também podem cicatrizar ou sofrer o processo de liquefação, no qual forma uma cavidade tuberculosa ideal para

proliferação, ativação e dispersão dos bacilos da tuberculose, tornando-se a doença altamente contagiosa, após o rompimento do tubérculo (MIRANDA et al., 2012; BRASIL, 2010). Assim, a disseminação inicia nas vias aéreas do pulmão e, posteriormente, passa para outros sistemas, como o circulatório e linfático (BRASIL, 2014; KNECHEL, 2009; VERVER et al., 2005; MIRANDA et al., 2012).

A infecção primária, geralmente, é assintomática e a sensibilidade à tuberculose é tardia, de forma, a somente se manifestar após algumas semanas ou anos, quando o sistema imunológico está debilitado (KORB; CHUTURGOON & MOODLEY, 2016). Brevemente, o indivíduo com infecção latente, que não desenvolveu a doença, pode vir a adoecer em virtude do processo de reativação ou reinfecção. Além disso, o HIV pode agilizar o contágio por *Mycobacterium tuberculosis* ao estimular o aumento da suscetibilidade do hospedeiro (FRIEDEN et. al., 2003; MUNIZ et al., 2006). Cabe salientar que somente indivíduos com tuberculose ativa transmitem a doença (CASTELO FILHO et al., 2004; MONROE et al., 2008). Os sintomas mais frequentes da doença no paciente são: perda de peso, tosse frequente com escarro sanguinolento, suor noturno, febre vespertina baixa e perda geral de vigor (WHO, 2016; BRASIL, 2010; MOÇAMBIQUE, 2012; BARKER, 2008). Todavia, a transmissão depende da concentração e grau de virulência dos bacilos, do tempo de exposição, do ambiente e de fatores imunológicos do hospedeiro em potencial (MOÇAMBIQUE, 2012; AHMAD, 2011; MORRISON; PAI & HOPEWELL, 2008).

1.4 Tratamento

Desde 1993, a OMS tem se preocupado em desenvolver planos e aplicar estratégias no combate, controle e erradicação da doença (HIJJAR & PROCÓPIO, 2006). A cada ano realiza um relatório epidemiológico e estatístico dos países com maior número de casos estimados com TB. A nova estratégia da organização (The End TB Strategy), de período 2016- 2020, tem o objetivo de reduzir em 35% e 25% os números de mortes e de incidência, respectivamente (WHO, 2016; BRASIL, 2016).

O tratamento padrão para a TB é por via de administração oral, em dose fixa e combinada, de múltiplos medicamentos (BRASIL, 2014). Ademais, o Ministério da Saúde adota o Tratamento Diretamente Observado (DOTs), que aplica uma medida de supervisão para tentar evitar o desenvolvimento de resistência bacteriana

provocado pelo uso inadequado/irregular dos antimicrobianos e o abandono no tratamento em consequência dos efeitos colaterais. (MONROE et al., 2008; MUNIZ et al., 2006; RODRIGUES, et al., 2012; BRASIL, 2010). O regime tem um perído total de 6 meses no qual o paciente é submetido, nos primeiros 2 meses, à Rifampicina (R), Pirazinamida (Z), Isoniazida (H) e Etambutol (E). Posteriormente, se mantém um intervalo de 4 meses com Rifampicina e Isoniazida (BRASIL, 2014; RAMAN; YETURU & CHANDRA, 2008; DUCATI et al., 2006). Muitos destes fármacos têm uma ação inibitória eficaz durante o crescimento celular do patógeno, permitindo reduzir significativamente a taxa de mortalidade (DI PERRI et al., 2005). Aliás, a vacina BCG (Bacilo de Calmette-Guerrin) foi introduzida em 1921 e até hoje é bastante empregada como medida de prevenção, nos países em desenvolvimento, a fim de impedir que as crianças contraiam formas mais graves da doença, como a TB miliar e meníngea (GRANJER et al, 1981; STARKE & CONNELLY, 2004; RAPPUOLI & ADEREM, 2011; HIJJAR & PROCÓPIO, 2006; BARRETO; PEREIRA & FERREIRA, 2006). Entretanto, por ser uma cepa atenuada de *Mycobacterium bovis* pode mostrar valor falso positivo no teste térmico da tuberculina. Ademais, o grau de segurança e eficiência da vacina é ainda controverso por não conferir imunidade na fase adulta (WHO, 2016; BARRETO, PEREIRA, FERREIRA, 2006; LUCA & MIHAESCU, 2013).

Portanto, uma identificação precoce, tratamento adequado e desenvolvimento de novas vacinas são necessários para que seja possível realizar um controle eficaz contra a TB (MOÇAMBIQUE, 2012; WHO, 2016; JAIN & MONDAL, 2008).

1.5 Via do ácido chiquímico e do corismato

O ácido chiquímico, também denominado de ácido carboxílico tri-hidroxi ciclohexeno ou chiquimato, sofre sete reações enzimáticas na rota metabólica que realiza a catálise dos precursores fosfoenolpiruvato e eritrose-4-fosfato para formar o produto final corismato, precursor metabólico importante da biossíntese dos aminoácidos aromáticos: fenilalanina, triptofano e tirosina (BENTLEY, 1990; DUCATI; BASSO & SANTOS, 2007; BOCHKOW et al., 2012). Na Figura 1, observa-se a rota metabólica do ácido chiquímico. As enzimas que constituem cada etapa do processo são: 3-deoxi-D-arabino-heptulosonato (a), 3-desidroquinato sintase (b), 3-desidroquinato desidratase (c), chiquimato desidrogenase (d), chiquimato quinase (e), 5-enolpiruvilchiquimato-3-fosfato sintase (f) e a corismato mutase (g).

Subsequentemente, o corismato fica disponível para participação de três processos de síntese de biomoléculas, em destaque na biossíntese de fenilalanina onde é convertido primeiramente em prefenato, depois em fenilpivurato e subsequentemente no produto final.

Figura 1. Esquema bioquímico da via do ácido chiquímico. Figura gerada pelo programa BKchem (http://bkchem.zirael.org/index.html).

Representação: 1) Eritrose 4-fosfato, 2) Fosfoenolpiruvato, 3) 3-Deoxi-D-arabino-ácido heptulosonato-7-fosfato, 4) 3-Dessidroquinato, 5) 3-Dessidrochiquimato, 6) Chiquimato, 7) Chiquimato-3-fosfato, 8) 5-Enolpirovil-chiquimato 3-fosfato, 9) Corismato.

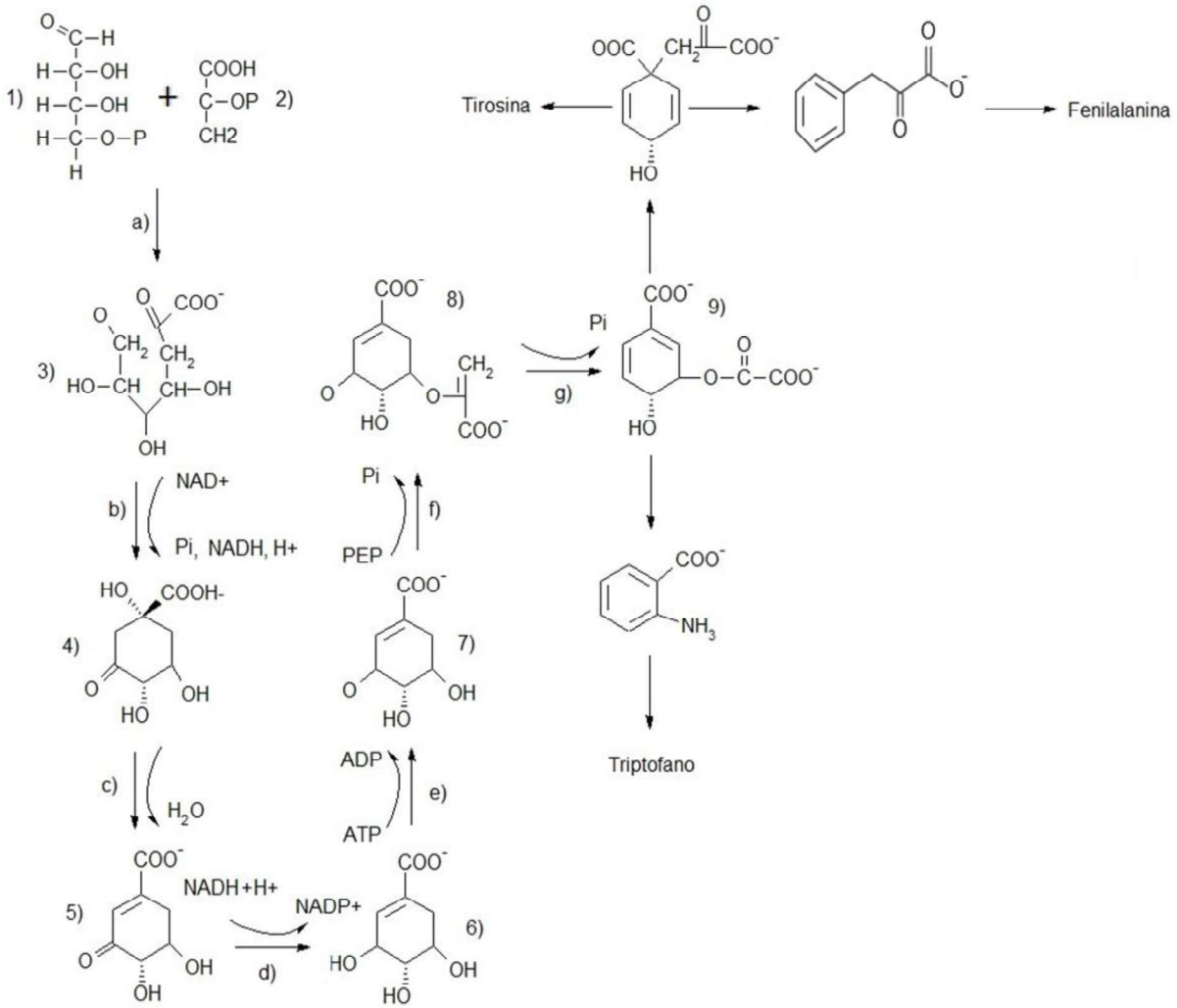

A presença desta via tem sido confirmada em diversos organismos como, por exemplo, plantas, algas, bactérias e fungos, estando ausente apenas nos mamíferos (BOCHKOW et al., 2012; PASQUALTTO & SCHWARZBOLD, 2000). Dentre estes

microrganismos, a presença das enzimas pertencentes à via do ácido chiquímico foi identificada no genoma do *Mycobacterium tuberculosis*, sendo, portanto, caracterizada como uma rota essencial para a sobrevivência da bactéria (PARISH & STOKER, 2002; AMER; EL-BEHEDY & MOHTADY, 2008). As enzimas presentes da via do ácido chiquímico e do corismato são potenciais alvos para a elaboração de novos agentes antibacterianos já que possuem propriedade de toxicidade seletiva, levando a redução significativa de efeitos colaterais em humanos (DUCATI; BASSO & SANTOS, 2007; AMER; EL-BEHEDY & MOHTADY, 2008; BOCHKOW et al., 2012).

1.6 Enzima prefenato desidratase

A enzima prefenato desidratase (PDT) de *Mycobacterium tuberculosis* possui 386 aminoácidos e é codificada pelo gene pheA (Rv3838), com 963 pares de bases. Essa enzima faz parte da via do corismato e realiza a descaboxilação e desidratação do prefenato a fenilpiruvato, com eliminação de dióxido de carbono e água (Figura 2) (POHNERT et al., 1999).

Figura 2. Reação de descarboxilação e desidratação de prefenato a fenilpiruvato catalisada pela enzima prefenato desidratase em *Mycobacterium tuberculosis*. Figura gerada pelo programa BKchem (http://bkchem.zirael.org/index.html).

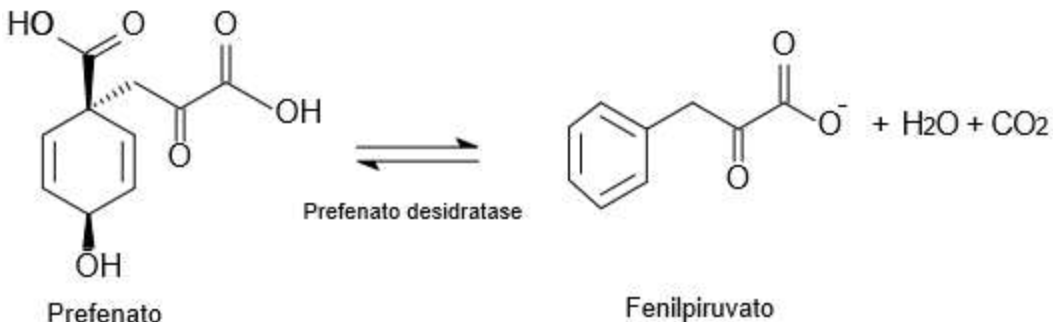

Por pertencer à via metabólica do corismato, indiretamente na via do ácido chiquímico, a prefenato desidratase é um excelente alvo para o desenvolvimento de novos inibidores antituberculose. Nos microrganismos, ela participa na biossíntese de fenilalanina e tirosina (HYUN et al., 2011). Em algumas bactérias, tais como a *Escherichia coli*, a PDT faz parte da enzima bifuncional denominada proteína P,

associando-se com a atividade da corismato mutase (CM) ao catalisar a conversão do corismato a fenilpiruvato. Em outras bactérias, a enzima é caracterizada como proteína monofuncional (PITTARD, 1996; POHNERT et al., 1999). Estudos cromatográficos realizados por COTTON & GIBSON (1965), usando extratos celulares e material parcialmente purificado de *Aerobacter aerogenes*, sugerem que um único complexo enzimático é capaz de realizar as duas primeiras reações na biossíntese da fenilalanina, metabolizando o corismato em prefenato e/ou corismato em fenilpiruvato através da atividade da CM e PDT. A PDT é uma enzima regulada pelo seu produto final L-fenilalanina que, por meio de um mecanismo alostérico, realiza um feedback negativo (POHNERT et al., 1999; CHO et al, 2007; HYUN et al., 2011). Além disso, a proteína é composta de dois domínios: o sítio catalítico desidratase localizado no N-terminal e o sítio regulatório no C-terminal (CHO et al, 2007; HYUN et al., 2011).

1.7 Planejamento racional de fármacos

Os fármacos são indispensáveis na prevenção e tratamento/cura de doenças, logo têm um papel crucial e indispensável no aumento da sobrevida dos pacientes por influênciar nas condições de estado saúde-doença (DUNNE et al., 2013). Atualmente, a compreensão da natureza da doença e dos mecanismos fisiológicos e metabólicos envolvidos, possibilitou aprimorar o planejamento e a síntese de novas entidades moleculares. Entretanto, a abordagem tradicional de tentativa e erro, que tem como base a intuição química sobre as moléculas, é ainda muito empregada no desenvolvimento de fármacos, embora a falta de otimização e seletividade de ligação possa acarretar efeitos secundários indesejáveis (FORSTER, 2002; BURGER & ABRAHAM, 2003). Outro fator limitante é a complexidade e o custo ao processar um novo fármaco, uma vez que a aplicação de diversas etapas de estudos clínicos ocasiona um aumento nas despesas e no tempo durante as etapas de aprovação, processamento e disponibilidade das novas entidades químicas no tratamento de patologias humanas (BURGER & ABRAHAM, 2003; DIMASI & GRABOWSKI, 2007). Segundo DUNNE e colaboradores (2013), a elaboração de um novo fármaco na indústria farmacêutica leva um período de 10-15 anos, com um custo que varia de US$800 milhões a US$ 2 bilhões de dólares. Uma melhor compreensão desse desfecho pode ser observada na Tabela 1 (YOUNG, 2009).

Tabela 1. Comparação dos custos dos experimentos

Experimentos	Custo por composto (US$)
Modelagem molecular	10
Ensaios Bioquímicos	400
Cultura de células	4000
Estudos de toxicidade aguda em ratos	12.000
Estrutura cristalográfica das proteínas	100.000
Ensaios em animais	300.000
Estudos de toxicidade crônica de ratos (2 anos)	800.000
Ensaio clínico randomizado	500.000.000

Fonte: Young, D. C. (2009). Computational Drug Design: A guide for computational and medicinal chemists, Wiley & Sons, Inc. Publications

Em razão disso, o planejamento racional de fármacos surgiu como uma alternativa viável e está, gradualmente, tornando-se uma abordagem mais popular nas empresas farmacêuticas e instituições de ensino (JUDY; CHOUDHARY & KISHORE, 2016). Em síntese, é uma estratégia que visa planejar, descobrir e desenvolver fármacos com suporte lógico, racional e teórico para garantir rapidez, custo/benefício acessível e maior produtividade na síntese e análise de novos compostos bioativos (BARREIRO & RODRIGUES, 1997; MAVROMOUSTAKOS et al., 2011). Cabe destacar o emprego de ferramentas computacionais, especialmente a modelagem molecular que possui uma vasta e notável aplicação na descoberta de novos de fármacos para predizer e gerar protótipos moleculares, com embasamento na informação estrutural do alvo biológico (BARREIRO & FRAGA, 2008; MAVROMOUSTAKOS et al., 2011).

O planejamento de fármacos pode ser dividido em dois métodos, aqueles com base na estrutura do receptor (SBDD) e os baseados na estrutura do ligante (LBDD), demonstrado na Figura 3 (XIONG, 2006). Evidenciam-se neste esquema também as subdivisões desses métodos junto com os principais programas/softwares computacionais, usados para cada fim específico nas pesquisas de compostos bioativos.

Figura 3. Esquema representativo do planejamento racional de fármacos.

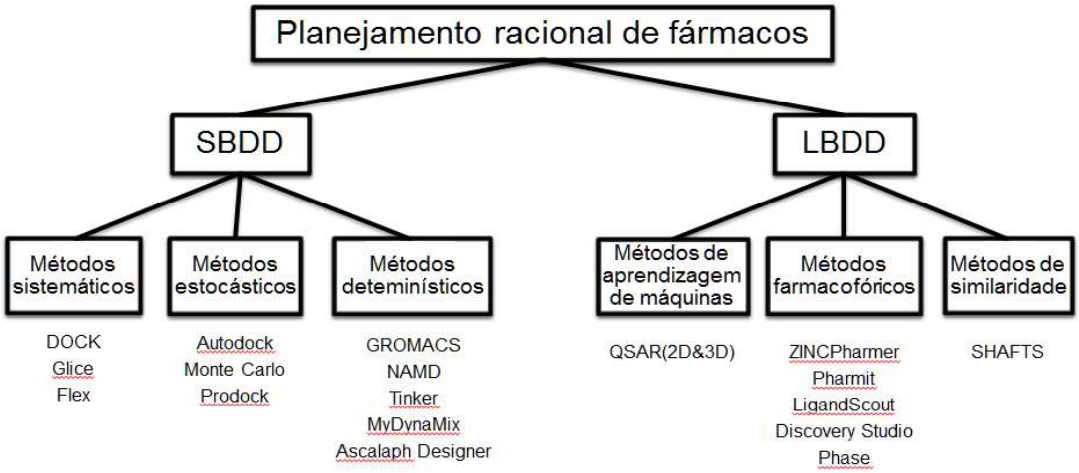

Fonte: XIONG, J. (2006). Essential Bioinformatics. New York: Cambridge University Press, p. 221.

Neste trabalho, serão aplicados os seguintes métodos de modelagem molecular: modelagem por homologia, docagem molecular e triagem virtual.

1.7.1 Modelagem por homologia

A modelagem molecular por homologia é um método bastante utilizado para predizer a estrutura tridimensional da enzima alvo de interesse, que não possui estrutura cristalográfica resolvida e usa como molde a estrutura 3D de outra proteína homóloga, cujas coordenadas cartesianas estejam depositadas no banco de dados de estruturas (BITAR & FRANGO, 2014; FORSTER, 2002; CALIXTO, 2013).

Fundamenta-se no princípio de evolução molecular, no qual estruturas de protéinas homológas mantêm alto grau de similaridade ao compartilhar um ancestral em comum, apesar das diferenças ocasionadas pelas mutações ao longo das gerações (SANTOS & ALENCASTRO, 2003; RÓZ et al., 2015). Na molécula, as regiões mais internas da estrutura são mais conservadas, enquanto as regiões localizadas nas superfícies, dobras ou alças (loops) são mais susceptíveis a mutações (WEBB & SALI, 2014; RÓZ et al., 2015).

Há diversos programas para a modelagem molecular sendo que os principais servidores empregados no contexto acadêmico e de pesquisa são os programas Modeller, Swiss-Model, Prime e Yasara (FLOUDAS et al., 2006; WEBB & SALI,

2014). A qualidade da predição é dependente do grau de identidade dos dados estruturais e das propriedades das moléculas que por meio de um alinhamento entre as sequências alvo e molde, pode-se efetuar a construção do modelo teórico desde que haja, no minímo, 30% de identidade (CALIXTO, 2013; WEBB & SALI, 2014). Quando esta condição ocorre há elevada probabilidade de ter proteínas com estruturas tridimensionais semelhantes (SANTOS & ALENCASTRO, 2003; WEBB & SALI, 2014; VERLI, 2014).

De modo geral, a modelagem molecular por homologia pode ser dividida em quatro etapas principais: (i) identificação do molde, (ii) alinhamento das sequências, (iii) construção e otimização dos modelos e (iv) validação (BITAR & FRANGO, 2014; CALIXTO, 2013). A seguir a descrição destas etapas que podem ser visualizadas na Figura 4.

Figura 4. Etapas da modelagem molecular por homologia. Adaptado do artigo de Webb & Sali, 2014.

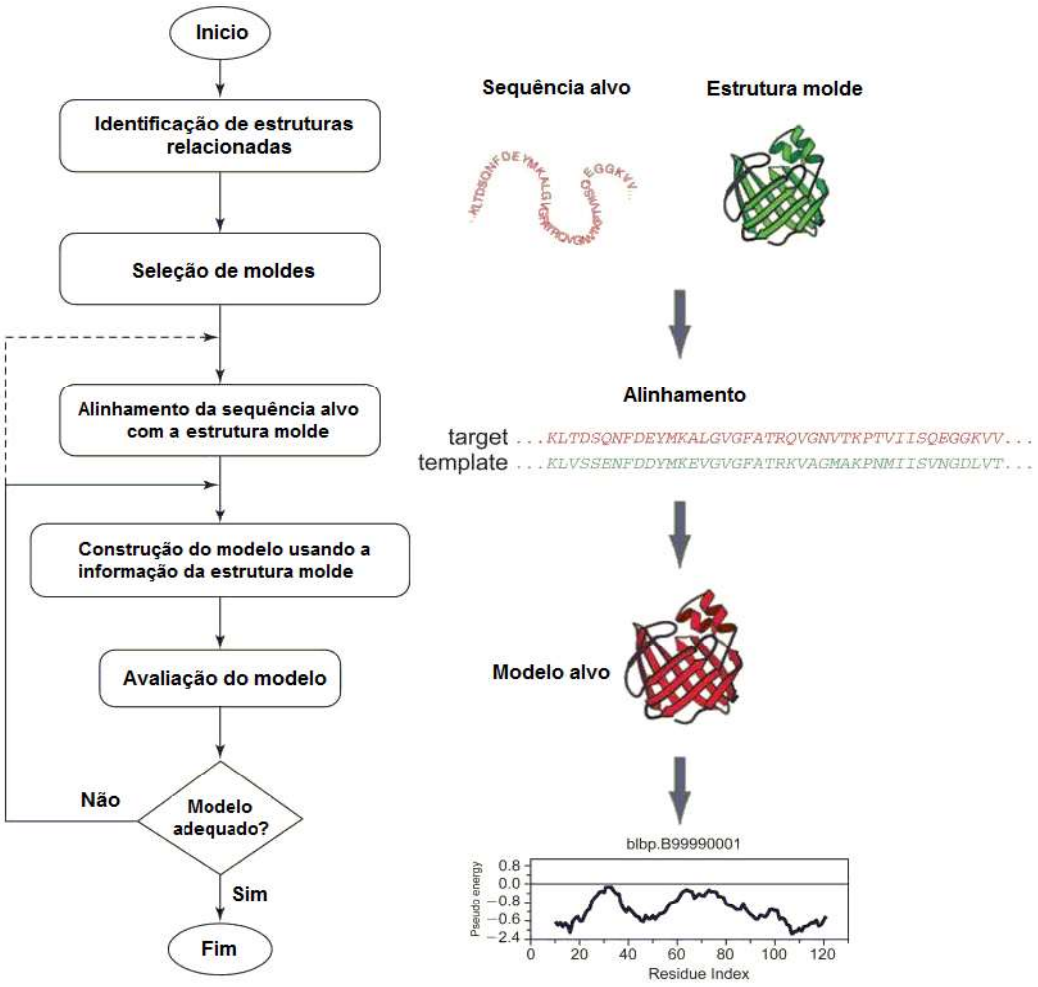

- Identificação e seleção do molde:

Identifica as sequências de aminoácidos de proteínas resolvidas experimentalmente que possuam similaridade com as sequências primárias da proteína-alvo a fim de selecionar o molde mais adequado (FLOUDAS et al., 2006; RÓZ et al., 2015). A estrutura preferencial deve apresentar o maior índice de similaridade, identidade e maior cobertura. Além disso, a seleção envolve outros critérios que podem estar presentes ou não: se pertence à mesma família, se desempenha a mesma função ou função correlacionada, se a estrutura resolvida possui resolução ≤ 2,0 Å e se a estrutura é complexada com ligante (WEBB & SALI, 2014; BITAR & FRANGO, 2014).

- Alinhamento entre as sequências:

Etapa que ocorre o alinhamento da sequência primária com o molde. Sucintamente, o alinhamento faz uma análise comparativa entre duas ou mais sequências de nucleotídeos ou aminoácidos com a finalidade de deduzir o grau de analogia estrutural, funcional e evolutiva entre as moléculas (ZAHA, FERREIRA & PASSAGLIA, 2012; DONKOR, DAYIE & ADIKU, 2014). Numa sequência alinhada: o pareamento é denominado de match, o não pareamento de mismatch, o espaçamento ou lacunas (gaps) são demonstrados em linhas tracejadas e a soma destes dados, por medidas escore, quantifica e determina a qualidade do alinhamento (ZAHA, FERREIRA & PASSAGLIA, 2012; VERLI, 2014).

Os alinhamentos são construídos com base em matrizes de substituição que permitem determinar a frequência de ocorrer substituições, inserções ou deleções, de um dado par de aminoácidos, nas sequências de uma proteína ao longo de sucessivas evoluções biológicas (ZAHA, FERREIRA & PASSAGLIA, 2012; SILVA, 2014). As principais matrizes, de amplo uso, são o PAM (Point Accepted Mutation) e o BLOSUM (BLOcks of Amino Acid SUbstitution Matrix), entretanto a segunda é mais empregada nas análises de nível protéico (SILVA, 2014; FRIZER, 2010; DONKOR, DAYIE & ADIKU, 2014; ZAHA, FERREIRA & PASSAGLIA, 2012).

Além disso, há duas formas de alinhamentos: o global e o local. No alinhamento global é caracterizado por alinhar, em toda a extensão, os resíduos das sequências, sendo os softwares ClustalW e Multialin, os mais utilizados. Por sua vez o alinhamento local prioriza alinhar alguns fragmentos, isto é, com regiões mais conservadas entre as duas sequências primárias, sendo o principal algoritmo

utilizado o BLAST (DONKOR, DAYIE & ADIKU, 2014; ZAHA, FERREIRA & PASSAGLIA, 2012; ALURU & JAMMULA, 2013).

- Construção dos modelos:

A construção do modelo é feito a partir da informação obtida do alinhamento da estrutura alvo-molde, sendo que os principais métodos utilizados nesta etapa são: os de corpos rígidos, por pareamento de fragmentos e por satisfação de restrições espaciais (WALLNER & ELOFSSON, 2005; FISER, 2010; VYAS et al., 2012). O método de corpos rígidos se baseia na separação de uma estrutura de proteína em regiões conservadas, alças e cadeias laterais, formando pequenos corpos rígidos a fim de construir, por partes, um novo modelo. Ao passo que o método por pareamento de fragmentos depende de um subconjunto de átomos conservados dos moldes para construir coordenadas de outros atómos, servindo como guia na obtenção do modelo final. Já o método por satisfação de restrições espaciais, se distingue dos demais, ao usar um ou mais alinhamentos do molde-alvo para gerar uma série de restrições estereoquímicas a fim de construir um modelo tridimensional adequado (WALLNER & ELOFSSON, 2005; FISER, 2010; VYAS et al., 2012). Isso ocorre pela presença de similaridade da distância geométrica entre os resíduos da estrutura do molde-alvo. As restrições são obtidas empiricamente pelo campo de força de mecânica molecular, sendo, em seguida, convertidos em funções de densidade de probabilidade (pdf) para cada restrição. Os critérios utilizados são: os ângulos de ligação, os ângulos diedrais, comprimento de ligação e átomos não-ligantes, posteriormente, há minimização de energia (FISER, 2010; BRABERG et al., 2012; VYAS et al., 2012).

- Validação do modelo:

A validação avalia a qualidade e confiabilidade do modelo, assim como verifica os prováveis erros estruturais durante todo o processo da modelagem. A obtenção do melhor modelo está, muitas vezes, associado à escolha do molde ideal e na acurácia do alinhamento (BAKER & SALI, 2001; VYAS et al., 2012; WEBB & SALI, 2014). Para determinar a qualidade estéreoquímica de uma estrutura proteica tem disponível o uso de distintos de softwares, em destaque o Procheck. O Procheck permite analisar o comprimento de ligação, os ângulos torcionais, a planaridade das ligações peptídicas, a quiralidade, as conformações das cadeias

laterais e o impedimento estérico (maus contatos), reproduzindo os dados no gráfico de Ramachandran. Este gráfico demonstra a distribuição dos ângulos phi (φ) e psi (ψ) para cada resíduo de aminoácido analisado, caracterizando as regiões em energeticamente mais favoráveis ou desfavoráveis (FLOUDAS et al., 2006; LASKOWSKI et al., 1993; HOLLINGSWORTH, S. A. & KARPLUS, 2010). Já na avaliação da compatibilidade do ambiente químico de cada aminoácido de uma proteína se utiliza o programa Verify-3D para verificar o enovelamento proteíco (EISENBERG, LUTHY & BOWIE, 1997). De modo geral, caso o modelo não seja aceitável, faz-se necessário checar o alinhamento utilizado e refazer todas as etapas do processo de modelagem até obter o modelo ideal (WEBB & SALI, 2014; BITAR & FRANGO, 2014).

No presente estudo, o s*oftware* empregado foi o MODELLER 9v14 (modeller). Neste programa, são necessários dois arquivos de entrada, um corresponde à sequência de aminoácidos (estrutura primária da proteína no formato *fasta*), cuja estrutura 3D e deseja obter, e uma estrutura cristalográfica já depositada no banco de dados de proteínas (*Protein Data Bank* - PDB), cujas coordenadas cristalográficas servirão como base para a construção do modelo da enzima alvo.

1.7.2 Docagem molecular

A docagem molecular realiza a predição da melhor posição, conformação e orientação da estrutura de uma pequena molécula (ligante) ao interagir no sítio de ligação de uma macromolécula-alvo (receptor) para formar um complexo, além de avaliar (função de pontuação) e classificar o modo de ligação (ALONSO; BLIZNYUK & GREADY, 2006; DE RUYCK et al., 2016). Consequentemente, a interação molecular do ligante pode provocar ativação ou inibição enzimática do respectivo alvo de interesse (GUEDES; MAGALHAES & DARDENNE, 2014). O processo de reconhecimento molecular, objetiva identificar e quantificar adequadamente o modo de interação de duas ou mais estruturas, como exemplo, o complexo proteína-ligante (FERREIRA, et al., 2015; DE RUYCK et al., 2016). A ligação do ligante com a macromolécula envolve um conjunto de interações intermoleculares no qual os principais tipos são: ligações de hidrogênio, interações de van der Walls, interações iônicas, interações hidrofóbicas, interações do tipo cátion-pi, anéis aromáticos, forças interatômicas e do grau de flexibilidade da molécula (CHEN, 2014; VERLI, 2014; GUEDES; MAGALHAES & DARDENNE, 2014). Também o conhecimento da

orientação entre duas moléculas permite prever a geometria e a afinidade de ligação do ligante com o alvo (GUEDES; MAGALHAES & DARDENNE, 2014; KITCHEN et al. 2004). Em contrapartida, o fator limitante da docagem se deve à dependência da informação tridimensional da biomolécula-alvo que, por sua vez, é obtida através de técnicas de ressonância magnética nuclear, cristalografia de raios-x ou modelagem por homologia (ALONSO; BLIZNYUK & GREADY, 2006; TAYLOR; JEWSBURY & ESSEX, 2002). Diversas técnicas de predição de docagem têm sido desenvolvidas para descobrir, refinar e otimizar os novos compostos líderes, podendo aplicar softwares livres, de âmbito acadêmico, como o Autodock, Autodockvina, DOCK, FDS, FRED, LigDockCSA and PyRx (DALLAKYAN & OLSON, 2015; FORLI et al., 2016; KITCHEN et al., 2004).

Os dois principais modelos de reconhecimento molecular, usados como base nos softwares de docagem para elucidar as reações dos sistemas biológicos são o modelo chave-fechadura e o encaixe induzido (GUEDES; MAGALHAES & DARDENNE, 2014; KITCHEN et al., 2004). O modelo chave-fechadura foi proposto por Emil Fisher em 1894 e tem por princípio buscar o melhor encaixe da chave (ligante) na fechadura (superfície da macromolécula). Ele considera a estrutura 3D do ligante e da proteína em forma rígida, tendo apenas exploração dos graus de liberdade translacional e rotacional (KITCHEN et al., 2004; MENG et al., 2011; HERNANDEZ-SANTOYO et al., 2013). Já o modelo encaixe induzido, proposto por Koshland em 1958, tem o principio de alcançar o melhor encaixe quando o ligante e a proteína ajustam a conformação entre eles, ocorrendo de forma simultânea. Tanto o ligante como o receptor são tratados como flexíveis, explorando todos os graus de liberdade do ligante (KITCHEN et al., 2004; MENG et al., 2011; HERNANDEZ-SANTOYO et al., 2013).

Os tipos de sistemas mais comuns nestes complexos são proteína-ligante, proteína-proteína e proteína-ácido nucléico (HERNANDEZ-SANTOYO et al., 2013; DE RUYCK et al., 2016). Ademais, a docagem tem grande aplicação na triagem virtual de bibliotecas, obtidas em banco de dados, na qual milhões de possíveis compostos são selecionados para se encaixarem em diferentes conformações e orientações no sítio de ligação da proteína-alvo (GUEDES; MAGALHAES & DARDENNE, 2014). Diversos cálculos de docagem são computados para cada interação e, posteriormente, todos os dados são armazenados e avaliados, gerando uma planilha de resultados com o respectivo ordenamento das moléculas que

obtiveram melhor pontuação ou afinidade de ligação. É importante ressaltar que a ferramenta deve distinguir, corretamente, as moléculas ligantes das não ligantes (CHEN, 2014; FERREIRA et al., 2015).

As ferramentas básicas de um método de docagem necessárias para gerar e avaliar as conformações do ligante são o algoritmo de busca e a função de pontuação (MENG et al., 2011; JACOB; ANDERSEN & MCDOUGL, 2012). O algoritmo de busca explora os graus de liberdade translacionais, rotacionais e conformacionais da molécula em relação à proteína-avo. Já com relação à flexibilidade do ligante, há três grupos de algoritmos: algoritmo de busca sistemático, estocástico e o determinístico (JACOB; ANDERSEN & MCDOUGL, 2012). A função de pontuação faz uma avaliação e ranqueamento dos modos de ligação, com base na energia de ligação do ligante com o complexo (ligante-receptor) (KITCHEN et al. 2004; MENG et al., 2011; VERLI, 2014). Tem o intuito de buscar o modo de interação mais favorável dos ligantes e a afinidade pela macromolécula-alvo.; Basicamente, realiza uma predição das afinidades de ligação (energia livre), das forças de interações não covalentes e das forças de interações intermoleculares (KITCHEN et al. 2004; MENG et al., 2011). A função de pontuação pode ser dividida em três tipos nos softwares de docagem: as baseadas no conhecimento, as empíricas e as baseadas no campo de força, está última é a mais utilizada nas avaliações de conformações geradas pelos algoritmos de busca (KITCHEN et al. 2004; JACOB; ANDERSEN & MCDOUGL, 2012; HERNANDEZ-SANTOYO et al., 2013). Atualmente, há vários métodos de avaliação nos softwares de docagem, sendo que neste trabalho empregamos o algoritmo genético lamarckiano (AGL), implementado no programa Autodock 4.2, para gerar a docagem dos ligantes selecionados (JACOB; ANDERSEN & MCDOUGL, 2012; MORRIS et al., 1998, 2009). O Autodock 4.2 é bastante utilizado no ambiente acadêmico em razão do grau de eficácia e robustez nas análises, sendo que a energia livre da função de pontuação é baseada no campo de força empírico e no AGL como algoritmo de busca rápido. O AGL tem sido demonstrado como a melhor ferramenta entre os algoritmos genéticos, a fim de simular as principais características da evolução Darwiniana e genética mendeliana em nível molecular (MORRIS et al., 1998, 2009).

1.7.3 Triagem virtual

A triagem virtual pode ser definida como uma seleção de compostos que satisfazem características específicas, utilizando ferramentas computacionais como, por exemplo, a docagem molecular (KLEBE, 2006; MERZ; RINGE & REYNOLDS, 2010). A triagem virtual permite a busca *in silico* em vastas bibliotecas de pequenas moléculas para a seleção de novos candidatos a fármacos (REDDY et al., 2007; HOU & XU, 2004). Basicamente, há dois tipos de abordagens para a busca por inibidores *in silico*. A primeira é a triagem virtual baseada no ligante (LBVS), frequentemente utilizada quando a estrutura alvo (macromolécula) a ser estudada ainda não foi elucidada (RODRIGUES et al., 2012; SOTRIFFER, 2011; MERZ; RINGE & REYNOLDS, 2010). Esta estratégia se baseia na utilização de informações de compostos conhecidos, que apresentem ação inibitória contra o alvo, a fim de identificar outros compostos que apresentem propriedades similares (MONTICELLI & SALOMEN, 2013; ZOETE; GROSDIDIER & MICHIELIN, 2009). Enquanto a segunda abordagem é a triagem virtual baseada na estrutura (SBVS), a qual envolve explicitamente a docagem de cada ligante dentro de um sítio ativo conhecido, estabelecendo um modo de ligação para cada composto de um banco de dados (RODRIGUES et al., 2012; SOTRIFFER, 2011). Essas informações servirão para selecionar os melhores ligantes, formando um pequeno conjunto de compostos, os quais poderão ser testados *in vitro* (REDDY et al., 2007).

As duas metodologias foram empregadas, sendo que para a LBVS foi aplicado o software ZINCPHARMER que realiza uma busca de pequenas moléculas com base no farmacóforo para gerar as respectivas bibliotecas. Subsequentemente, na SBVS foi empregado o software PyRx na análise de cada interação do ligante no sítio da macromolécula alvo por docagem molecular (MERZ; RINGE & REYNOLDS, 2010).

2. OBJETIVOS

2.1 Objetivo geral

- O objetivo geral deste estudo é predizer e investigar a estrutura da prefenato desidratase de *Mycobacterium tuberculosis*, além de propor potenciais inibidores utilizando técnicas de desenho racional de fármacos assistidos por computador.

2.2 Objetivos específicos

- Predizer a estrutura da enzima prefenato desidratase de *Mycobacterium tuberculosis* através da técnica de modelagem molecular por homologia;

- Construir modelos farmacofóricos 3D baseados no ligante, L-fenilalanina;

- Construir uma biblioteca de pequenas moléculas análogas ao substrato da prefenato desidratase de *Mycobacterium tuberculosis;*

- Realizar a triagem virtual de pequenas moléculas a partir da biblioteca construída;

- Excecutar análises farmacológicas e toxicológicas dos potenciais candidatos a fármacos *in silico*.

3. REFERÊNCIAS BIBLIOGRÁFICAS

1. AMER, F. A.; EL-BEHEDY, E. M.; MOHTADY, H. A. New targets for antibacterial agents. Biotechnology and Molecular Biology Reviews. v. 3, n. 3, p. 046-057, 2008.

2. AHMAD, S. Pathogenesis, Immunology, and Diagnosis of Latent *Mycobacterium tuberculosis* Infection. Clinical and Developmental Immunology, p. 17, 2011.

3. ALONSO, H.; BLIZNYUK, A. A.; GREADY, J. E. Combining docking and molecular dynamic simulations in drug design. Med Res Rev, v. 26, n. 5, p. 531-68, 2006. ISSN 0198-6325.

4. ALURU, S. & JAMMULA, N. A review of hardware acceleration for computational genomics. IEEE Design & Test, v. 31, n. 1, p. 19-30, 2013.

5. BAKER, D.; SALI, A. Protein structure prediction and structural genomics. Science, v. 294, n. 5540, p. 93-6, 2001. ISSN 0036-8075.

6. BARKER, R. D. Clinical tuberculosis. Medicine, v. 36, n. 6, p. 300-305, 2008.

7. BARREIRO, E. J.; FRAGA, C. A. M. Química Medicinal: as bases moleculares da ação dos fármacos. 3.ed. Porto Alegre: Artmed. p. 536, 2008. ISBN 9788582711187.

8. BARRETO, M. L.; PEREIRA, S. M.; FERREIRA, A. A. Vacina BCG: eficácia e indicações da vacinação e da revacinação. J. Pediatr. (Rio J.), Porto Alegre, v. 82, n. 3, supl. p. s45-s54, 2006.

9. BARREIRO, E. J.; RODRIGUES, C. R. Modelagem molecular: uma ferramenta para o planejamento racional de fármacos em química medicinal. Química nova, v. 20, n. 1, 1997.

10. BENTLEY, R. The shikimate pathway – a metabolic tree with many branches. Biochem Mol Bio. v. 1990, n. 25, p. 307-84, 1990.

11. BITAR, M.; FRANCO, G. R. A Basic Protein Comparative Three-Dimensional Modeling Methodological Workfloe Theory and Practice. IEEE/ACM Trans Comput Biol Bioinform, v. 11, n. 6, p. 1052-65, 2014. ISSN 1545-5963.

12. BOCHKOW, D. V. et al. Shikimic Acid: Review of Its Analytical, Isolation, and Purification Techniques from Plant and Microbial Sources. Journal of Chemical Biology v.5, n.1, p. 5-17, 2012.

13. BURGER, A.; ABRAHAM, D. J. Burger's: Medicinal Chemistry & Drug Discovery. 6.ed. Wiley, 2003. ISBN 9780471270904.

14. BRABERG, H.; WEBB, B. M.; TJIOE, E.; PIEPER, U.; SALI, A.; MADHUSUDHAN, M. S. SALIGN: a web server for alignment of multiple protein sequences and structures. Bioinformatics, v. 28, n. 15, p. 2072-2073, 2012.

15. BRASIL. Ministério da Saúde. Secretaria de Vigilância em Saúde. Departamento de Vigilância Epidemiológica. Manual nacional de vigilância laboratorial da tuberculose e outras micobactérias. 1. ed. Brasília: Ministério da Saúde, 2008.

16. BRASIL. Ministério da Saúde. Secretaria de Vigilância em Saúde. Departamento de Vigilância Epidemiológica. Doenças infecciosas e parasitárias: guia de bolso. 8. ed. rev. Brasília: Ministério da Saúde, 2010.

17. BRASIL. Ministério da Saúde. Secretaria de Vigilância em Saúde. Guia de Vigilância em Saúde. Volume único. Brasília: Ministério da Saúde, 2014.

18. BRASIL. Ministério da Saúde. Secretaria de Vigilância em Saúde. Perspectivas brasileiras para o fim da tuberculose como problema de saúde pública. Boletim Epidemiológico, Brasília, v. 47, n. 13, p. 1-15, 2016

19. CALIXTO, P. H. M. Aspectos gerais sobre a modelagem comparativa de proteínas. Ciência Equatorial, v. 3, n. 1, p. 9-16, 2013. ISSN 2179-9563.

20. CASTELO FILHO, A. et al. II Consenso Brasileiro de Tuberculose: Diretrizes Brasileiras para Tuberculose 2004. Jornal Brasileiro de Pneumologia., São Paulo, v. 30, p. S57-S86, 2004. ISSN 1806-3713.

21. CAFÉ OLIVEIRA, L. N. et al. Detection of multidrug-resistant *Mycobacterium tuberculosis* strains isolated in Brazil using a multimaker genetic assay for KatG and rpoB genes. Braz J Infect Dis, v. 20, n. 2, p. 166-72, 2016. ISSN 1413-8670.

22. CAMPOS, H. S. Etiopatogenia da tuberculose e formas clínicas. Pulmão. RJ., Rio de Janeiro, v. 15, n. 1, p. 2ão. RJ., Rio de Janeiro, v. 15, n. 1, p. 29-35, 2006.

23. COTTON, R. G. H.; GIBSON, F. The biosynthesis of phenylalanine and tyrosine: enzymes converting chorismic acid into prephenic acid and their relationship to prephenate dehydratase and prephenate dehydrogenase. Biochimica et Biophysica Acta, v. 100, n. 100, p. 75-88, 1965.

24. CHEN, Y. C. Beware of docking! Trends in Pharmacological Sciences, v. 36, n. 2, p. 78-95, 2014. ISSN 0165-6147

25. CHO, M. H. et al. Phenylalanine biosynthesis in Arabidopsis thaliana. Identification and characterization of arogenate dehydratases. J. Biol Chem, v. 282, n. 42, p. 30827-35, 2007. ISSN 0021-9258.

26. DALLAKYAN, S.; OLSON, A.J. Small-molecule library screening by docking with PyRx. Methods Mol Biol, v. 1263, p. 243-50, 2015. ISSN 1064-3745.

27. DE RUYCK, J. et al. Molecular docking as a popular tool in drug design, an in silico travel. Adv Appl Bioinform Chem, v.9, p. 1-11, 2016. ISSN 1178-6949.

28. DI PERRI, G. et al. Drug-drug interactions and tolerance in combining antituberculosis and antirretroviral therapy. Expert Opin Drug Saf, v. 4, n. 5, p. 821-36, 2005. ISSN 1474-0338.

29. DIMASI, J. A.; GRABOWSKI, H. G. The cost of biopharmaceutical R&D: is biotech different? Special Issue: Economic and Policy Issues in the Pharmaceutical Industry, v. 28, n. p. 469-479, 2007.

30. DONKOR, E. S.; DAYIE, N. T. K. D. & ADIKU, T. K. Bioinformatics with basic local alignment search tool (BLAST) and fast alignment (FASTA). Journal of Bioinformatics and Sequence Analysis, v. 6, n. 1, p. 1-6, 2014.

31. DUCATI, R. G.; RUFFINO-NETO, A.; BASSO, L. A.; SANTOS, D. S. The resumption of consumption: a review on tuberculosis. Memórias do Instituo Oswaldo Cruz, Rio de janeiro, v. 101 suppl. 7, p. 697-714, 2006.

32. DUCATI, R. G.; BASSO, L. A.; SANTOS, D. S. *Mycobacterium* Shikimate Pathway Enzymes as Targets for Drug Design. Current Drug Targets, v. 2007, n. 8, p. 423-435, 2007.

33. DUNNE, S.; SHANNON, B.; DUNNE, C. & CULLEN, W. A review of the differences and similarities between generic drugs and their originator counterparts, including economic benefits associated with usage of generic medicines, using Ireland as a case study. BMC Pharmacology and Toxicology,v. 2013, n.14, p. 1, 2013.

34. ELKS, P. M.; BRIZEE, S.; VAN DER VAART, M.; WALMSLEY, S. R.; VAN EEDEN, F. J.; RENSHAW, S. a; MEIJER, A. H. Hypoxia inducible factor signaling modulates susceptibility to mycobacterial infection via a nitric oxide dependent mechanism. PLoS pathogens, v. 9, n. 12, p. e1003789, 2013.

35. EISENBERG, D.; LUTHY, R.; BOWIE, J. U. VERIFY3D: assessment of protein models with three-dimensional profiles. Methods in Enzymology, v. 277, n. 6364, p. 396-404, 1997.

36. FERREIRA, L. G. et al. Molecular docking and structure-based drug design strategies. Molecules, v. 20, n. 7, p. 13384-421, 2015. ISSN 1420-3049.

37. FISER, A. Template-Based Protein Structure Modeling. Methods in Molecular Biology (Clifton, N. J.), v. 673, p. 73-94, 2010.

38. FORLI, S. et al. Computational protein-ligand docking and virtual drug screening with the AutodDock suíte. Nat Protoc, v. 11, n. 5, p. 905-19, 2016. ISSN 1750-2799

39. FLOUDAS, C. A. et al. Advances in protein structure prediction and de novo protein design: A review. Chemical Engineering Science, v. 61, n. 3, p. 966-988, 2006. ISSN 0009-2509.

40. FORSTER, M. J. Molecular modeling in structural biology. Micron, v. 33, n. 4, p. 365-84, 2002. ISSN 0968-4328.

41. FRIEDEN, T. R. et al. Tuberculosis. Lancet, v. 362, n. 9387, p. 887-99, 2003. ISSN 0140-6736.

42. GUEDES, I. A.; DE MAGALHÃES, C. S.; DARDENNE, L. E. Receptor-ligand molecular docking. Biophysical Reviews, v. 6, n. 1, p. 75-87, 2014. ISSN 1867-2469.

43. HIJJAR, M. A.; PROCÓPIO, M. J. Tuberculose – Epidemiologia e Controle no Brasil. Revista Hospital Universitário Pedro Ernesto, v. 5, n. 2, p. 15-23, 2006.

44. HERNÁNDEZ-SANTOYO, A. et al. Protein-Protein and Protein-Ligand Docking. Protein Engineering – Technology and Application, Dr. Tomoshisa Ogawa, InTech, DOI: 10.5772/56376, 2013.

45. HYUN, M. W.; YUN, Y. H; KIM, J. Y.; KIM, S. H. Fungal and Plant Phenylalanine Ammonia-lyase. Mycobiology. v. 39, n. 4, p. 257-265, 2011.

46. HOLLINGSWORTH, S. A. & KARPLUS, P. A. A fresh look at the Ramachandran plot and the occurrence of standard structures in proteins. Biomolecular Concepts, v. 1, n.3-4, p. 271-283, 2010.

47. HOU, T.; XU, X. Recent development and application of virtual screening in drug discovery: an overview. Curr Pharm Des, v. 10, n. 9, p. 1011-33, 2004. ISSN 1381-6128.

48. JACOB, R. B.; ANDERSEN, T.; MCDOUGAL, O. M. Accessible high-throughput virtual screening molecular docking software for students and educators. PLoS Comput Biol, v. 8, n. 5, p. e1002499, 2012. ISSN 1553-734x.

49. JAIN, A.; MONDAL, R. Extensively drug-resistant tuberculosis: current challenges and threats. FEMS Immunol Med Microbiol, v. 53, n. 2, p. 145-50, 2008. ISSN 0928-8244.

50. JUDY, E.; CHOUDHARY, S. & KISHORE N. Rational drug desin and future directions: Thermodynamic perspective. Austin Biomol Open Acess, v.1, n. 1, p. 1003, 2016.

51. KAUFMANN, S. H.; HUSSEY, G.; LAMBERT, P. H. New vaccines for tuberculosis. Lancet, v. 375, n. 9731, p. 2110-9, 2010.

52. KAUFMANN, S. H. E.; MCMICHAEL, A. J. Annulling a dangerous liaison: vaccination strategies against AIDS and tuberculosis. Nature Medicine, v. 11, n. 4s, p. S33-S44, 2005.

53. KLEBE, G. Virtual ligand screening: strategies, perspectives and limitations. Drug Discov Today, v. 11, n. 13-14, p. 580-94, 2006. ISSN 1359-6446.

54. KNECHEL, N. A. Tuberculosis: Pathophysiology, Clinical Features, and Diagnosis. Critical Care Nurse, v. 29, n. 2, p. 34-43, 2009.

55. KITCHEN, D. B. et al. Docking and scoring in virtual screening for drug discovery: methods and applications. Nat Rev Drug Discov, v. 3, n. 11, p. 935-49, 2004. ISSN 1474-1776.

56. KIRBY, T. Extensively drug-resistant tuberculosis hovers threateningly at Australia's door. Med J Aust, v. 198, n. 7, p. 355-356, 2013.

57. KORB, V. C.; CHUTURGOON, A. A. & MOODLEY, D. *Mycobacterium tuberculosis*: Manipulator of Protective Immunity. Esposito S, ed. International Journal of Molecular Sciences, v. 17, n. 3, p.131-144, 2016.

58. KUMAR, V. et al. Robbins & Cotran Patologia: Bases Patológicas das Doenças. 8.ed. Rio de Janeiro: Elsevier,p. 120 , 2010. ISBN 9788535234596.

59. LASKOWSKI, R. A.; MACARTHUR, M. W.; MOSS, D. S.; THORNTON, J. M. PROCHECK – a program to check the stereochemical quality of protein structures. J. App. Cryst., v. 26, p. 283-291, 1993.

60. LEMOS, A. C. M. Co-infecção tuberculose/HIV. J. bras. Pneumol v. 34, n. 10, p. 753-755, 2008.

61. LUCA, S., & MIHAESCU, T. History od BCG Vaccine. Maedica (Buchar), v. 8, n. 1, p. 53-58, 2013.

62. MIRANDA, M. S.; BREIMAN, A.; ALLAN, S.; DEKNUYDT, F.; ALTARE, F. The Tuberculous Granuloma: An Unsuccessful Host Defence Mechanism Providing a Safety Shelter for the Bacteria? Clinical and Developmental Immunology, v. 2012, p. 1-14, 2012.

63. MENG, X. Y. et al. Molecular docking: a powerful approach for structure-based drug discovery. Curr Comput Aided Drug Des, v. 7, n. 2, p. 146-57, 2011. ISSN 1573-4099.

64. MERZ, K. M.; RINGE, D; REYNOLDS, C. H. Drug Design: Structure and ligand-based approaches. New York: Cambridge University Press, p.132, 2010. ISBN 9780521887236.

65. MOÇAMBIQUE. Ministério da Saúde. Manual de Baciloscopia da Tuberculose. Programa Nacional de Controle da Tuberculose. Instituto Nacional de Saúde. Maputo, 2012.

66. MONTICELLI, L.; SALOMEN, E. Biomolecular Simulations: methods and protocols. New York: Humana, p.702, 2013. ISBN: 9781627030168.

67. MONROE, A. A.; GONZALES, R. I. C.; PALHA, P. F.; SASSAKI, C. M.; RUFFINO NETTO A.; VENDRAMINI S. H. F. et al. Envolvimento de equipes de

atenção básica à saúde no controle da tuberculose. Revista da Escola de Enfermagem da USP, v. 42, n. 2, p. 262-267, 2008.

68. MORRISON, J.; PAI, M.; HOPEWELL, P. C. Tuberculosis and latent tuberculosis infection in close contacts of people with pulmonary tuberculosis in low-income and middle-income countries: a systematic review and meta-analysis. Lancet Infect Dis, v. 8, n. 6, p. 359-68, 2008. ISSN 1473-3099.

69. MORRIS, G. M., GOODSELL, D. S., HALLIDAY, R.S., HUEY, R., HART, W. E., BELEW, R. K. and OLSON, A. J. Automated Docking Using a Lamarckian Genetic Algorithm and and Empirical Binding Free Energy Function J. Computational Chemistry, n.19, p. 1639-1662, 1998.

70. MORRIS, G. M., HUEY, R., LINDSTROM, W., SANNER, M. F., BELEW, R. K., GOODSELL, D. S. and OLSON, A. J. (2009) Autodock4 and AutoDockTools4: automated docking with selective receptor flexiblity. J. Computational Chemistry, n. 16, p. 2785-91, 2009.

71. MAVROMOUSTAKOS, T.; DURDAGI, S.; KOUKOULITSA, C.; SIMCIC, M.; PAPADOPOULOS, M. G.; HODOSCEK, M. & GRDADOLNIK, S. G. Strategies in the Rational Drug Design. Current Medicinal Chemistry, v. 2011, n.18, p. 2517-2530, 2011.

72. MUNIZ, J. N.; RUFFINO-NETTO, A.; VILLA, T. C.; YAMAMURA, M.; ARCENCIO, R.; CARDOZO-GONZALEZ, R. I. Epidemiological aspects of human immunodeficiency virus/tuberculosis co-infection in Ribeirão Preto, Brazil from 1998 to 2003. J. Bras. Pneumol. v. 32, n. 6, p. 529-34, 2006.

73. OTTENHOFF, T. H. Overcoming the global crisis: “yes, we can”, but also for TB ... ? Eur J Immunol, v. 39, n. 8, p. 2014-20, 2009.

74. O’GARRA, A.; REDFORD, P. S.; MCNAB, F. W.; BLOOM, C. I.; WILKINSON, R. J.; BERRY, M. P. R. The imune response in tuberculosis. Annual review of immunology, v. 31, p. 475-527, 2013.

75. PATEL, K.; JHAMB, S. S.; SINGH, P. P. Models of latente tuberculosis: Their saliente features, limitations, and development. Journal of Laboratory Physicians, v. 3, n. 2, p. 75-79, 2011.

76. PARISH T., STOKER N. G. The common aromatic amino acid biosynthesis pathway isessential in *Mycobacterium tuberculosis*. Microbiology. v. 2002, n. 148, p. 3069–77, 2002.

77. POHNERT, G.; ZHANG, S.; HUSAIN, A.; WILSON, D.B.; GANEM, B. Regulation of Phenylalanine Biosynthesis. Studies on the Mecanism of Phenylalanine Binding an dfeedback Inhibition in the Eschericha coli P Protein. Biochemistry, v. 1999, n. 38, p. 12212-12217, 1999.

78. PITTARD A. J. Escherichia coli and Salmonella: Cellular and Molecular Biology, ed. Neidhardt, Washington: ASM Press, p. 458–484, 1996.

79. RAVIGLIONE, M. et al. Scaling up interventions to achieve global tuberculosis control: progress and new developments. Lancet maio v. 379, n. 9829, p. 1902-13, 2012.

80. RAPPUOLI, R.; ADEREM, A. A 2020 vision for vacines against HIV, tuberculosis and malária. Nature, v. 473, n. 7348, p. 463-9, 2011.

81. RAMAN, K.; YETURU, K.; CHANDRA, N. targetTB: A target identification pipeline for *Mycobacterium tuberculosis* through an interactome, reactome and genome-scale structural analysis. BMC Systems Biology, v. 2008, n. 2, p. 109, 2008.

82. REDDY, A. S. et al. Virtual screening in drug discovery – a computational perspective. Curr Protein Pept Sci, v. 8, n. 4, p. 329-51, 2007. ISSN 1389-2037.

83. RODRIGUES, R. P. et al. Virtual Screening Strategies in Drug Design[Estratégias de Triagem Virtual no Planejamento de fármacos]. Revista Virtual de Química, v. 4, n. 6, p. 739-776, 2012.

84. RÓZ, A. L.; LEITE, F. L.; FERREIRA, M.; OLIVEIRA, O. N. Grandes áreas da nanociência: princípios e aplicações. Coleção nanociência e nanotecnologia. Rio de Janeiro: Elsevier, v. 2, 2015.

85. RUSSELL, D. G. Who puts the tubercle in tuberculosis? Nature Reviews Microbiology, v. 5, n. 1, p. 39-47, 2007.

86. RUSTAD, T. R.; HARRELL, M. I.; LIAO, R.; SHERMAN, D. R. The enduring hypoxic response of *Mycobacterium tuberculosis*. PloS one, v. 3, n. 1, p. e1502, 2008.

87. SANTOS, J. S.; BECK, S. T. The coinfection HIV/Tuberculosis: a importante challenge- A review. Rev. Bras. Anal. Clin. v. 41, n. 3, p. 209-150, 2009.

88. SANTOS, F. O. A.; ALENCASTRO, R. B. Modelagem de proteínas por homologia. Química Nova, v. 26, n. 2, p. 253-259, 2003.

89. SILVA, M. S. Comparação de matrizes de substituição para alinhamento de pequenos fragmentos de proteínas. Brazilian Journal of Bioinformatics, v. 2, n. 3, 2014.

90. STARKE, J. R.; CONNELLY, K. K.; Bacille Calmette-Guerin vaccine. In: Plotkin MEA, editor. Vaccines. Philadelphia: WB Saunders, p. 456-89, 2004.

91. SOTRIFFER, C. Virtual Screening: principles, challenges, and practical guidelines. Weinheim: Wiley-VCH, p. 519, 2011. ISBN 9783527326365.

92. SNIDER, D. E.; RAVIGLIONE, M.; KOCHI, A. Tuberculosis pathogenesis, protection and control. p. 3-11, 1994.

93. TAYLOR, R. D.; JEWSBURY, P. J.; ESSEX, J. W. A review of protein-small molecule docking methods. J Comput Aided Mol Des, v. 16, n. 3, p. 151-66, 2002. ISSN 0920-654X.

94. TORTORA, G. J.; FUNKE, B. R., & CASE, C. L. Microbiologia. 6 ed. Porto Alegre: Artmed, 2000.

95. URDAHL, K. B.; SHAFIANI, S. & ERNST, J. Initiation and regulation of T-cell responses in tuberculosis. Mucosal immunology, v. 4, n. 3, p. 288-293, 2011.

96. VYAS, V. K.; UKAWALA, R. D.; GHATE, M.; & CHINTHA, C. Homology Modeling a Fast Tool for Drug Discovery: Current Perspectives. Indian Journal of Pharmaceutical Sciences, v. 74, n. 1, p. 1-17, 2012.

97. VERLI, H. (Org.). Bioinformática da Biologia à Flexibilidade Molecular. Porto Alegre: 1 ed., 2014.

98. VERONESI-FOCACCIA, R. Tratado de infectologia. 4.ed. São Paulo: Atheneu, 2009. ISBN 9788538801016.

99. VERVER, S.; WARREN, R. M.; BEYERS, N.; RICHARDSON, M.; VAN DER SPUY, G. D.; BORGDORFF, M. W.; ENARSON, D.a.; BEHR, M.a.; VAN HELDEN, P. D. Rate of Reinfection Tuberculosis after Successful Treatment Is Higher than Rate of New Tuberculosis. American Journal of Respiratory and Critical Care Medicine, v. 171, n. 12, p. 1430-1435, 2005.

100. WALLNER, B.; ELOFSSON, A. All are not equal: A benchmark of different homology modeling programs. Protein Science: A Publication of the Protein Society, v. 14, n. 5., p. 1315-1327, 2005.

101. WEBB, B.; SALI, A. Comparative Protein Structure Modeling Using Modeller. Current Protocols in Bioinformatics, John Wiley & Sons, Inc., 5.6.1-5.6.32, 2014.

102. WILDNER, L. M. et al. Micobactérias: Epidemiologia e diagnostic. Rev. Patol. Trop., Goiânia, v. 40, n. 3, p. 227-229, 2011.

103. WORLD HEALTH ORGANIZATION (WHO). Global Tuberculosis Control: report. Geneva: WHO, 2016.

104. XIONG, J. Essential Bioinformatics. New York: Cambridge University Press, p. 221, 2006. ISBN 9780521600828.

105. YOUNG, D. C. Computational Drug Design: A Guide for Computational and Medicinal Chemists. Wiley, 2009. ISBN 9780470451847.

106. ZAHA, A.; FERREIRA, H. B.; PASSAGLIA, L. M. P. (Org) Biologia molecular básica. 4. ed. Porto Alegre: Artmed, 2012.

107. ZOETE, V.; GROSDIDIER, A.; MICHIELIN, O. Docking, virtual high throughput screening and in silico fragment-based drug design. J Cell Mol Med, v. 13, n. 2, p. 238-48, 2009. ISSN 1582-1838.

4. ARTIGO

O artigo foi elaborado conforme as normas da revista Journal of Molecular Modeling (Fator de impacto:1,438, 2015). Posteriormente, será submetido.

Structural study and design of new inhibitors of Prephenate dehydratase enzyme from *Mycobacterium tuberculosis*

Mauricio Alves Alte[1], Rafael Andrade Caceres[1,2]

1 Programa de Pós-Graduação em Ciências da Saúde, Universidade Federal de Ciências da Saúde de Porto Alegre (UFCSPA).

2 Departamento de Farmacociências, Universidade Federal de Ciências da Saúde de Porto Alegre , R. Sarmento Leite 245, 90050-170 Porto Alegre, RS, Brazil

ABSTRACT

Tuberculosis is considered a serious public health problem by keeping high rate of incidence, prevalence and mortality in the population worldwide, being the second most lethal disease of humanity, following the human immunodeficiency virus. The World Health Organization estimates that a third of the population is infected with the *Mycobacterium tuberculosis.* The increase of multidrug resistant strains and the complexity of HIV/TB coinfection have led to the search of more efficient antimicrobial agents. The enzyme prephenate dehydratase belongs to the pathway of chorismate, an essential mechanism to the survival of the microorganism, consequently, was chosen as a potential therapeutic target. The aim of this study was to obtain and investigate the 3D structure of prephenate dehydratase of *Mycobacterium tuberculosis,* beyond to propose potential inhibitors using bioinformatics tools. The tertiary structure was resolved by homology modeling based on the 3MWB crystallographic structure. The 3D model showed 93.7% of the amino acid residues in more favorable regions and 5.4% in additionally favorable in the Ramachandran Plot. The Verify-3D profile exhibit 90.34% of residues. In relation to the molecular docking were selected, from a library of 30.908 compounds, 100 ligands with higher binding affinity ranging from -12.45 to -10.52 kcal/mol about the phenylalanine (-7.8 kcal/mol). Among the top ten compounds are ZINC69138131 and ZINC28047676, which are derived from benzomidazol. These results are useful for a better understanding of interactions of active sites of enzyme and in the selection of potential prototypes to be tested *in vitro* and *in vivo*.

Key words: Tuberculosis, Prephenate dehydratase, Rational drug design, Structural Bioinformatics.

INTRODUCTION

Tuberculosis (TB) is an infectious and contagious disease caused by the microorganism *Mycobacterium tuberculosis* (Mtb), which mainly affects the lungs, but can also be evident in other parts of the body, such as the kidneys, the bones, the lymph glands, the pleura, the larynx, the intestines and the brain (extrapulmonary tuberculosis) [1-4]. TB is a serious public health problem and continues to be an alarming factor in view of the present spread of infected persons and deaths [1, 5-6]. Indeed, it is the second most lethal disease on human species, after the human immunodeficiency virus (HIV), with which it often shows signs of coinfection [1,7,8]. The World Health Organisation (WHO) estimates that one third of the population, which is about two or three billion people, is currently infected with the Mtb bacillus [1]. In 2015, there were 10.4 million new cases and 1.4 million deaths (1.1 million HIV negative and 0.4 million HIV positive) caused by TB in the world [1]. Brazil is included in this global scenario, currently being in 18th position in the ranking of countries with most cases of TB [9]. The capital of the state of Rio Grande do Sul has the second highest level of incidence and the first on the percentage of TB-HIV co-infection in the country [1,9]. According to the Ministry of Health/SINAN and the IBGE, the city of the Porto Alegre shows 88.8 cases for every 100 thousand people, while the mortality rate stands at 4.5 cases per 100 thousand people [9]. In addition, the emergence of Mtb strains that are resistant to multiple drugs has aggravated the problem although other factors, such as social and economic conditions, abandonment of treatment, and unfavourable interactions between the drugs involved, may also contribute to the increase in the number of infected people [10-13]. Several research studies have reported the emergence of multi-resistant strains (MDR), extensively resistant strains (XDR) and, more recently, totally resistant strains (TDR) [12, 14-16]. The need to understand the distinct metabolic pathways of *M. tuberculosis* has allowed the growth of studies to identify molecular targets as well as to search and investigate potential compounds with inhibitory action [18]. In addition, developing new drugs may contribute to disease control and eradication [1, 17-19].

The prephenate dehydratase of *Mycobacterium tuberculosis* has 386 amino acids and is encoded by pheA gene (Rv3838). This enzyme performs the decarboxylation and dehydration of the prephenate to phenylpyruvate with elimination of carbon dioxide and water [20-23]. Because it belongs to the metabolic

pathway of shikimic acid, the inhibition of any enzyme present in this pathway makes the organism unviable and also contains a selective toxicity property [20-26, 65]. Therefore, the prephenate dehydratase is a very promising and essential target in the development of new antituberculosis inhibitors [18, 24-26]. The main objective of this study is to obtain and investigate the structure of prephenate dehydratase of *Mycobacterium tuberculosis* and propose potential inhibitors using computer aided rational drug design techniques.

MATERIAL AND METHODS

Molecular modelling by homology and validation of the model

The primary sequence of amino acids that encodes the target enzyme, prephenate dehydratase of Mtb, was obtained on the National Centre of Biotechnological Information (NCBI, http://www.ncbi) database, with access number NP_218355 [27]. The sequence has a total lengtht of 321 amino acids and was used to identify homologs and also to generate a 3D structure through modelling by homology [28-30]. The Blast tool (Basic Local Alignment Search Tool) allows the identification of possible templates, on the protein database or Protein Data Bank (PDB) and the structure of the dimer complexed with phenylalanine (PDB ID: 3MWB) was chosen as a model for molecular analysis [31]. The water molecules and the magnesium ion were excluded from PDB file, and four residues (21, 53, 139 and 214) from selenomethionine (Se-Met) were altered to methionine (Met), in both chains A and B, using the Swiss PDB Viewer software package (SPDBV, http://spdbv.vital-it.ch/) [32]. It was also performed the reconstruction of missing atoms from each side chain. The alignment between the target sequence and the model was carried out by command SALIGN() that employs a dynamic programming algorithm and an BLOSUM62 similarity matrix, using the program 9.v.14 modeller [30, 33-34]. The alignment file was used to generate one thousand 3-D models by satisfaction of spatial restraints [30, 33-34]. In the analysis, the best structure of the model is represented by the lowest DOPE-Score value.

The stereochemical and structural quality of the model were analysed and validated by the Swiss-model workspace servers and SAVES (server for analysis and

structural verification) [32-33]. The Procheck program analyses the general geometry and also that of each residue within the structure, being represented by Ramachandran plot that shows the statistical data and also the phi and psi angles of torsion. The Verify-3D package analyses the three-dimensional environment of each residue using the sequence of amino acids [29-34].

Construction of the pharmacophore model and virtual screening

The pharmacophore model was constructed based on phenylalanine ligand, while maintaining the molecule's active ingredient. The structural information and the drawing of the compound were performed with the aid of PDB, PDBsum and Molview software [31, 35-36]. In the screening process, the Zincpharmer server subjected the pharmacophore to the ZINC database, to seek and analyse analogous molecules, creating six libraries of small molecules through adoption of six types of parameters in the regions of the pharmacophore [37-38]. The parameters that have been included in these models are: hydrogen bonding vectors (donor and acceptor), hydrophobic volume, and negative ion [37-38]. The concept of this methodology is that the molecules could have similar biological activities when sharing structural similarity [37-38]. The other reason behind the selection of the compounds is the probability of establishing good interaction with the target receptor [39-43]. All the libraries of the ligands, as supplied by the ZINC database, were downloaded in the .sdf file format, being minimized and converted into the .pdbqt format by the Open Babel software package of PyRx 0.8 [37,44]. No filters were applied to Zincpharmer during the process of virtual screening on the database.

Molecular docking

The Autodock 4.2 software package (autodock.scripps.edu) with the PyRx 0.8 graphic interface(http://pyrx.sorceforge.net), based on python 2.7 language, was used to perform the calculations for docking of phenylalanine and the six ligand libraries against enzyme prephenate dehydratase and predicts interaction and bond affinity for each ligand [34,40-44,66]. All the ligands were contained within the bonding site of the target macromolecule, in a type of autogrid (box or cube). In this grid, there is a spatial search with spacing of 0.375 Å, dimensions (x, y, z) (Å) of (30, 30, 30) and a geometric centre of co-ordinates (x, y, z) at (26.190, 35.462, 65.548). The Lamarckian genetic algorithm was used to analyse the conformity of each

docked molecule [45-46]. The parameters of simulation consist of producing ten conformations (runs) for each protein-ligand complex with an initial population of 150 individuals, an evaluation of maximum energy set at 1000.000, maximum generation of 27.000, a mutation rate of 0.02 and a crossover rate of 0.8. The AutoDock results for the conformations of each molecule were then grouped according to the root-mean-square deviation (RMSD) less than 2.0 Å [34, 46]. The ligands with the best bonding energy are represented by higher binding affinity, expressed in kcal/mol. All the structures were analysed and viewed by the following programmes: Swiss PDB Viewer (spdbv), Visual Molecular Dynamics (vmd), UCSF Chimera and PyMOL [32, 47-49]. High-quality images were generated by these two last-mentioned programmes.

Pharmacokinetic and toxicological analysis

The best one hundred ligands were submitted to a pharmacological analysis of the physico-chemical properties and ADME-tox (Absorption, Distribution, Metabolism, Excretion and Toxicity). They were estimated by the servers FAF-Drugs3 (http://fafdrugs3.mti.univ-paris-diderot.fr/), that uses several molecular describers, and DataWarrior (www.openmolecules.org/datawarrior/) to evaluate toxicological profiles, such as mutagenic, tumorigenic, reproductive effective and irritant (allergic) [50-52].

Analysis of protein-ligand complex

A molecular analysis of the interaction of the best ten ligands, which are candidates to drugs, with the prephenate dehydratase of *Mtb* was performed composing both dimensional 2D-3D structures. The software packages that were used for the inspection and viewing of the receptor-ligand complexes were PyMOL 1.9.1 and Ligplot+v.1.4.5 [47, 54].

Environment of molecular analysis

Computer simulations were performed using the Linux Ubuntu operating system, version 12.04, in a Dell XP58700 computer, intel@Core i7-4770, operating at 3.4GHZ in a total of 12GB of random-access memory (RAM).

Ethical considerations

This project has been sent and duly registered at the Research Committee of the Federal University of the Health Sciences in Porto Alegre (ComPesq), under number 079/2015.

RESULTS

Molecular modelling

The BLAST software package was used to look for homologous sequences of the target enzyme, which have their 3D structure available in PDB databank [27, 31]. The selection criteria used to choose the best model are as follows: identity index, area of coverage, resolution of the structure, E-value, structure complexed with the ligand or modulated through a co-factor (metal). The results of this search are presented in Table 1 below, which also shows the most important parameters in analysis. All the structures have been solved by X-ray crystallography, presenting one or more substrates as a ligand or a co-factor.

In this present study, the crystallographic structure of code PDB 3MWB was identified and then selected as an appropriate template to build an accurate model for prephenate dehydratase of *Mycobacterium tuberculosis*. The structure chosen showed an identity of 38%, an E-value of 3.7 E-43, 4% of Gaps, resolution of 2.00 Å and it is complexed with substrate phenylalanine. The modeler 9v14 software performed the alignment (fig. 1) and the modelling, generating one thousand models for the PDT-PHE complex. Those models were ranked according to the values of the energy function estimated by the program, these being the DOPE-score, the Normalized DOPE-score, molpdf and GA341 [30, 33]. The fig. 2 shows the 3D structure of the best model of prephenate dehydratase of Mtb generated by modeller 9v14.The best model, mphe.909999045.pdb was chosen. It has a DOPE-score of –68241.9, a Normalized DOPE-score of –0.3213, molpdf of 3033.16 and GA341 of 1.0.

To validate the structure and evaluate its stereochemical quality, the model was then analised by Procheck and Verify-3D programs. It is well known that in order to obtain a decent and good model, it is necessary to have at least 90% of the residues in the more favourable regions [28, 33, 34]. The Ramachandran Plot (Fig. 3) shows the distribution of the phi and psi torsion angles for each amino acid, thus

defining those which are in the regions that are energetically more favourable or unfavourable. In the representation shown on the plot, the more favourable regions (A, B, L) are coloured red; other permitted regions (a, b, l, p) are in yellow; regions generously permitted (~a, ~b, ~l, ~p) are in light yellow, and regions not permitted are in white. The current amino acids are represented by black dotted lines. While the statistical analysis of the Ramachandran Plot are represented in table 2. The model showed 93.7% of amino acid residues in the most favourable regions, 5.4% in additional allowed regions, 5.4% in generously allowed region, and no residue in disallowed regions (0%). All the amino acids residues are shown as squares, except for glycines that are represented as triangles. In addition, the amino acid residues Ala24, Met342, Ala344, Val348 and Asp636 are highlighted on the Ramachandran plot for being situated in the flexible regions of loops, and they are not involved in the site of binding of the target macromolecule (fig. 4). This picture shows in detail, the positions of these amino acids and also that of phenylalanine in the respective protein, builded by the PyMOL program. We can also perceive that in the secondary structure of model have 23 α-helix, 26 β-sheet and 51 loops. While the Verify-3D program shows the compatibility of the three-dimensional model (3D) with the sequence of amino acids (1D) of the structure, determining the quality of the chemical environment of each residue in the model and also the level of reliability of the protein folding of the macromolecule [33-34]. It is necessary to have at least 80% of the residues showing a score of 0.2 or greater. In the analysis of this model to chains A and B (fig. 5), it was verified that 90.34% of the residues has a medium 3D-1D score value of 0.2 of more, meaning that it is indeed satisfactory [34].

Preparation of the ligand and construction of the libraries

Based on the knowledge of molecules available on the PDBsum (https://www.ebi.ac.uk/pdbsum/) and PDB (www.rcsb.org/) databanks, it has been possible to draw the phenylalanine molecule and use it as a template, downloaded file in .mol format, in the building of the pharmacophore model using the Molview software package, which is an online tool available for drawing molecules (molview.org/) [31, 35-36]. The fig. 6 showed the 2D-3D structure of phenylalanine.

After build the pharmacophore, a virtual screening was carried out based on the ZINC database (http://zinc.docking.org) in the Zincpharmer server (http://zincpharmer.csb.pitt.edu/pharmer.html), which uses a rapid and wide-scale

search of small molecules that have pharmacophore characteristics similar to those of the original compound. It identifies possible drugs that most likely show good interaction and inhibitory activities over enzyme prephenate dehydratase [37-38]. In the screening against the ZINC database, which currently contains over 35 million compounds deposited and commercially available, we identified a total of 80,008 molecules from the six libraries builded, in sdf format, compliant with the pharmacophore standard of interest. In fig. 7, there are illustrations of the six variations of parameters considering the x, y and z co-ordinates and the radius, for the six pharmacophores models, so seek and generate to the their corresponding libraries.

Molecular docking

To carry out molecular docking, initially was used the template to correctly reproduce the binding mode and also to check the degree of accuracy of the software. After, the molecular docking protocol was validated using simulations of re-docking for the generated model. The method considers the protein to be a rigid structure and the ligand bond rotations as flexible [39-44]. The RMSD was used as a measurement evaluation, being able to describe the quality of a docking simulation, which accepts values below 2 Å. There was also the development of a protocol based on free bonding energy [42]. The Autodock 4.2 software [45-46] present in the PyRx platform was used for the analysis of molecule interaction and the results obtained, both for the template and the generated model were: RMSD of 0.48 Å for the bonding energy of -7.59 kcal/mol, and 0.44 Å for bonding energy of -7.80 kcal/mol, respectively. The table 3 shows the respective values of RMSD for all ten runs, considering the template and model. To carry the standardization and approved of the protocol must be agreement with the values of RMSD and bonding energy, so can to seek the most stable conformation between the ligand and its molecular target [40,43].

All libraries of ligands have been converted into .pdbqt format, consisting of a total of 30.908 compounds, and then docked against the enzyme prephenate dehydratase to generate the respective bonding affinities, through the Autodock 4.2 software package, of PyRx 0.8 [34,45]. The reduction in the size of the library occurs through the presence of isomerism in the compounds, and also detection and discard by exclusion criteria of 2.609 molecules that were duplicated between the six

different libraries. The table 4 shows the results of the one hundred best ligands with good potential to have inhibitory pharmacological action. The estimate of free bonding energy is a result of the sum of other molecular energies (non-bonded + intermolecular + internal + torsional) in which the ligands have been ranked based on their respective docking scores, with the more negative values correspond to higher binding affinity. It means there is a higher possibility of the molecule bond with the respective molecular target [441-44]. We see that the ligands have high binding energy when compared with substrate phenylalanine (-7.8 kcal/mol), ranging between -12.45 and -10.52 kcal/mol. All the docked molecules have been visualized using PyMOL, for inspection and analysis of the results [47].

Subsequently, the selected ligands were subjected to pharmacokinetic and toxicological analysis, to verify the likelihood that the new candidate drug having, or not having, a harmful effect on the human being [50-52].

Pharmacokinetic and toxicological analysis

The results of the analyses of the ADME-Tox properties of one hundred ligands were generated by the FAF-Drugs3 web-server, as shown in Tables 6 and 7. The chemical compounds were subjected to the rules proposed by VEBER, EGAN, Lipinski and Bayer Oral Physchem score to check the quality of oral bioavailability. At the same time that the rules of the GlaxoSmithKline 4/400; those of Pfizer, of 3/75; and the level of phospholipidosis induction are to check how safe and efficient is the profile of the prospective drug [50-51]. Other physical and chemical analyses were also performed: including checking for solubility, flexibility and molecular size [53-54]. In the table 6 and fig. 8, we see that all the ligands exhibiting good conditions of oral Bioavailability for rules of EGAN and VEBER, except for the Oral Physchem score, which showed three poor molecules (with a score of 4), one for a value of 3, and two for the value of 2 (median), as well as 19 with a score of 1 and 66 molecules with a score of zero (ideal value). According to Lipinski's rule, shown in detail in Table 7, 97 compounds were within the parameters, while three did not satisfied the rule: ZINC83411094, ZINC59381777 and ZINC06576259. Based on the 4/400 rule, all the ligands showed good results. In contrast, according to the 3/75 rule only 84 compounds were good, twelve with a warning and four poor. For phospholipidosis, 91 compounds showed no induction, while 9 induced; and with regard to solubility (not shown), 81 were good while 19 showed a meaningful

reduction. In the last assessment, in general, all the molecules were accepted by the FAF-Drugs server for later development or for streamlining of the prototypes.

For a deeper study of the toxicological risk prediction, considering the categories of mutagenic, tumorigenic and irritant and reproductive effects, together with complementary calculations of molecular properties, druglikeness and drugscore, we used the Datawarrior software [52]. In table 8 and fig. 9 are shown some of theses status. In both *in silico* prediction tools, standard values were used for parameters of filtering and molecular analysis, these having been supplied by the software itself. In relation to the ligands, with regard to mutagenesis, 10 were high, low in 1 and absent in 89. While in terms of tumorigenesis, there were 89 compounds with no effect, 10 considered of risk, and 1 of low risk. Last but not least, the irritant effect was absent in 89 molecules, low in three, and with significant increase in the rate in eight molecules.

Analysis of interactions

The ten best structures obtained (fig. 10) were submitted to studies of protein-ligand interaction, using the software package ligplot+v.1.4.5 [54]. The program generated a 2D diagram to each complex based on the ligand binding in the .pdb file of target, in which the respective intermolecular interactions were analysed by hydrogen bonds and by hydrophobic interaction [54]. In addition, PyMOL was also used to show, in 3D, details of the interactions between amino acid residues, in the binding site of enzyme [47]. The fig. 11 shows the 2D schematic diagram of ten ligands complexed with the protein, with their respective bonds and also distance measurements, generated by ligplot [54]. Details of the visualization and analysis of these interactions are showed in ligplot and PyMOL in the fig. 12-21, being puts in summary form by the table 5.

DISCUSSION

The drugs rifampicin, isoniazid, pyrazinamide and ethambutol may not be enough for the treatment and control of tuberculosis. Even though it may be effective in the cure of the disease, the application of this therapy comes up against difficulties regarding the presence of strains that bring bacterial resistance, degree of toxicity, bigotry, and co-infection by HIV. This leads to the need to change the intervention by

adopting second-line drugs in the medication process [9-11,55]. According to Sarkar and Jain & Mondal, second-line drugs are often less efficient, more expensive and more toxic than the previous line, and in this category we can include drugs such as streptomycin, kanamycin, fluoroquinolones, ethionamide, and para-acetyl salicylic acid [12, 56].

This therapeutic procedure has been available to the human population approximately by 60 years [10, 55]. Regarding other infecto-contagious diseases caused by bacteria, this drug stands out for having a total duration period of six months [55-56]. Countless research studies have confirmed the side effects of these antibiotics used against tuberculosis, including gastrointestinal reactions, exanthema, neurological syndrome and, mainly, hepatoxicity [56-60]. The exception is ethambutol, which sometimes causes sight disorders or loss of sight when applied [61-63].

The trend towards technological and scientific advances in areas of drug planning is that of expanding the testing process and the analysis of toxicological risk, as also the quest for simpler options with accessible cost and short term for the treatment of pathologies [18, 19, 56]. In this way, prephenate dehydratase was chosen as a therapeutic target as it is an enzyme that belongs to the chorismate pathway, which is essential for the survival of the pathogen. The pathway is absent in human population, only being shared by bacteria, fungi and plants [20-21, 23]. Depending on the type of organism, there could be PDT in the form of monofunctional or bifunctional protein, being associated with chorismate mutase [20, 23]. In the description of Mtb made by Prakash, PDT and CM showed no activity and association between themselves, being monofunctional proteins. *In vitro* studies on cloning, sequencing and expression of PDT in cells of Escherichia coli, the presence of this enzyme in the genome of Mtb has been confirmed [25, 26]. In the report description up by Vivan, the characterization of the PDT of Mtb was performed through techniques of Small angle X-rays Scattering (SAXS), ultracentrifugation, molecular dichroism and molecular modeling. Theys shows that the protein is like a flattened disk, symmetrical, with the structure of a tetramer when in solution [24]. On the other hand, Prakash characterized the oligomeric structure of the PDT of Mtb as a dimer and the catalytic and regulatory domains as monomers [21, 26]. However, Vivan also determines the three-dimensional structure of the molecule with the software PARMODEL, but the low level of identity (15%) of the built model with

based on the template phenyalanine hydroxylase (PDB ID: 2PHM) did not exhibit significants results. This occurred because, in that time, it did not have protein structures with higher identity in the PDB. Thus, a bad template could lead to errors in structure and also in the folding of the loops, thereby reducing the quality and accuracy of the model as proposed [24, 28, 34]. There is a need for an identity rate of at least 30% so that the model brings ideal conditions for molecular prediction [28, 34]. In comparison with our template, the identity was 38%, satisfying these conditions. Regarding secondary structures, our model consists of 23 α-helix and 26 β-sheet in relation to the model of Vivan (17 α-helix and 18 β-sheet) [24, 25]. Between models, there is a significant difference, in Ramachandran Plot, the residues in most favoured region showed value of 93.7% and 89.6%, while Verify3D profile value was 93.7% and 35.52%.

In this regard and knowing that there are few studies about the enzyme, we used the software modeller to obtain the 3D structure of the prephenate dehydratase of Mtb based on the crystallographic structure 3MWB of the microorganism *Arthobacter aurescens* [30, 33]. The quality of the model showed itself to be good and also ideal for the continuity of the analyses. Supplementary, there was the exploration of mechanisms and characteristics of the phenylalanine bond to build a 3D pharmacophore model and also to generate libraries of small molecules. The choice arose from the fact that PDT is regulated by allosteric activation by Phe, in which low concentrations lead to an increase in enzymatic activity, while there is an evident inhibition at high concentrations [20-21, 23, 26]. In addition, it is already quite evident that the aromatic amino acid brings a change in the conformational state of the protein in its regulatory domain [20, 23]. In results of these studies of molecular docking, the interaction of these compounds with the target macromolecule allowed us to observe the spatial orientation and the bond affinity, shown in kilocalories per mole (kcal/mol). As shown in the previous section, most ligands showed good results of interaction when submitted by FAF-Drugs3 and Datawarrior to evaluate the ADME-Tox profile and, so, can be found aspects of pharmaceutical relevancy. Overall Drug-score ranged from 0.13 to 0.95 and druglikeness of 74.1 to 93.5. The Stacked Column Chart was used in analyzes to obtain a better reproducibility and synthesis of the data provided by the tables 6, 7 and 8 (fig. 8 and fig. 9). Usually, we can see that in the chart approximately 75%, of all ligands, presented good conditions to pharmacological prediction and 80% to prediction of toxicological risk.

Among one hundred ligands analyzed, the top ten compounds were subjected to calculations of intermolecular interaction of complex receptor-ligand with Ligplot. Available in table 5, allows to check the hydrogen bonds and the hydrophobic contacts of the complex, highlighting the frequencies of the most common interactions of the ligands with the molecular target. The presence of hydrophobic contacts, among the ligands, in the residues: Arg231 and Tyr565 have an estimate of 10/10 and Gly223, Gly534, Ile232 and Ile227 of 9/10, whereas Pro533 and Gln532 are of 8/10. For the hydrogen bonds, the Leu225 and Asn531 residues were more common being 7/10, that is, 70 % of these residues bind at the receptor of macromolecule. These values may predict, at degree of probability, which keys residues are generally present and involved in the interaction with the target binding site, being able considered essential in the process of inhibition and molecular recognition. It is also worth emphasize, as part of this analysis, that the ten molecules highlighted included the two promising molecules ZINC69138131 and ZINC28047676, which has been given the name of 1-(1H-benzimidazol-2-yl)-3-[2-(4-methyl-1,3-thiazol-2-yl)ethyl]urea and N-(1H-benzimidazol-2-yl)-2,4-dioxo-1H-pyrimidine-5-sulfonamide by the International Union of Pure and Applied Chemistry (IUPAC). They are derived from benzimidazol and showed potential biological activity and clinical applications. Although these two compounds share benzomidazole as a common ancestor, there are differents peculiarities. The ZINC69138131 has a higher binding affinity, but with reduced solubility, high reproductive effect and a drugscore value of 0.507. While the ZINC28047676 doesn’t have these effects and has a drugscore value of 0.824, being a more ideal value [64]. The drugscore allows to indicate the potential of a compound to become a drug, in which the degree of the estimate is proportional to values close to one [68]. Anyway, both it brings a wide variety of characteristics such as antimicrobial and antiviral activities, antidiabetic effects, anticancer effects, antioxidant effects, antiparasite action, anticonvulsion, anti-inflammatory, anti-hypertension and others applications [64]. Recent studies highlight the effective action of benzomidazole against *Mycobacterium tuberculosis* [67], being another reason to choose the ZINC69138131 and ZINC28047676 can be candidates for inhibition of tuberculosis.

CONCLUSIONS AND PERSPECTIVES

The results obtained in this work shall be very useful to have a better understanding about the structure and the molecular interaction of prephenate dehydratase with different ligands, as well as being a base for future research *in vivo* and *in vitro* related to the development of new prototypes of drugs.

ACKNOLEDGMENT

We thank the Federal University of Health Sciences of Porto Alegre (UFCSPA) and CAPES – Coordination of Improvement of Higher Education Personnel for the master degree scholarship.

REFERENCES

1. WORLD HEALTH ORGANIZATION (2016) Global Tuberculosis Control: report. Geneva: WHO

2. BRASIL. Ministério da Saúde. Secretaria de Vigilância em Saúde. Departamento de Vigilância Epidemiológica (2010) Doenças infecciosas e parasitárias: guia de bolso. 8. ed. rev. Brasília: Ministério da Saúde

3. BRASIL. Ministério da Saúde. Secretaria de Vigilância em Saúde (2014) Guia de Vigilância em Saúde. Volume único. Brasília: Ministério da Saúde

4. Barker RD (2008) Clinical tuberculosis. Medicine. 36(6):300-305

5. Rappuoli R, Aderem A (2011) A 2020 vision for vacines against HIV, tuberculosis and malária. Nature. 473(7348):463-9

6. Raviglione M, Marais B Fau - Floyd K, Floyd K Fau - Lonnroth K et al (2012) Scaling up interventions to achieve global tuberculosis control: progress and new developments. Lancet maio. 379(9829):1902-13

7. Campos HS (2006) Etiopatogenia da tuberculose e formas clínicas. Pulmão. RJ. 15(1):29-35

8. Frieden TR, Sterling Tr Fau - Munsiff SS et al (2003) Tuberculosis. Lancet. 362(9387):887-99

9. BRASIL. Ministério da Saúde. Secretaria de Vigilância em Saúde (2016) Perspectivas brasileiras para o fim da tuberculose como problema de saúde pública. Boletim Epidemiológico, Brasília. 47(13):1-15

10. Di Perri G, Aguilar Marucco D Fau - Mondo A, Mondo A Fau - Gonzalez de Requena D et al (2005) Drug-drug interactions and tolerance in combining antituberculosis and antirretroviral therapy. Expert Opin Drug Saf. 4(5):821-36

11. Arbex MA, Varella MdCL, Siqueira HRd, Mello FAFd (2010) Drogas antituberculose: interações medicamentosas, efeitos adversos e utilização em situações especiais - parte 1: fármacos de primeira linha. Jornal Brasileiro de Pneumologia 36:641-56

12. Jain A, Mondal R (2008) Extensively drug-resistant tuberculosis: current challenges and threats. FEMS Immunol Med Microbiol. 53(2):145-50

13. WILDNER LM, Nogueira CL, SOUZA BS et al (2011) Micobactérias: Epidemiologia e diagnostic. Rev. Patol. Trop., Goiânia. 40(3):227-229

14. Café Oliveira LN, Muniz-Sobrinho JdS, Viana-Magno LA, Oliveira Melo SC, Macho A, Rios-Santos F (2016) Detection of multidrug-resistant *Mycobacterium tuberculosis* strains isolated in Brazil using a multimarker genetic assay for katG and rpoB genes. Brazilian Journal of Infectious Diseases. 20:166-72

15. Velayati AA, Farnia P, Masjedi MR, Ibrahim TA, Tabarsi P, Haroun PRZ, Kuan HO, Ghanavi J, Farnia P, Varahram M (2009) Totally drug-resistant tuberculosis strains: evidence of adaptation at the cellular level. Eur Respir J. England. 34:1202-3

16. Kirby T (2013) Extensively drug-resistant tuberculosis hovers threateningly at Australia's door. Med J Aust. 198(7):355-356

17. Floudas CA, Fung HK, McAllister SR, Monnigmann M, Rajgaria R (2006) Advances in protein structure prediction and de novo protein design: A review. Chemical Engineering Science. 61(3):966-988

18. Amer FA, El-behedy EM, Mohtady HA (2008) New targets for antibacterial agents. Biotechnology and Molecular Biology Reviews. 3(3):046-057

19. Judy E, Choudhary S, Kishore N (2016) Rational drug desin and future directions: Thermodynamic perspective. Austin Biomol Open Acess. 1(1):p. 1003

20. Cotton RGH, Gibson F (1965) The biosynthesis of phenylalanine and tyrosine: enzymes converting chorismic acid into prephenic acid and their relationship to prephenate dehydratase and prephenate dehydrogenase. Biochimica et Biophysica Acta. 100:75-88

21. Prakash P, Pathak N, Hasnain SE (2005) pheA (Rv3838c) of *Mycobacterium tuberculosis* encodes an allosterically regulated monofunctional prephenate dehydratase that requires both catalytic and regulatory domains for optimum activity. J Biol Chem. 280(21):20666-71. doi: 10.1074/jbc.M502107200

22. Cho MH, Corea OR, Yang H, Bedgar DL, Laskar DD, Anterola AM, et al (2007) Phenylalanine biosynthesis in Arabidopsis thaliana. Identification and characterization of arogenate dehydratases. J Biol Chem. 282(42):30827-35. doi: 10.1074/jbc.M702662200

23. Shin MH, Ku HK, Song JS, Choi S, Son SY, Yang HJ, et al (2014) X-ray structure of prephenate dehydratase from Streptococcus mutans. J Microbiol. 52(6):490-5. doi: 10.1007/s12275-014-3645-8

24. Vivan AL, Caceres RA, Abrego JR, Borges JC, Ruggiero Neto J, Ramos CH, et al (2008) Structural studies of prephenate dehydratase from *Mycobacterium tuberculosis* H37Rv by SAXS, ultracentrifugation, and computational analysis. Proteins. 72(4):1352-62. doi: 10.1002/prot.22034

25. Vivan AL, Dias MV, Schneider CZ, de Azevedo WF, Jr., Basso LA, Santos DS (2006) Crystallization and preliminary X-ray diffraction analysis of prephenate dehydratase from *Mycobacterium tuberculosis* H37Rv. Acta Crystallogr Sect F Struct Biol Cryst Commun. 62(4):357-60. doi: 10.1107/s1744309106006385

26. Prakash P, Aruna B, Sardesai AA, Hasnain SE (2005) Purified recombinant hypothetical protein coded by open reading frame Rv1885c of *Mycobacterium tuberculosis* exhibits a monofunctional AroQ class of periplasmic chorismate mutase activity. J Biol Chem. 280(20):19641-8. doi: 10.1074/jbc.M413026200

27. NCBI Resource Coordinators (2016). Database resources of the National Center for Biotechnology Information. Nucleic Acids Research. 44(Database issue), D7–D19. http://doi.org/10.1093/nar/gkv1290

28. Calixto PHM (2013) Aspectos gerais sobre a modelagem comparative de proteínas. Ciência Equatorial. 3(1):9-16

29. Pimentel AS, Guimarães CRW, Miller Y (2013) Molecular Modeling: Advancements and Applications. Journal of Chemistry. 2013:2. doi: 10.1155/2013/875478

30. Sali A, Blundell TL (1993) Comparative protein modeling by satisfaction of spatial restraints. J Mol Biol. 234(3):779-815

31. H.M. Berman, J. Westbrook, Z. Feng, G. Gilliland, T.N. Bhat, H. Weissig, I.N. Shindyalov, P.E. Bourne (2000) The Protein Data Bank Nucleic Acids Research. 28:235-242

32. Guex N, Peitsch MC (1997) SWISS-MODEL and the Swiss-Pdb Viewer: an environment for comparative protein modeling. Electrophoresis. 18(15):2714-23

33. Eswar, N., Webb, B., Marti-Renom, M. A., Madhusudhan, M., Eramian, D., Shen, M.-y., Pieper, U. and Sali, A (2006) Comparative Protein Structure Modeling Using Modeller. Current Protocols in Bioinformatics. 15:5.6:5.6.1–5.6.30

34. Forster MJ (2002) Molecular modelling in structural biology. Micron. 33(4):365-84

35. De Beer TA, Berka K, Thornton JM, Laskowski RA (2014) PDBsum additions. Nucleic Acids Research. 42(D1):D292-D296

36. Laskowski RA (2009) PDBsum new things. Nucleic Acids Res. 37:D355-9

37. Koes DR, Camacho CJ (2012) ZINCPharmer: pharmacophore search of the ZINC database. Nucleic Acids Res. 40(Web Server issue):W409-14. doi: 10.1093/nar/gks378

38. Koes DR, Pabon NA, Deng X, Phillips MA, Camacho CJ (2015) A Teach-Discover-Treat Application of ZincPharmer: An Online Interactive Pharmacophore Modeling and Virtual Screening Tool. PLoS One. 10(8):e0134697. doi: 10.1371/journal.pone.0134697

39. Guedes IA, de Magalhães CS, Dardenne LE (2014) Receptor–ligand molecular docking. Biophysical Reviews. 6(1):75-87. doi: 10.1007/s12551-013-0130-2

40. Hernández-Santoyo A, Tenorio-Barajas AY, Altuzar V, Vivanco-Cid H, Mendoza-Barrera C (2013) Protein-Protein and Protein-Ligand Docking. Protein Engineering – Technology and Application, Dr. Tomoshisa Ogawa, InTech, DOI: 10.5772/56376

41. Kitchen DB, Decornez H, Furr JR, Bajorath J (2004) Docking and scoring in virtual screening for drug discovery: methods and applications. Nat Rev Drug Discov. 3(11):935-49. doi: 10.1038/nrd1549

42. Meng XY, Zhang HX, Mezei M, Cui M (2011) Molecular docking: a powerful approach for structure-based drug discovery. Curr Comput Aided Drug Des. 7(2):146-57

43. Zoete V, Grosdidier A, Michielin O (2009) Docking, virtual high throughput screening and in silico fragment-based drug design. J Cell Mol Med. 13(2):238-48

44. Dallakyan S, Olson AJ (2015) Small-molecule library screening by docking with PyRx. Methods Mol Biol. 1263:243-50. doi: 10.1007/978-1-4939-2269-7_19

45. Morris GM, Goodsell DS, Halliday RS, Huey R, Hart WE, Belew RK, Olson AJ (1998) Automated Docking Using a Lamarckian Genetic Algorithm and and Empirical Binding Free Energy Function J. Computational Chemistry. 1998(19):1639-1662

46. Morris GM, Huey R, Lindstrom W, Sanner MF, Belew RK, Goodsell DS, Olson AJ (2009) Autodock4 and AutoDockTools4: automated docking with selective receptor flexiblity. J. Computational Chemistry. (16):2785-91

47. Schrödinger LLC The PyMOL Molecular Graphics System, Version 1.8. https://www.pymol.org/citing

48. Pettersen EF, Goddard TD, Huang CC, Couch GS, Greenblatt DM, Meng EC, Ferrin TE (2004) UCSF Chimera—a visualization system for exploratory research and analysis. Journal of computational chemistry 25(13):1605–1612

49. Humphrey W, Dalke A, Schulten K (1996) VMD: Visual Molecular Dynamics. J Mol Graph. 14(1):33-8, 27-8

50. Lagorce D, Sperandio O, Baell JB, Miteva MA, & Villoutreix BO (2015) FAF-Drugs3: a web server for compound property calculation and chemical library design. Nucleic Acids Research. 43(Web Server issue):W200–W207

51. Miteva MA, Violas S, Montes M, Gomez D, Tuffery P, & Villoutreix, BO (2006) FAF-Drugs: free ADME/tox filtering of compound collections. Nucleic Acids Research. 34(Web Server issue):W738–W744

52. Sander T, Freyss JF, Rufener C et al (2015) DataWarrior: An Open-Source Program For Chemistry Aware Data Visualization And Analysis. Journal of Chemical Information and Modeling. 55(2):460-473

53. Hou T, Xu X (2004) Recent development and application of virtual screening in drug discovery: an overview. Curr Pharm Des. 10(9):1011-33

54. Laskowski RA, Swindells MB (2011) LigPlot+: multiple ligand-protein interaction diagrams for drug discovery. J Chem Inf Model. 51(10):2778-86. doi: 10.1021/ci200227u

55. Horsburgh CRJ, Barry CEI, Lange C (2015) Treatment of Tuberculosis. New England Journal of Medicine. 373(22):2149-60. doi:10.1056/NEJMra1413919

56. Sarkar S, Ganguly A, Sunwoo HH (2016) Current Overview of Anti-Tuberculosis Drugs: Metabolism and Toxicities. Mycobact Dis 6:209. doi:10.4172/2161-1068.1000209

57. Araújo-Mariz C, Lopes E P, Acioli-Santos B, Maruza M, Montarroyos UR, Ximenes RA Albuquerque, M. de F. P. M (2016). Hepatotoxicity during Treatment for Tuberculosis in People Living with HIV/AIDS. PLoS ONE, 11(6), e0157725. http://doi.org/10.1371/journal.pone.0157725

58. Lee CM, Lee SS, Lee JM et al (2016). Early monitoring for detection of antituberculous drug-induced hepatotoxicity. The Korean Journal of Internal Medicine. 31(1):65–72. http://doi.org/10.3904/kjim.2016.31.1.65

59. CUSACK, R. P. et al. Predictors of hepatotoxicity among patients treated with antituberculous medication. Qjm, pii: hcw160, 2016. ISSN 1460-2393

60. Lima, MFSM, Heloísa RL (2012) Hepatotoxicity induced by antituberculosis drugs among patients coinfected with HIV and tuberculosis. Cadernos de Saúde Pública. 28(4):698-708

61. Levy M, Rigaudiere FF, Lauzanne AF et al (2015) Ethambutol-related impaired visual function in childrens less than 5 years of age treated for a mycobacterial infection: diagnosis and evolution. Pediatr Infect Dis J. 34(4):346-50

62. Huang SP, Chien JY, TSAI RK (2015) Ethambutol induces impaired autophagic flux and apoptosis in the rat retina. Dis Model Mech. 8(8):977-87

63. Mustak H, Rogers G, Cook C (2013) Ethambutol induced toxic optic neuropathy in HIV positive patients. Int J Ophthalmol. 6:542-5

64. Singh N, Pandurangan A, Rana K, Anand P, Ahmad A, and Tiwari AK (2012) Benzimidazole: a short review of their antimicrobial activities. International Current Pharmaceutical Journal. 1(5):119–127

65. BENTLEY, R.; HASLAM, E (1990) The Shikimate Pathway-A Metabolic Tree with Many Branche. Critical reviews in biochemistry and molecular biology. 25(5): 307-384

66. Forli S, Huey R, Pique ME, Sanner MF, Goodsell DS, Olson AJ (2016) Computational protein-ligand docking and virtual drug screening with the AutoDock suite. Nat Protoc. 11(5):905-19. doi: 10.1038/nprot.2016.051

67. Gong Y, Somersan KS, Guo X et al (2014) Benzimidazole-based compounds kill *Mycobacterium tuberculosis*. Eur J Med Chem. 21;75:336-53. doi: 10.1016/j.ejmech.2014.01.039

68. Velec HFC, Gohlke H, Klebe G. (2005) DrugScore(CSD)-knowledge-based scoring function derived from small molecule crystal data with superior recognition rate of near-native ligand poses and better affinity prediction. J Med Chem. 48(20):6296-6303

FIGURES

Fig. 1 Sequence alignment of the prephenate dehydratase from *Mycobacterium tuberculosis* with its homologous 3MWB, performed by modeler 9v.14. (*) are conserved residues

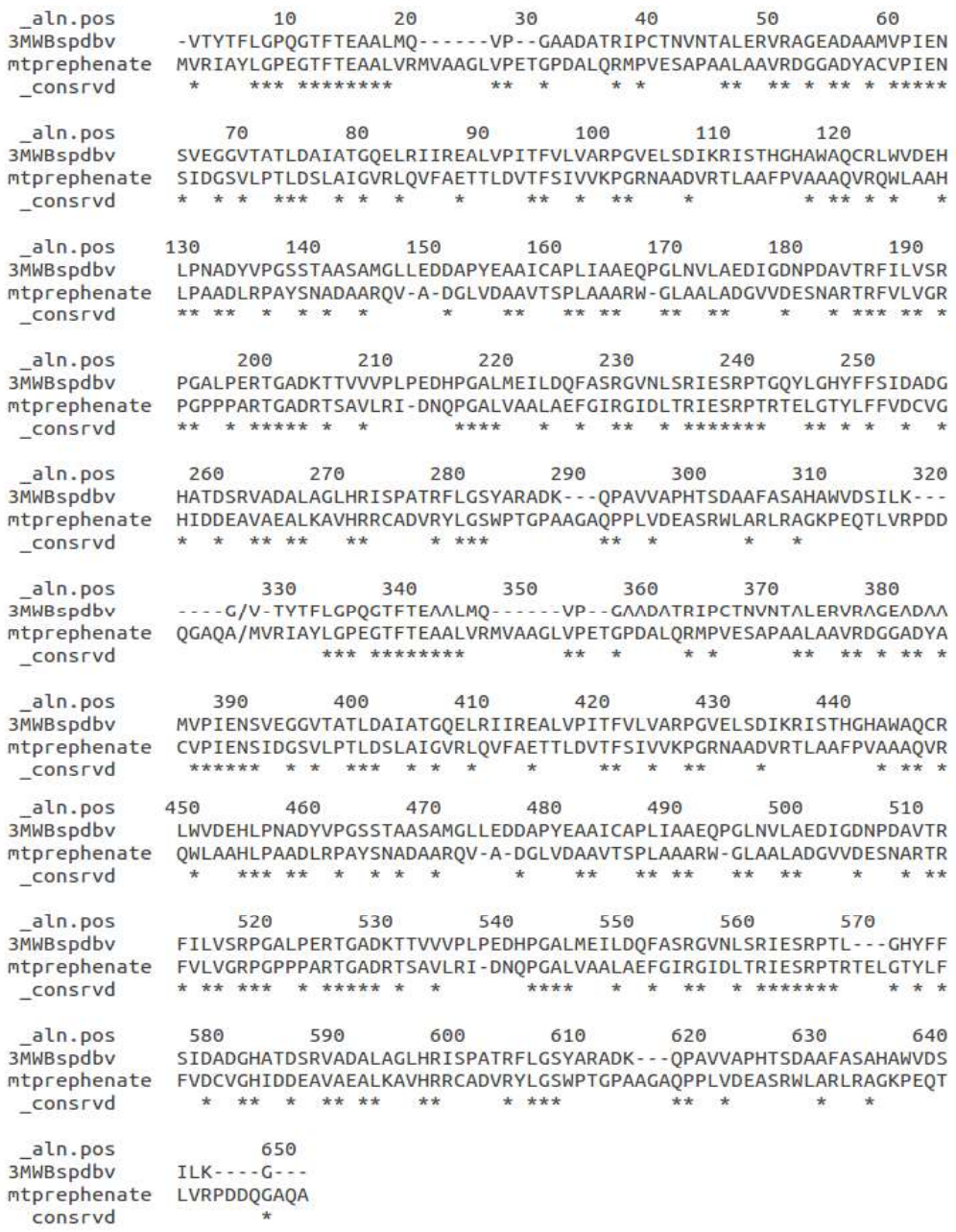

Fig. 2 Structure of the prephenate dehydratase model generated by software package modeler 9v.14, based on crystallographic structure (PDB 3MWB). The figures (A and B) were generated in PyMOL, with the residue of amino acids being shown in cartoons and inhibitors phenylalanine in sticks

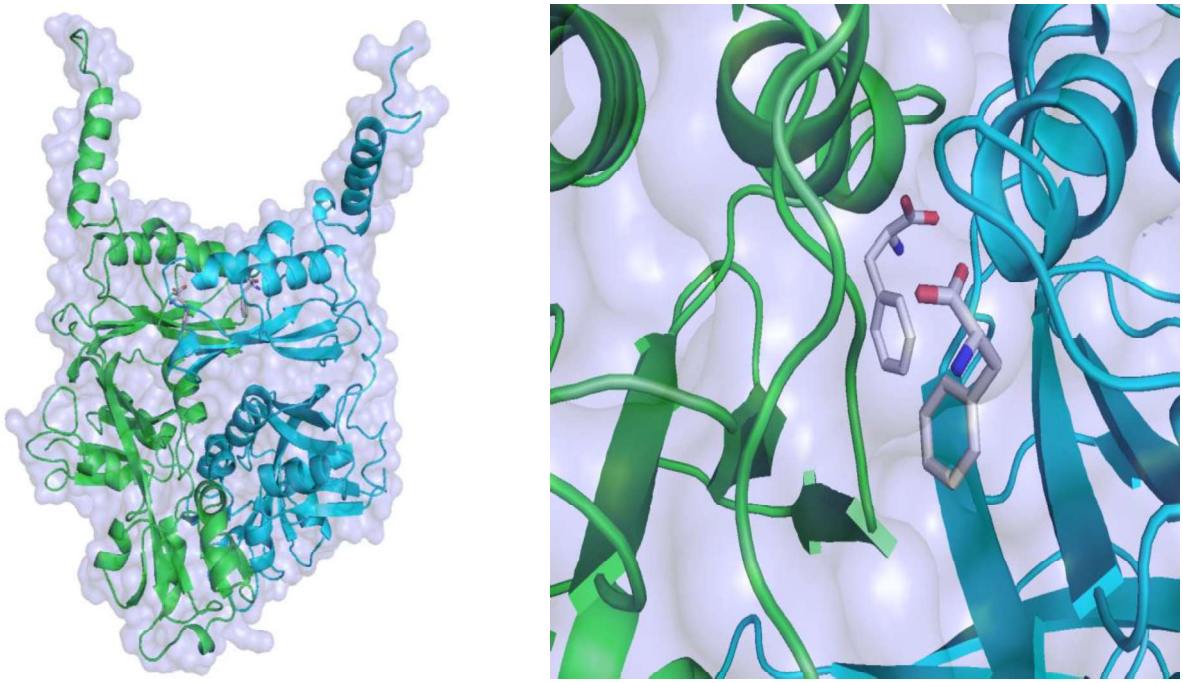

Fig. 3 Ramachandran Plot for each residue that makes up the prephenate dehydratase enzyme for *Mycobacterium tuberculosis*, generated with the Procheck of Swiss-model workspace server. This model was builded by modeller 9v.14 based on model 3MWB

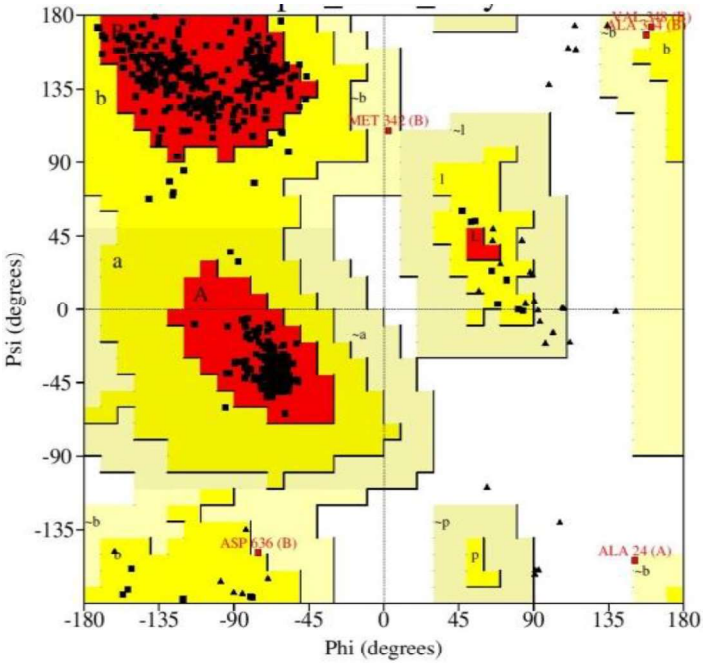

Fig. 4 Structure of the prephenate dehydratase model generated by software package modeler 9v.14, based on crystallographic structure (PDB 3MWB). This figure was generated in PyMOL

It is show the amino acid residues Asp636, Ala24, Met342, Ala344 and Val348, highlighted on the Ramachandran plot. They are situated in the flexible regions of the loops, so are not involved in the site of binding of the target macromolecule

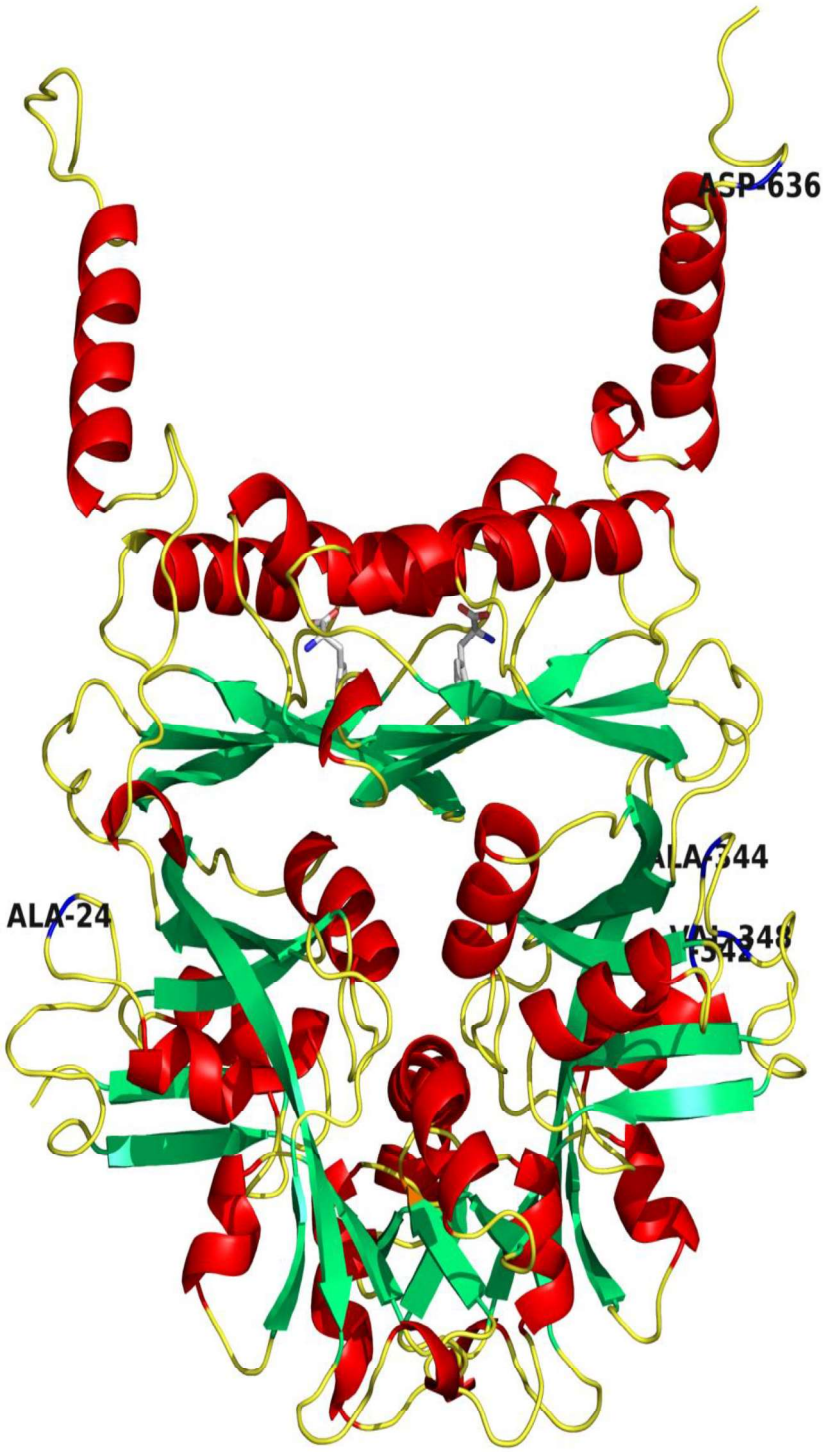

Fig. 5 Verify3D plot results for chain A and B for model. The vertical axis represents the average 3D-1D profile score and horizontal axis to residue number

Chain A

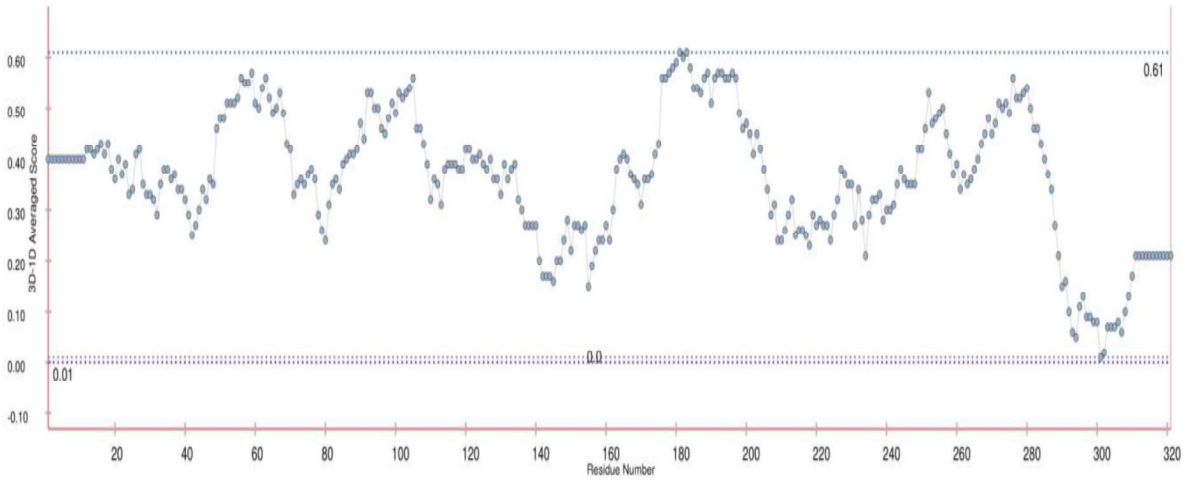

Chain B

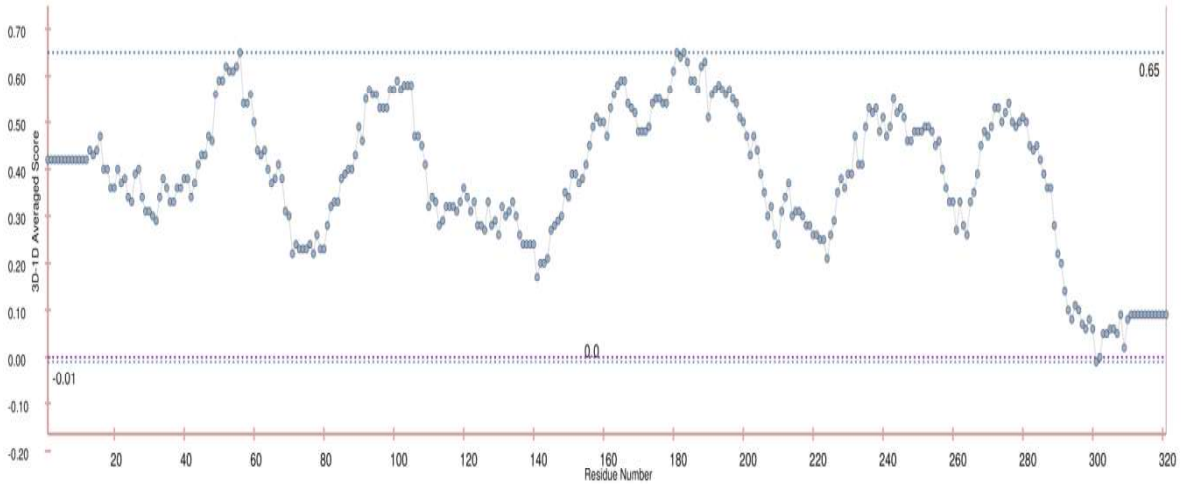

Fig. 6 Schematic representation in 2D and 3D of the known phenylalanine structure, where there has been structural changes through substitution and addition of oxygen atoms to the construction of the pharmacophore, in order to expand the search for compounds, but without losing the active ingredient of the original molecule

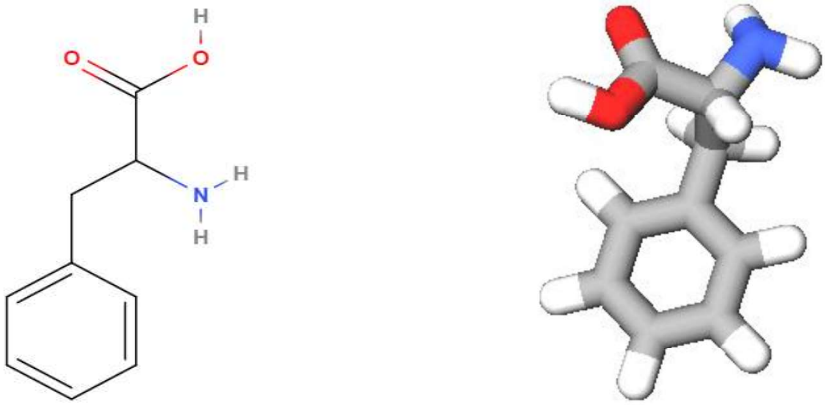

Fig. 7 Structure and parameters used in the six pharmacophore as a models for the construction of libraries of ligands in .sdf format, through Zincpharmer: 10,994 compounds for library 1 (a), 464 compounds for library 2 (b), 15,555 compounds for library 3 (c), 429 compounds for library 4 (d), 20,082 compounds for library 5 (e), and 32,484 compounds for library 6 (f)

In this picture, we show hydrophobicity in green, the aromatics in red, hydrogen donors in white, and the acceptors in yellow

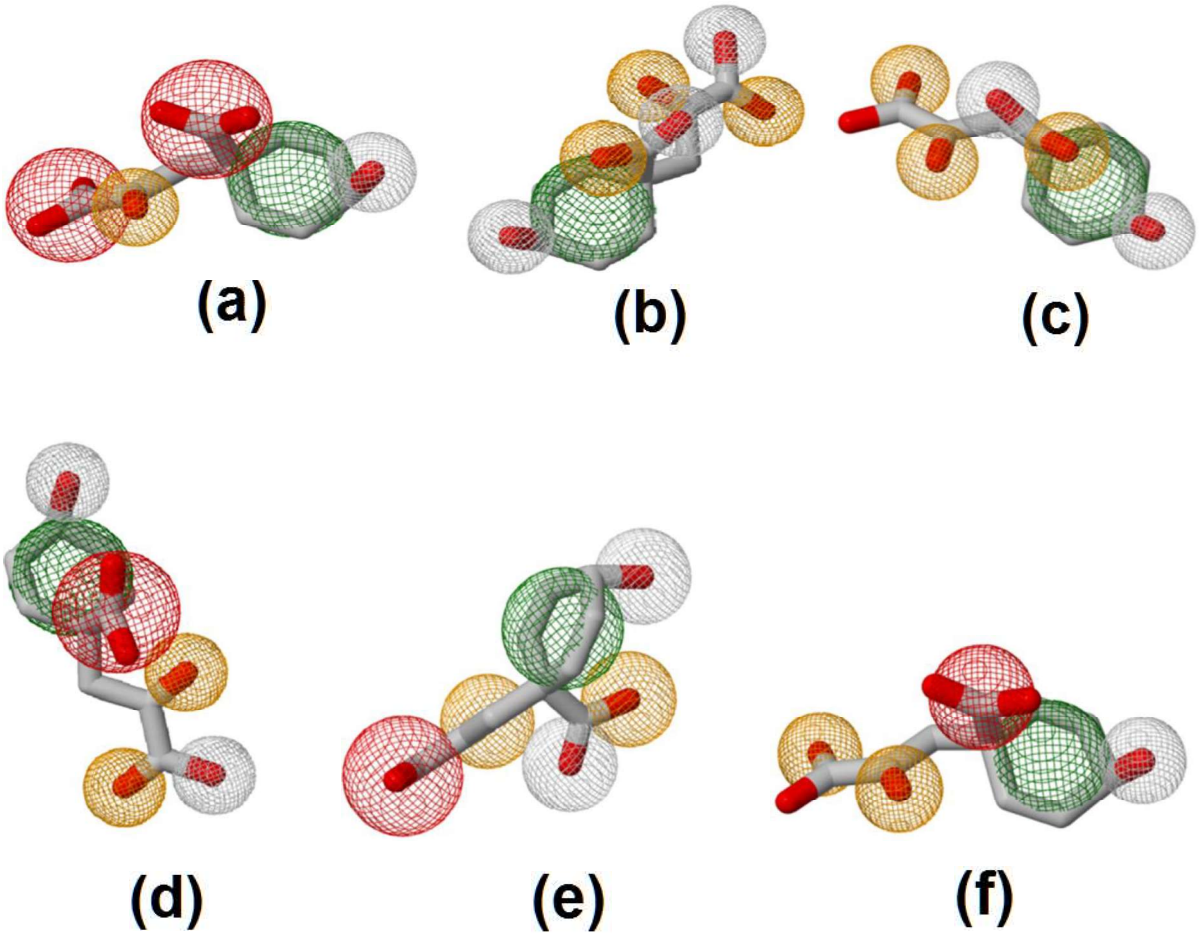

Fig. 8 Stacked Column Chart show the percentage of each rule applied to one hundred chemical compounds, based on analyses of the ADME-Tox properties by the FAF-Drugs3 web-server

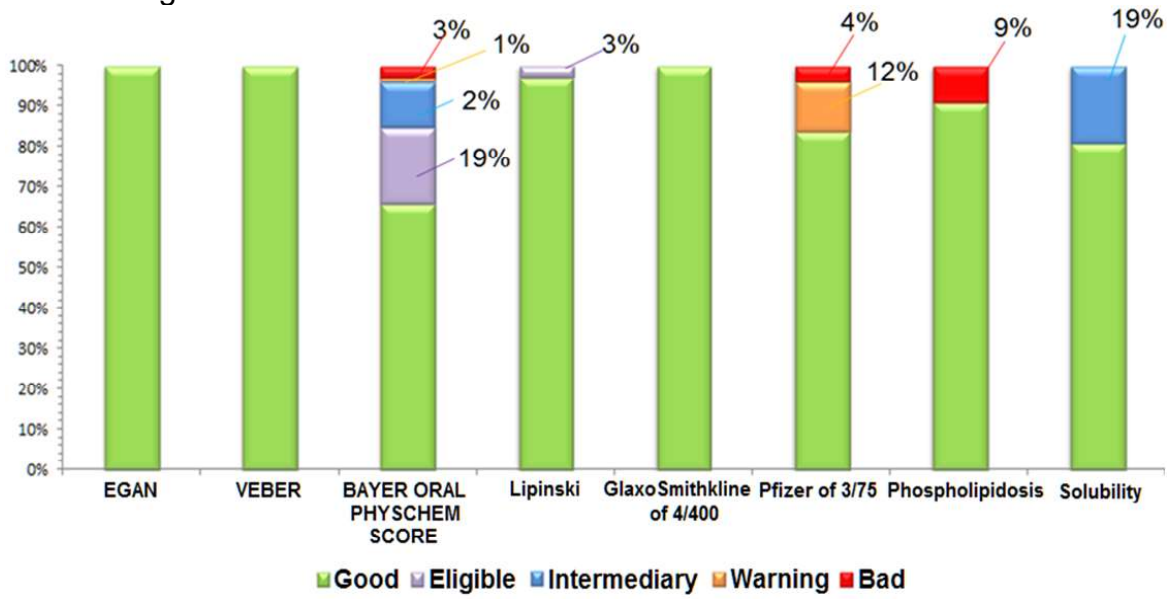

Fig. 9 Stacked Column Chart show the results of percentage of toxic profiles (Mutagenic, Tumorigenic, Reproductive Effective and Irritant) to one hundred chemical compounds, based on DataWarrior software. For each isolated case, can be observerd that 80% of the ligands showing good results

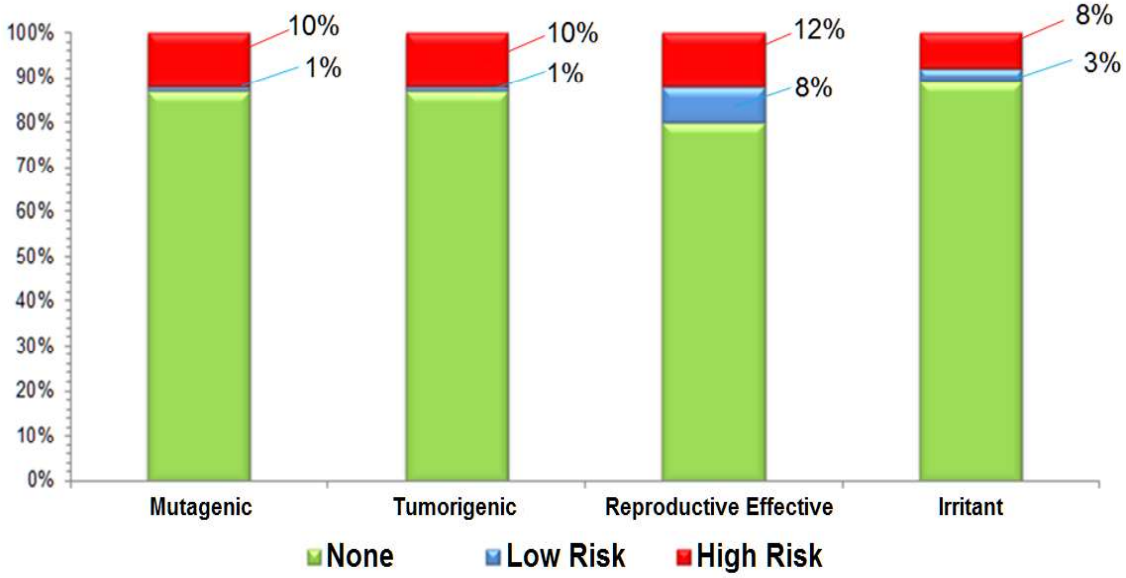

Fig. 10 Visualization of the ten best binders with higher binding affinity. The pictures, in sticks, were drawn using UCSF Chimera

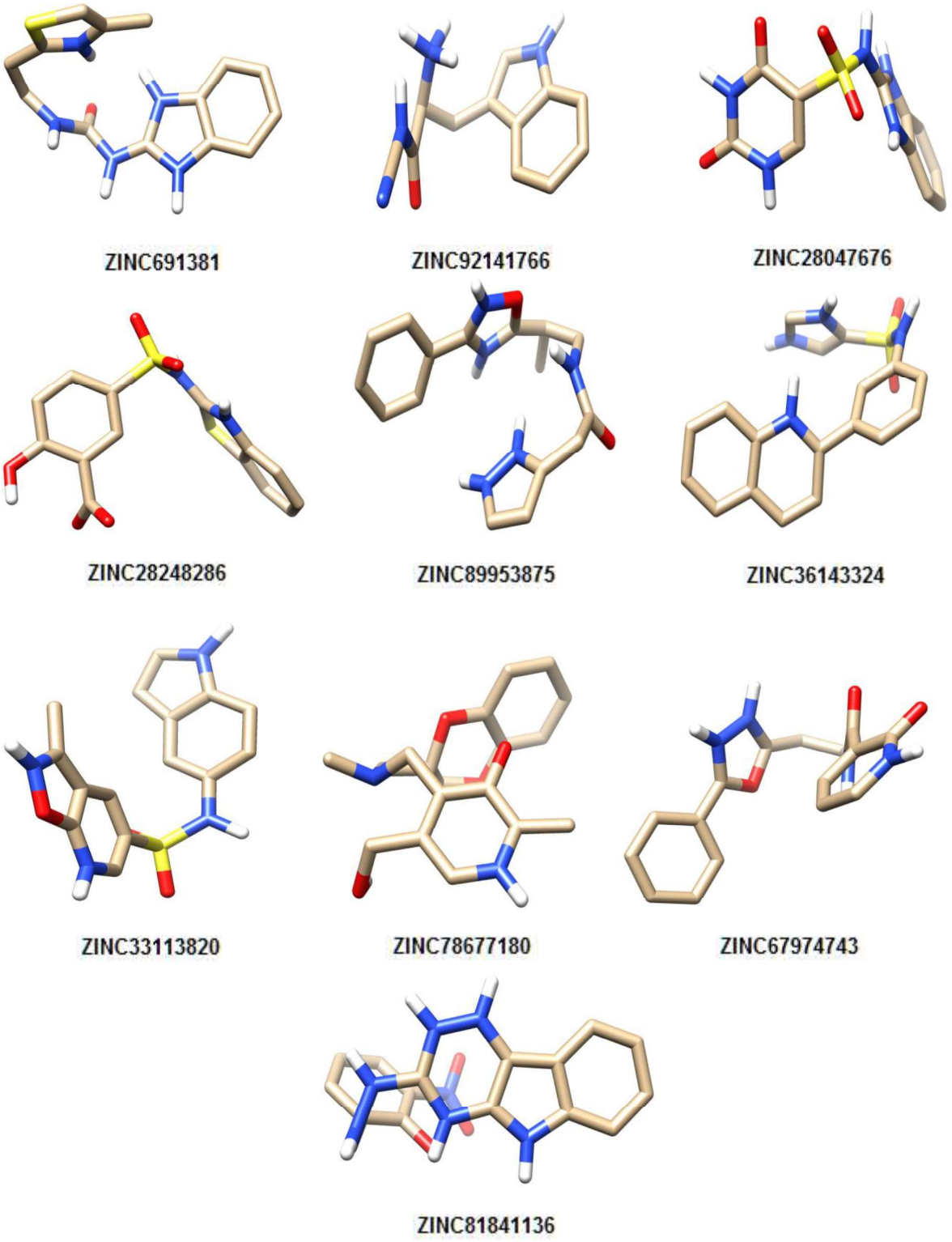

Fig. 11 Ligplot diagram for the ten ligands and their respective interactions with enzyme prephenate dehydratase

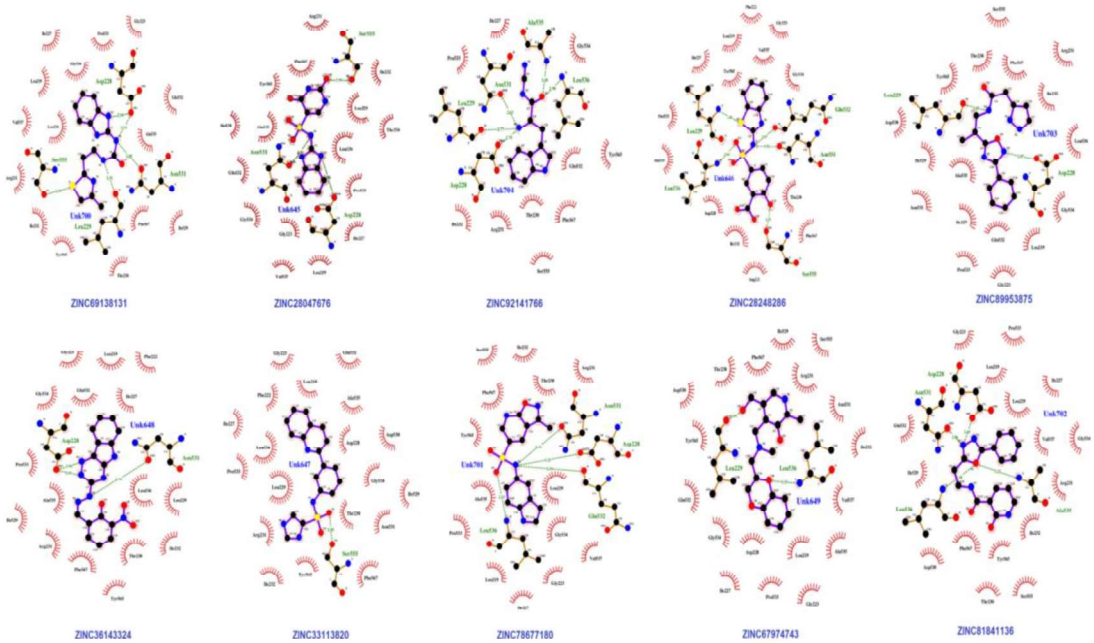

Fig. 12 Schematic representation of binding interactions in 2D and 3D of ZINC69138131, showing intermolecular interactions of ligand with the binding site of the target protein. The figures were generated with ligplot and PyMOL

In the illustration below : In ligplot are expressed how oxygen atoms (in red); carbon atoms (black); nitrogen atoms (blue); hydrogen bonds (green dotted lines with measurements of the respective radii); bonds between the atoms of the ligand (in lilac); connections between the enzyme atoms (in orange) and hydrophobic contacts (red semicircles). And in PyMOL the hydrogen bonds are shown in yellow dotted lines and the hydrophobic contacts in balls

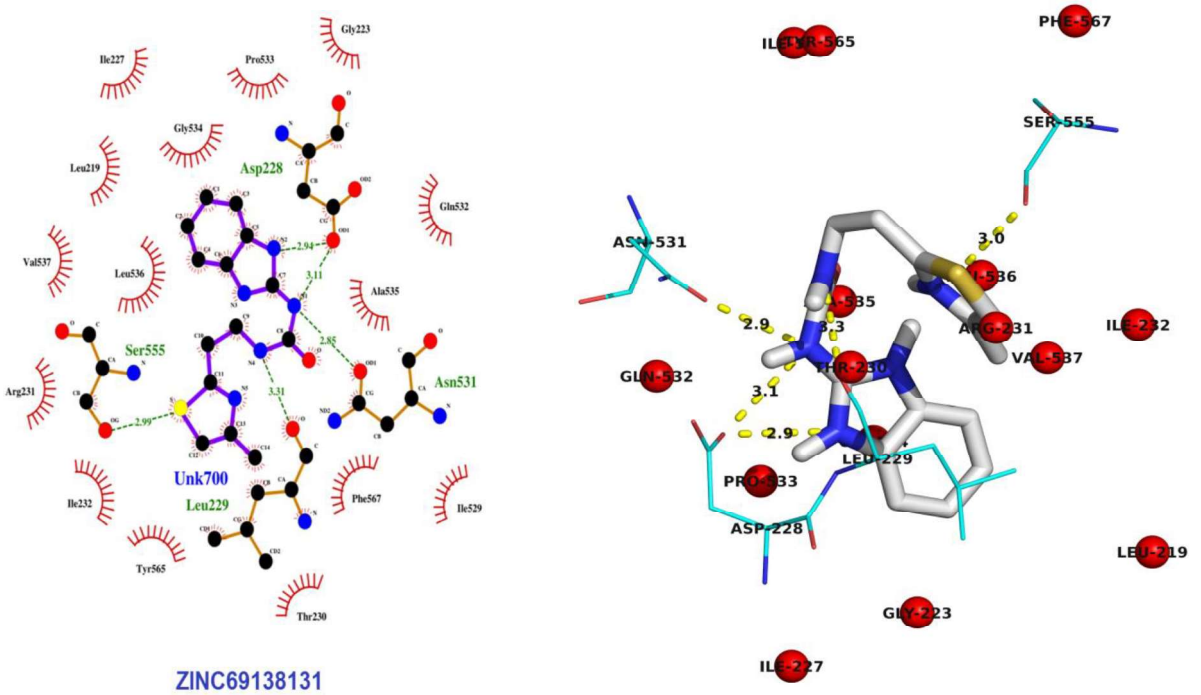

Fig. 13 Schematic representation of binding interactions in 2D and 3D of ZINC92141766, showing intermolecular interactions of ligand with the binding site of the target protein. The figures were generated with ligplot and PyMOL

In the illustration below : In ligplot are expressed how oxygen atoms (in red); carbon atoms (black); nitrogen atoms (blue); hydrogen bonds (green dotted lines with measurements of the respective radii); bonds between the atoms of the ligand (in lilac); connections between the enzyme atoms (in orange) and hydrophobic contacts (red semicircles). And in PyMOL the hydrogen bonds are shown in yellow dotted lines and the hydrophobic contacts in balls

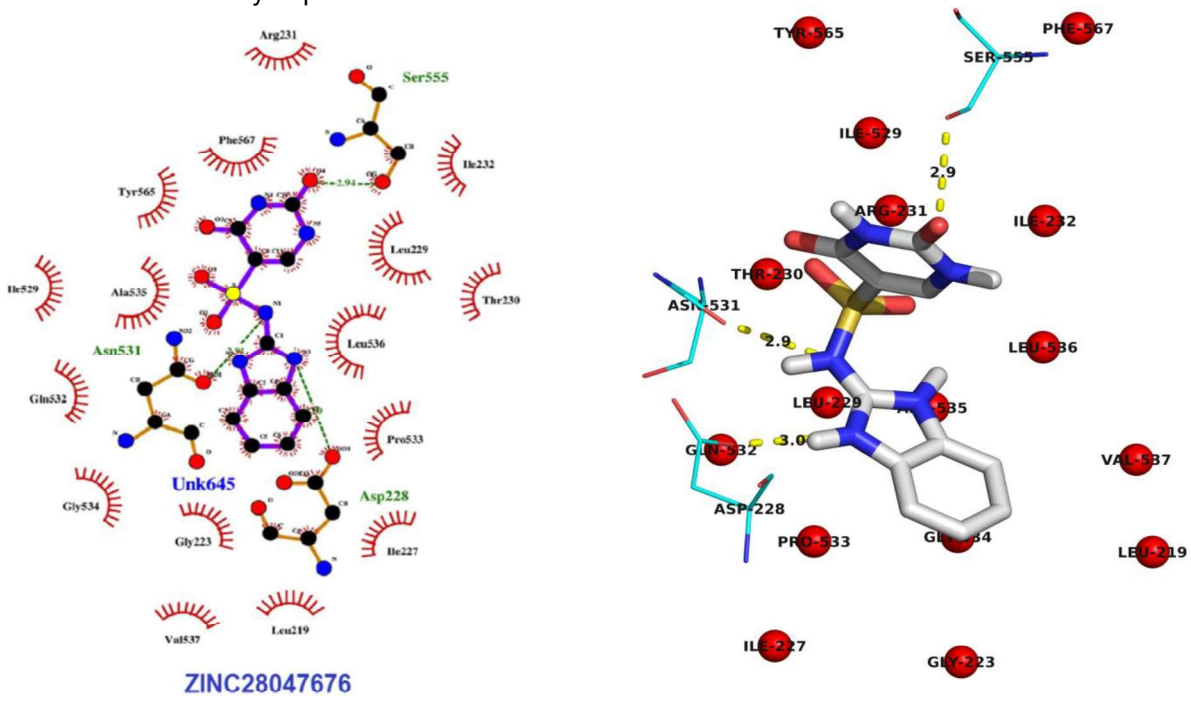

Fig. 14 Schematic representation of binding interactions in 2D and 3D of ZINC2804766, showing intermolecular interactions of ligand with the binding site of the target protein. The figures were generated with ligplot and PyMOL

In the illustration below: In ligplot are expressed how oxygen atoms (in red); carbon atoms (black); nitrogen atoms (blue); hydrogen bonds (green dotted lines with measurements of the respective radii); bonds between the atoms of the ligand (in lilac); connections between the enzyme atoms (in orange) and hydrophobic contacts (red semicircles). And in PyMOL the hydrogen bonds are shown in yellow dotted lines and the hydrophobic contacts in balls

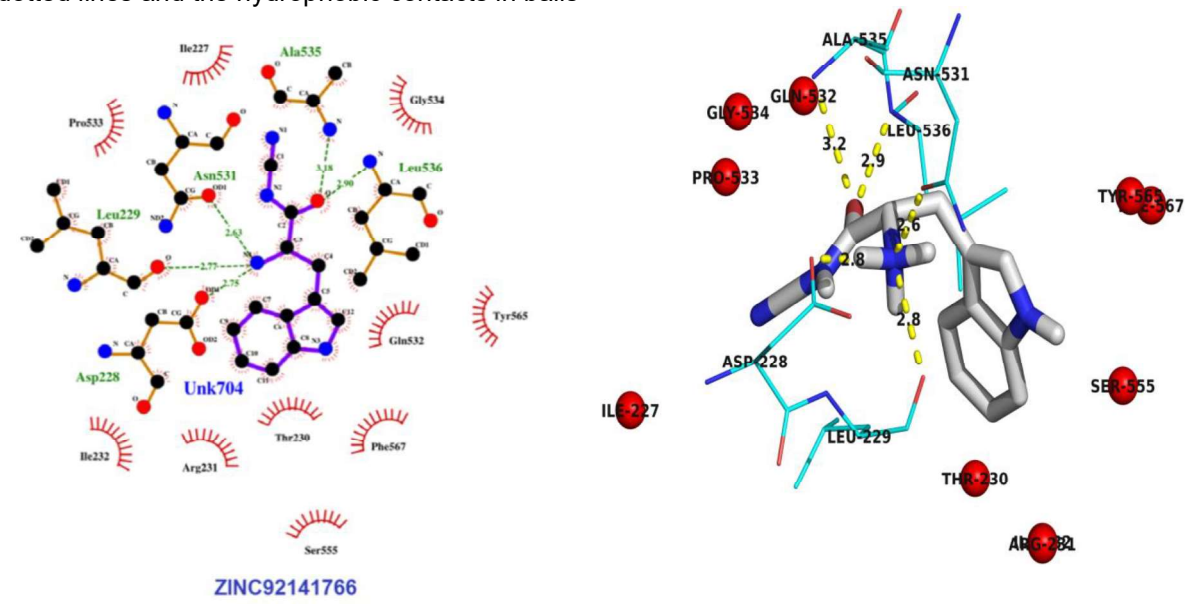

Fig. 15 Schematic representation of binding interactions in 2D and 3D of ZINC28248286, showing intermolecular interactions of ligand with the binding site of the target protein. The figures were generated with ligplot and PyMOL

In the illustration below: In ligplot are expressed how oxygen atoms (in red); carbon atoms (black); nitrogen atoms (blue); hydrogen bonds (green dotted lines with measurements of the respective radii); bonds between the atoms of the ligand (in lilac); connections between the enzyme atoms (in orange) and hydrophobic contacts (red semicircles). And in PyMOL the hydrogen bonds are shown in yellow dotted lines and the hydrophobic contacts in balls

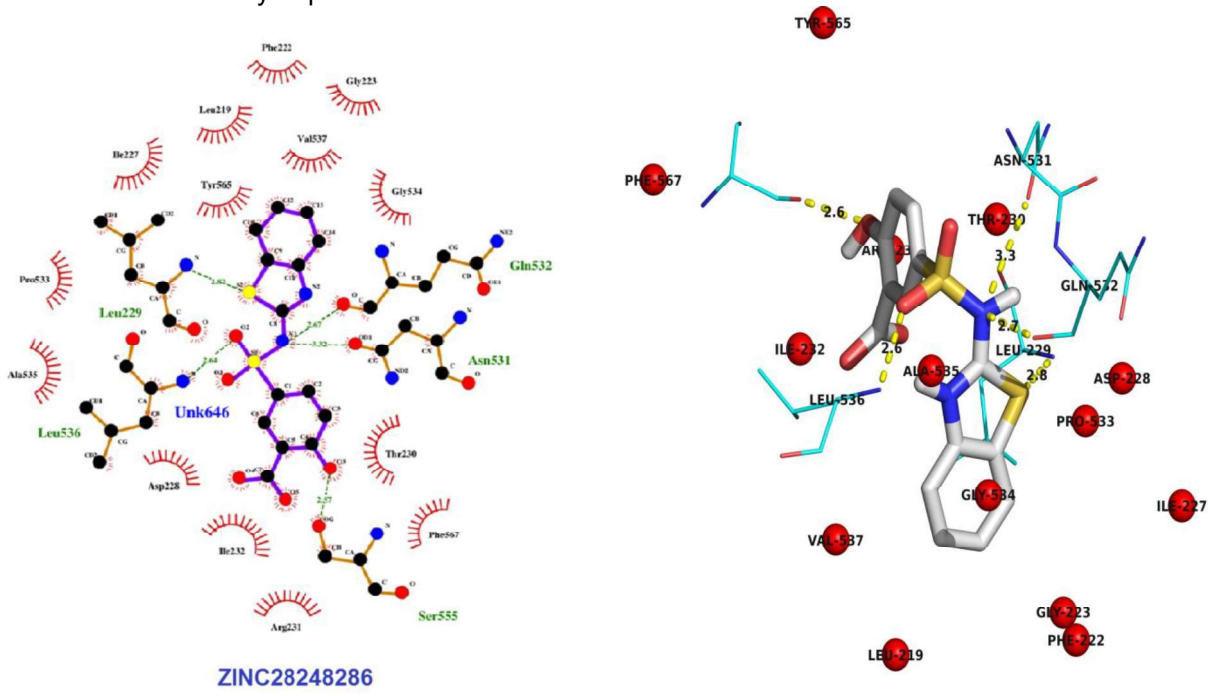

Fig. 16 Schematic representation of binding interactions in 2D and 3D of ZINC89953875, showing intermolecular interactions of ligand with the binding site of the target protein. The figures were generated with ligplot and PyMOL

In the illustration below: In ligplot are expressed how oxygen atoms (in red); carbon atoms (black); nitrogen atoms (blue); hydrogen bonds (green dotted lines with measurements of the respective radii); bonds between the atoms of the ligand (in lilac); connections between the enzyme atoms (in orange) and hydrophobic contacts (red semicircles). And in PyMOL the hydrogen bonds are shown in yellow dotted lines and the hydrophobic contacts in balls

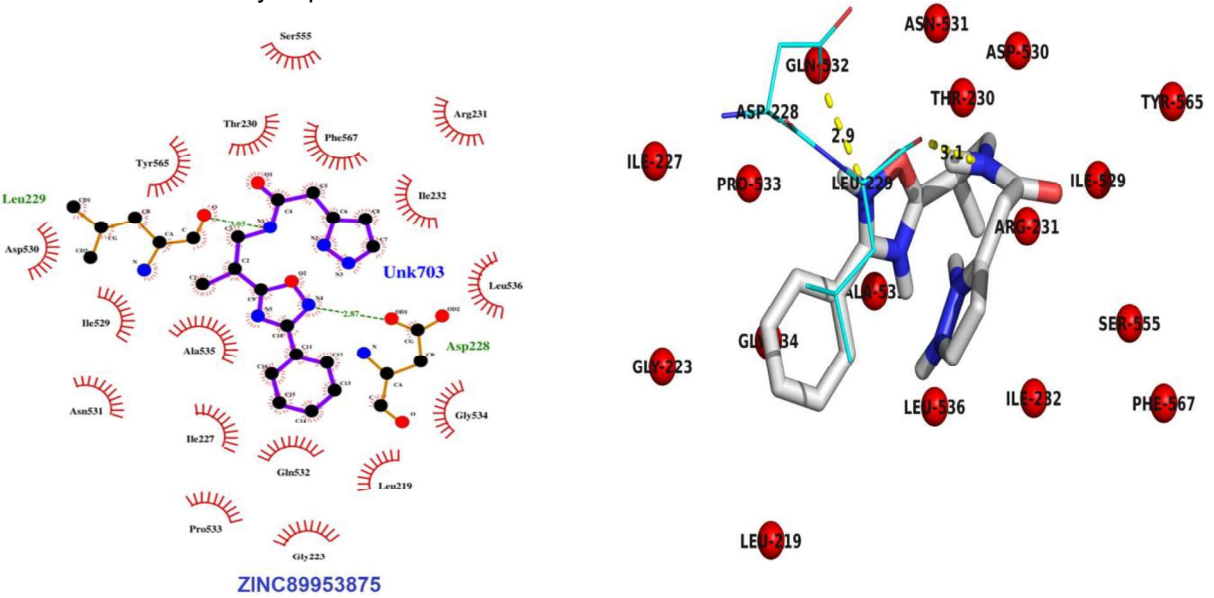

Fig. 17 Schematic representation of binding interactions in 2D and 3D of ZINC36143324, showing intermolecular interactions of ligand with the binding site of the target protein. The figures were generated with ligplot and PyMOL

In the illustration below: In ligplot are expressed how oxygen atoms (in red); carbon atoms (black); nitrogen atoms (blue); hydrogen bonds (green dotted lines with measurements of the respective radii); bonds between the atoms of the ligand (in lilac); connections between the enzyme atoms (in orange) and hydrophobic contacts (red semicircles). And in PyMOL the hydrogen bonds are shown in yellow dotted lines and the hydrophobic contacts in balls

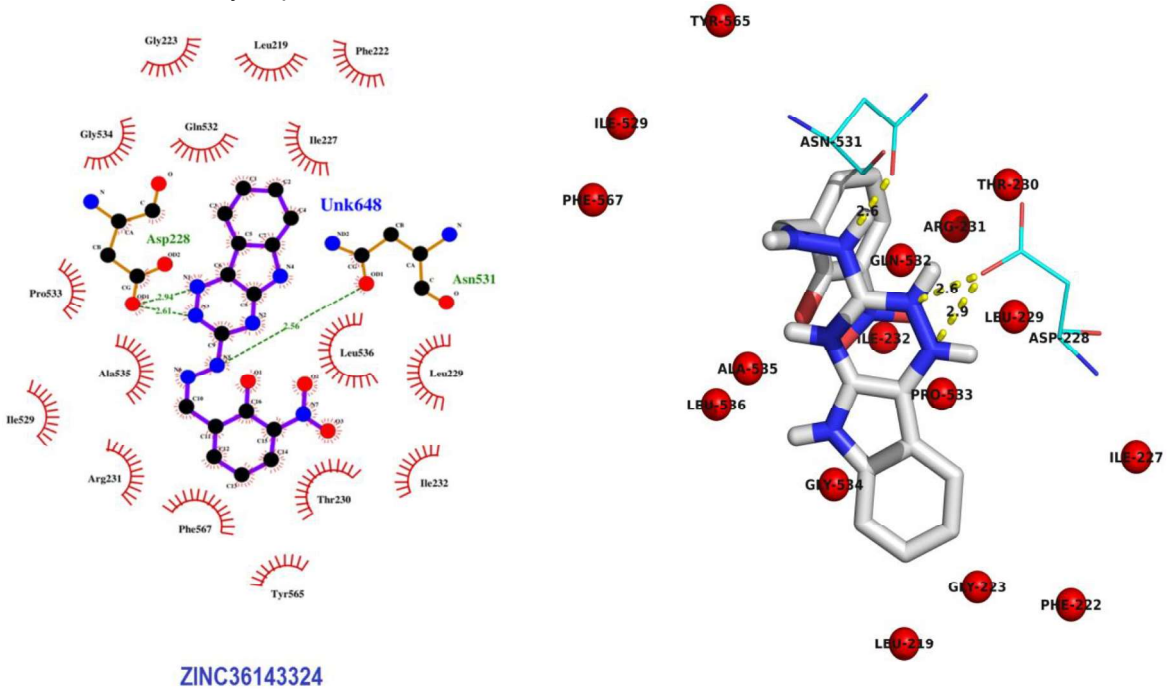

Fig. 18 Schematic representation of binding interactions in 2D and 3D of ZINC33113820, showing intermolecular interactions of ligand with the binding site of the target protein. The figures were generated with ligplot and PyMOL

In the illustration below: In ligplot are expressed how oxygen atoms (in red); carbon atoms (black); nitrogen atoms (blue); hydrogen bonds (green dotted lines with measurements of the respective radii); bonds between the atoms of the ligand (in lilac); connections between the enzyme atoms (in orange) and hydrophobic contacts (red semicircles). And in PyMOL the hydrogen bonds are shown in yellow dotted lines and the hydrophobic contacts in balls

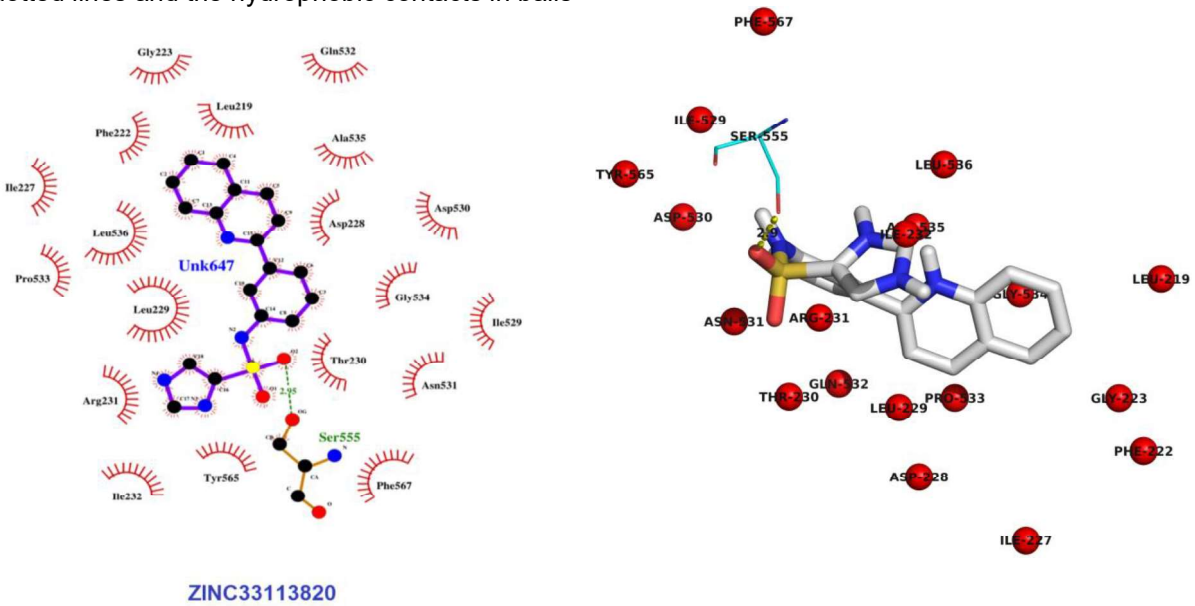

Fig. 19 Schematic representation of binding interactions in 2D and 3D of ZINC78677180, showing intermolecular interactions of ligand with the binding site of the target protein. The figures were generated with ligplot and PyMOL

In the illustration below: In ligplot are expressed how oxygen atoms (in red); carbon atoms (black); nitrogen atoms (blue); hydrogen bonds (green dotted lines with measurements of the respective radii); bonds between the atoms of the ligand (in lilac); connections between the enzyme atoms (in orange) and hydrophobic contacts (red semicircles). And in PyMOL the hydrogen bonds are shown in yellow dotted lines and the hydrophobic contacts in balls

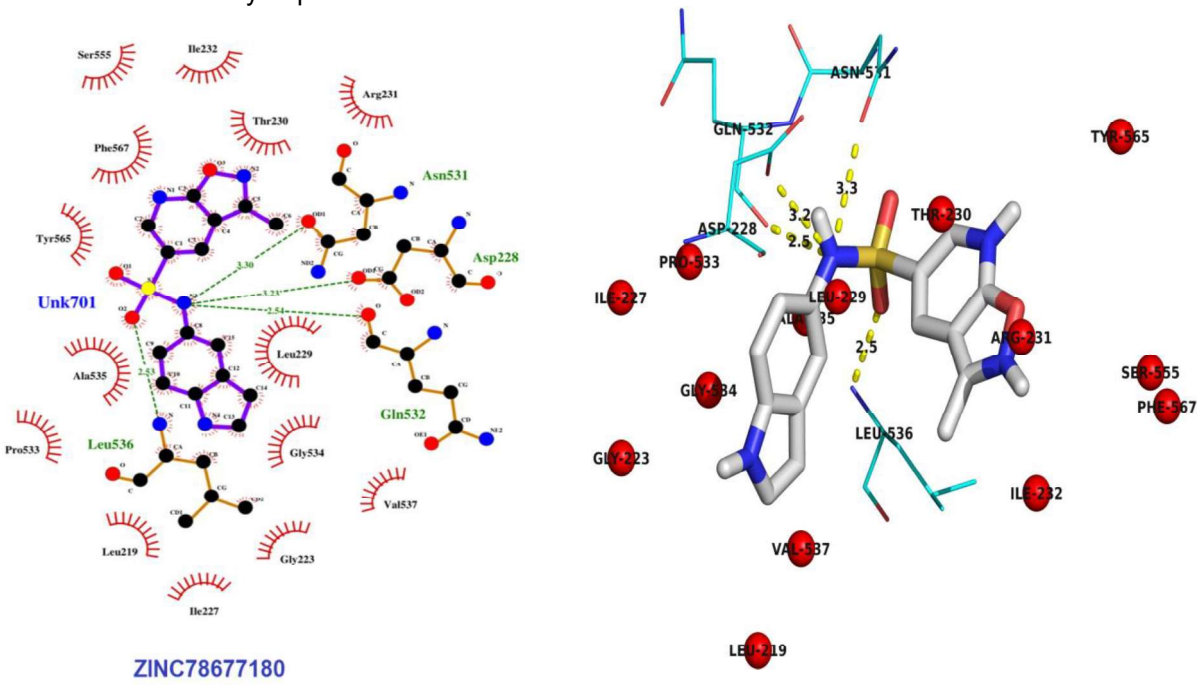

Fig. 20 Schematic representation of binding interactions in 2D and 3D of ZINC67974743, showing intermolecular interactions of ligand with the binding site of the target protein. The figures were generated with ligplot and PyMOL

In the illustration below: In ligplot are expressed how oxygen atoms (in red); carbon atoms (black); nitrogen atoms (blue); hydrogen bonds (green dotted lines with measurements of the respective radii); bonds between the atoms of the ligand (in lilac); connections between the enzyme atoms (in orange) and hydrophobic contacts (red semicircles). And in PyMOL the hydrogen bonds are shown in yellow dotted lines and the hydrophobic contacts in balls

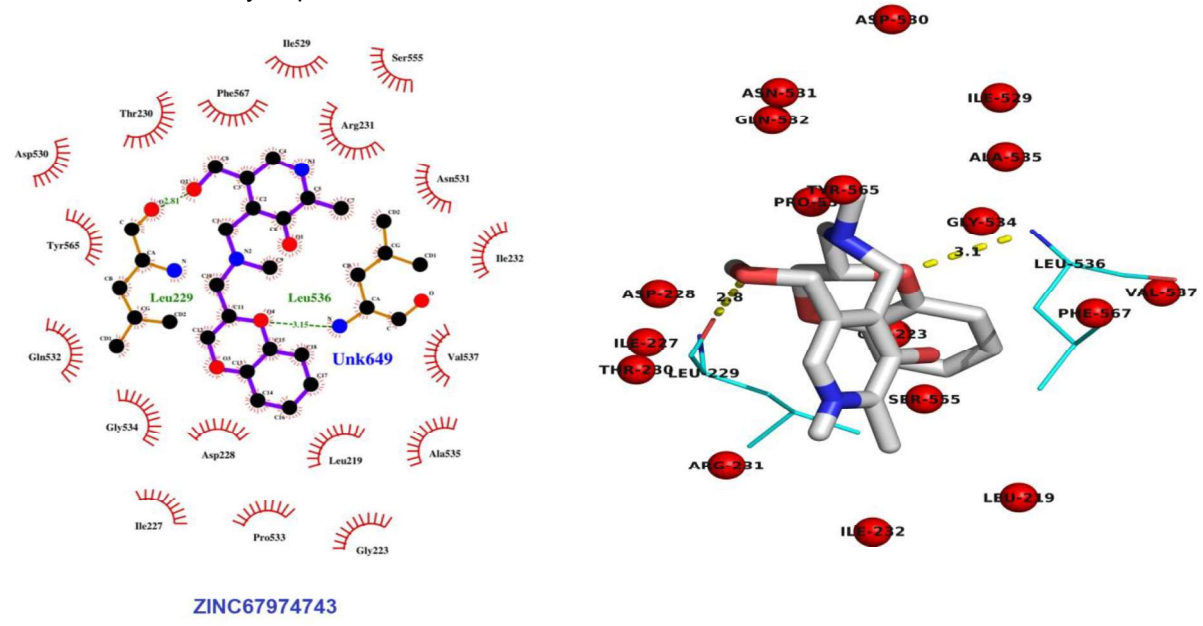

Fig. 21 Schematic representation of binding interactions in 2D and 3D of ZINC81841136, showing intermolecular interactions of ligand with the binding site of the target protein. The figures were generated with ligplot and PyMOL

In the illustration below: In ligplot are expressed how oxygen atoms (in red); carbon atoms (black); nitrogen atoms (blue); hydrogen bonds (green dotted lines with measurements of the respective radii); bonds between the atoms of the ligand (in lilac); connections between the enzyme atoms (in orange) and hydrophobic contacts (red semicircles). And in PyMOL the hydrogen bonds are shown in yellow dotted lines and the hydrophobic contacts in balls

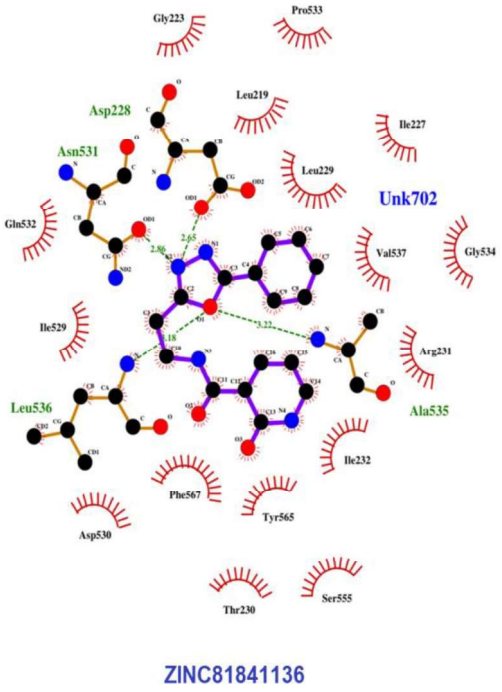

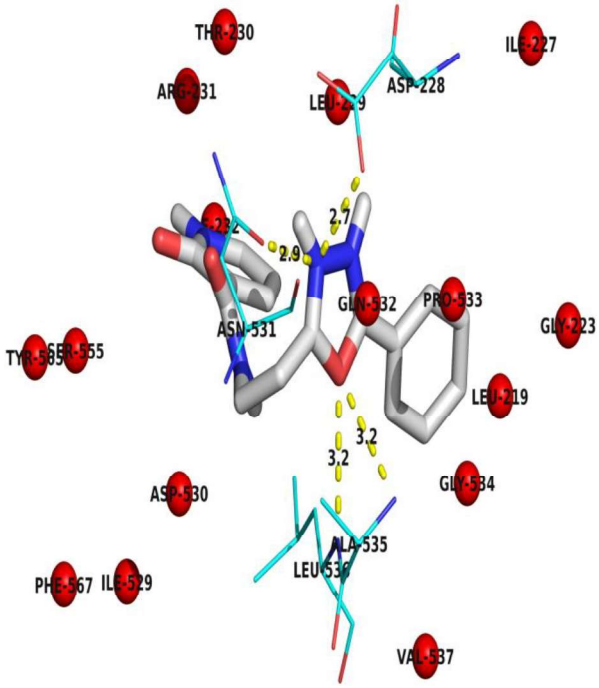

TABLES

Table 1 Blast Results for target PDT.

ID	Chain	E-value	Identities	Gaps	Resolution	Resídues	Ligands
3MWB	A, B	3.7 E-43	38%	4%	2.00	626	PHE MG
2QMX	A, B	3.0 E-27	31%	8%	2.30	566	PHE, EDO
4LUB	A, B	6.6 E-35	32%	9%	2.10	552	ACT, O
3LGY	A	8.7 E-17	29%	6%	2.00	329	PPY
2QMW	A, B	4.9 E-14	26%	11%	2.30	534	PEG, EDD
5FGJ	A, B, C, D	0.0868	39%	0%	3.60	1812	FE,MG,
5DEN	A, B, C, D	0.0875	39%	0%	2.90	1812	FE
5EGQ	A, B, C, D	0.0883	39%	0%	2.50	1812	SO4
1PHZ	A	0.0928	39%	0%	2.20	429	FE
2PHM	A	O.0928	39%	0%	2.60	429	PHER
5FII	A, B, C, D	0.1432	38%	7%	1.80	408	PHE

Table 2 Statistical analysis of the ramachandran chart.

	Model	
	Residues	%
Residues in most favoured region	506	93.7%
Residues in additional allowed regions	29	5.4%
Residues in generously allowed region	5	0.9%
Residues in disallowed regions	0	0.0%
Number of non-glycine and non-proline residues	510	100.0%
Number of end-residues (excl. Gly and Pro)	4	
Number of glycine residues	50	
Number of proline residues	48	
Total number of residues	642	

Table 3 RMSD values and binding free energy for template and model.

Template					Model				
Rank	Run	Binding Energy	Cluster RMSD	Reference RMSD	Rank	Run	Binding Energy	Cluster RMSD	Reference RMSD
1	2	-7.59	0.00	0.48	1	5	-7.80	0.00	0.44
2	6	-7.51	0.72	0.52	2	4	-7.80	0.10	0.48
3	3	-7.51	0.84	0.52	3	2	-7.75	0.12	0.52
4	8	-7.37	0.87	0.91	4	1	-7.74	0.23	0.57
5	5	-7.30	0.80	0.79	5	8	-7.74	0.41	0.57
6	9	-7.28	0.64	0.82	6	3	-7.74	0.32	0.65
7	1	-7.22	1.02	0.86	7	6	-7.73	0.15	0.52
8	7	-7.16	0.94	0.79	8	10	-7.72	0.15	0.54
9	4	-6.85	1.02	0.83	9	7	-7.72	0.29	0.65
10	10	-6.84	0.99	1.18	10	9	-7.63	0.00	3.54

Table 4 Binding free energys (kj/mol) and their energy components for hundred docked complexes with Autodock4 in PyRx. (continue)

Ligand	Bonding energy	Non-bonded energy	Intermolecular energy	Internal energy	Torsional energy
ZINC69138131	-12.45	-0.08	-13.35	-0.08	0.89
ZINC28047676	-12.43	-0.08	-13.32	-0.08	0.89
ZINC92141766	-12.12	-0.2	-13.31	-0.2	1.19
ZINC28248286	-11.87	-0.56	-13.36	-0.56	1.49
ZINC89953875	-11.78	-1.17	-13.57	-1.17	1.79
ZINC36143324	-11.78	1.05	-12.67	1.05	0.89
ZINC33113820	-11.74	0.06	-12.63	0.06	0.89
ZINC78677180	-11.72	0.27	-12.61	0.27	0.89
ZINC67974743	-11.67	0.92	-13.45	0.92	1.79
ZINC81841136	-11.64	-0.45	-13.13	-0.45	1.49
ZINC89953900	-11.56	-1.08	-13.65	-1.08	2.09
ZINC47973221	-11.51	0.59	-13.01	0.59	1.49
ZINC04488159	-11.44	0.15	-12.93	0.15	1.49
ZINC72310844	-11.44	0.64	-12.94	0.64	1.49
ZINC72725050	-11.41	-0.19	-12.3	-0.19	0.89
ZINC72310843	-11.40	-0.09	-12.89	-0.09	1.49
ZINC74489165	-11.39	0.01	-12.88	0.01	1.49
ZINC89794093	-11.36	-0.36	-12.56	-0.36	1.19
ZINC81251469	-11.32	-0.32	-13.11	-0.32	1.79
ZINC69414439	-11.29	-0.69	-13.38	-0.69	2.09
ZINC78236323	-11.28	-0.19	-13.07	-0.19	1.79
ZINC68326065	-11.27	-0.31	-12.76	-0.31	1.49
ZINC79759898	-11.27	-0.43	-12.47	-0.43	1.19
ZINC78601901	-11.23	-1.07	-12.12	-1.07	0.89
ZINC34864608	-11.23	-0.05	-12.72	-0.05	1.49
ZINC08445929	-11.18	-0.02	-12.07	0.31	0.89
ZINC76463896	-11.17	-0.24	-12.96	-0.24	1.79
ZINC92877478	-11.15	-0.53	-12.34	-0.53	1.19
ZINC20467622	-11.13	0.2	-12.62	0.2	1.49
ZINC78235761	-11.13	1.63	-12.32	1.63	1.19
ZINC59158219	-11.13	1.08	-12.92	1.08	1.79
ZINC83411094	-11.12	-1.37	-13.21	-1.37	2.09
ZINC73765427	-11.11	1.03	-13.19	1.03	2.09
ZINC94263938	-11.08	-0.03	-11.98	-0.03	0.89
ZINC94233008	-11.07	-0.54	-12.56	-0.54	1.49
ZINC72310845	-11.04	0.7	-12.53	0.7	1.49
ZINC15973895	-11.04	1.78	-12.54	1.78	1.49
ZINC89510990	-11.04	-0.7	-11.93	-0.7	0.89
ZINC13466561	-11.03	-0.04	-11.62	-0.04	0.6
ZINC17003701	-11.03	0.1	-11.63	0.1	0.6
ZINC54293756	-11.03	-0.05	-12.22	-0.05	1.19
ZINC07913920	-11.02	4.6	-12.22	4.6	1.19
ZINC14849722	-11.02	-0.29	-12.22	-0.29	1.19
ZINC56447933	-11.01	0.57	-12.8	0.57	1.79
ZINC78179327	-11.01	-0.69	-13.1	-0.69	2.09
ZINC06786506	-10.95	0.68	-13.04	0.68	2.09
ZINC40521657	-10.91	0.02	-12.4	0.02	1.49
ZINC59472609	-10.91	0.15	-11.8	0.15	0.89
ZINC94593912	-10.89	-0.48	-11.78	-0.48	0.89

Table 4 Binding free energys (kj/mol) and their energy components for hundred docked complexes with Autodock4 in PyRx. (conclusion)

Ligand	Bonding energy	Non-bonded energy	Intermolecular energy	Internal energy	Torsional energy
ZINC94593831	-10.86	-0.38	-11.75	-0.38	0.89
ZINC93365350	-10.85	-0.62	-12.34	-0.62	1.49
ZINC94263851	-10.84	-0.19	-12.03	-0.19	1.19
ZINC94593832	-10.83	-0.43	-11.73	-0.43	0.89
ZINC64025793	-10.80	0.15	-11.99	0.15	1.19
ZINC95445378	-10.80	-0.12	-12.3	-0.12	1.49
ZINC04062324	-10.78	-0.86	-11.97	-0.86	1.19
ZINC69704955	-10.78	1.54	-12.27	1.54	1.49
ZINC04579041	-10.77	0.37	-11.36	0.37	0.6
ZINC89269515	-10.75	0.45	-12.84	0.45	2.09
ZINC91444049	-10.75	-0.37	-12.84	-0.37	2.09
ZINC06672415	-10.74	0.28	-11.33	0.28	0.6
ZINC42232219	-10.70	-0.99	-12.79	-0.99	2.09
ZINC47972375	-10.68	-0.32	-12.17	-0.32	1.49
ZINC04488161	-10.68	-0.44	-12.17	-0.44	1.49
ZINC52794213	-10.68	-0.26	-11.58	-0.26	0.89
ZINC67756223	-10.68	-0.0	-12.47	-0.0	1.79
ZINC29434885	-10.67	1.05	-12.16	1.05	1.49
ZINC42322899	-10.67	-0.09	-11.86	-0.09	1.19
ZINC69618255	-10.67	-0.18	-12.16	-0.18	1.49
ZINC29435548	-10.67	1.97	-12.16	1.97	1.49
ZINC77845816	-10.66	-0.32	-12.15	-0.32	1.49
ZINC15732045	-10.66	0.76	-11.85	0.76	1.19
ZINC92421552	-10.64	-0.39	-11.53	-0.39	0.89
ZINC47972369	-10.63	-0.35	-12.13	-0.35	1.49
ZINC59381777	-10.63	-1.74	-12.72	-1.74	2.09
ZINC89953901	-10.62	-1.63	-12.71	-1.63	2.09
ZINC06576259	-10.62	2.32	-11.52	2.32	0.89
ZINC32617403	-10.61	0.36	-12.4	0.36	1.79
ZINC04785895	-10.61	0.6	-10.91	0.6	0.3
ZINC59155358	-10.60	0.81	-12.69	0.81	2.09
ZINC94291680	-10.60	-1.09	-12.39	-1.09	1.79
ZINC40139487	-10.58	-0.16	-11.78	-0.16	1.19
ZINC68329714	-10.58	-0.35	-12.37	-0.35	1.79
ZINC93909337	-10.58	-0.14	-12.37	-0.14	1.79
ZINC94991865	-10.58	-0.03	-11.77	-0.03	1.19
ZINC12204753	-10.57	0.25	-12.06	0.25	1.49
ZINC00517811	-10.57	-0.21	-12.06	-0.21	1.49
ZINC04297058	-10.57	-0.35	-11.47	-0.35	0.89
ZINC71081891	-10.57	-0.09	-11.76	-0.09	1.19
ZINC94263974	-10.56	-0.03	-11.15	-0.03	0.6
ZINC93909314	-10.56	0.01	-11.76	0.01	1.19
ZINC59947565	-10.55	0.11	-11.74	0.11	1.19
ZINC67157807	-10.55	0.66	-12.34	0.66	1.79
ZINC72296120	-10.55	1.86	-12.04	1.86	1.49
ZINC48533147	-10.54	-0.96	-11.74	-0.96	1.19
ZINC38714907	-10.53	-0.26	-11.42	-0.26	0.89
ZINC77888125	-10.53	0.59	-11.72	0.59	1.19
ZINC55119488	-10.52	-0.5	-12.01	-0.5	1.49

Table 5 Sumary of receptor-ligand interactions of the ligplot diagram.
The most frequent residues among the compounds are highlighted in bold.

ID	Hydrophobic bonds	Hydrogen bonds
ZINC69138131	**Gly223**, **Gly534**, **Pro533**, **Ile227**, **Ile232** ,Ile529,**Leu219**,Leu536, Val537, **Gln532** , Ala535,**Arg231**, **Tyr565**, **Thr230**, **Phe567**	**Leu229**, **Asn531**, Ser555, **Asp228**
ZINC92141766	**Gly223**, **Gly534**, **Pro533**, **Ile232,** **Ile227**, Ile529, Leu 229,**Leu219**, Leu 536, Val537, **Gln532**, Ala535, **Arg231**, **Phe567**, **Tyr565**, **Thr230**	**Asn531**,**Asp228**, Ser555
ZINC28047676	**Gly534**, **Pro533**,**Ile232**, **Ile227**, **Gln532** ,**Arg231**, **Phe567**, Ser555, **Thr230**,**Tyr565** **Gly223**,**Gly534**, Pro553, **Ile232**,	**Asn531**,Ala535,**Leu536**,**Leu229**,**Asp228**
ZINC28248286	**Leu219**, Val537, **Arg231**, **Phe567**, Phe222, **Thr230**, **Tyr565**,Ala535, Asp228	**Asn531**, Ser555,**Leu536**, **Leu229**, Gln532
ZINC89953875	**Gly223**, **Gly534**, **Pro533**,**Ile227**, Ile529, **Ile232**, **Leu219**, **Arg231**, **Phe567**, **Gln532**,Asn531, Ala535, Leu536,Asp530,**Tyr565**,**Thr230**	**Leu229**, **Asp228**,
ZINC36143324	**Gly223**, **Gly534**, **Pro533**, **Ile227**, Ile529, **Leu219**, Leu536, Leu229, Phe222,**Phe567**, **Gln532**, Leu229, Ala535, **Arg231**, **Thr230**, **Ile232**, **Tyr565**	**Asp228**, **Asn531**
ZINC33113820	**Gly223**,**Gly534**,**Pro533**, **Gln532**, **Ile227**,Ile529, **Ile232**, **Leu219**, Leu229,Leu536,**Arg231**,Ala535, Asp228,Asp530,Asn531, **Thr230**, Phe222,**Tyr565**, **Phe567**	Ser555
ZINC78677180	**Gly223**, **Gly534**,**Pro533**, **Ile227**, **Ile232**, **Leu219**,Leu229, **Arg231**, Ala535,Val537,**Tyr565**,**Phe567**,**Thr230**,Ser555	**Asn531**, **Asp228**, Gln532,**Leu536**
ZINC67974743	**Gly534**, **Gly223**,Pro553, Ile529, **Ile232**, **Ile227**, **Leu219**, Ala535, **Arg231**,Val537,Ser555,**Phe567, Thr230** Asp530,Asn531, **Tyr565**, **Gln532**, Asp228	**Leu229**, **Leu536**,
ZINC81841136	**Gly223**,**Gly534**, **Pro533**, **Ile227**, Ile529, **Ile232**, **Ile227**, **Leu219**, Leu229,Val537,**Arg231**, **Tyr565**, **Gln532**, **Phe567**, Asp530,**Thr230**, Ser555	**Asp228**, **Asn531**, Ala535,**Leu536**,

Table 6 Results of physicochemicals properties to compounds calculated using FAF-Drugs3. (continuation)

ID	Oral Bioavailability (VEBER)	Oral Bioavailability (EGAN)	4_400	3_75	Phospholipidosis	Result
ZINC69138131	Good	Good	Good	Good	NonInducer	Accepted
ZINC28047676	Good	Good	Good	Good	NonInducer	Accepted
ZINC92141766	Good	Good	Good	Good	Inducer	Accepted
ZINC28248286	Good	Good	Good	Good	NonInducer	Accepted
ZINC36143324	Good	Good	Good	Good	NonInducer	Accepted
ZINC89953875	Good	Good	Good	Good	Inducer	Accepted
ZINC33113820	Good	Good	Good	Good	NonInducer	Accepted
ZINC78677180	Good	Good	Good	Good	NonInducer	Accepted
ZINC67974743	Good	Good	Good	Good	Inducer	Accepted
ZINC81841136	Good	Good	Good	Good	NonInducer	Accepted
ZINC89953900	Good	Good	Good	Good	NonInducer	Accepted
ZINC47973221	Good	Good	Good	Good	NonInducer	Accepted
ZINC04488159	Good	Good	Good	Bad	NonInducer	Accepted
ZINC72310844	Good	Good	Good	Warning	NonInducer	Accepted
ZINC72725050	Good	Good	Good	Good	NonInducer	Accepted
ZINC72310843	Good	Good	Good	Warning	NonInducer	Accepted
ZINC74489165	Good	Good	Good	Good	Inducer	Accepted
ZINC89794093	Good	Good	Good	Good	NonInducer	Accepted
ZINC81251469	Good	Good	Good	Good	NonInducer	Accepted
ZINC69414439	Good	Good	Good	Good	NonInducer	Accepted
ZINC78236323	Good	Good	Good	Good	NonInducer	Accepted
ZINC68326065	Good	Good	Good	Good	NonInducer	Accepted
ZINC79759898	Good	Good	Good	Good	NonInducer	Accepted
ZINC34864608	Good	Good	Good	Warning	NonInducer	Accepted
ZINC78601901	Good	Good	Good	Warning	NonInducer	Accepted
ZINC08445929	Good	Good	Good	Good	NonInducer	Accepted
ZINC76463896	Good	Good	Good	Warning	NonInducer	Accepted
ZINC92877478	Good	Good	Good	Good	NonInducer	Accepted
ZINC20467622	Good	Good	Good	Good	NonInducer	Accepted
ZINC59158219	Good	Good	Good	Good	NonInducer	Accepted
ZINC78235761	Good	Good	Good	Warning	NonInducer	Accepted
ZINC83411094	Good	Good	Good	Good	NonInducer	Accepted
ZINC73765427	Good	Good	Good	Good	NonInducer	Accepted
ZINC94263938	Good	Good	Good	Good	NonInducer	Accepted
ZINC94233008	Good	Good	Good	Good	Inducer	Accepted
ZINC15973895	Good	Good	Good	Good	NonInducer	Accepted
ZINC72310845	Good	Good	Good	Warning	NonInducer	Accepted
ZINC89510990	Good	Good	Good	Good	Inducer	Accepted

Table 6 Results of physicochemicals properties to compounds calculated using FAF-Drugs3. (continuation)

ID	Oral Bioavailability (VEBER)	Oral Bioavailability (EGAN)	4_400	3_75	Phospholipidosis	Result
ZINC07913920	Good	Good	Good	Good	NonInducer	Accepted
ZINC14849722	Good	Good	Good	Good	NonInducer	Accepted
ZINC56447933	Good	Good	Good	Warning	NonInducer	Accepted
ZINC78179327	Good	Good	Good	Good	NonInducer	Accepted
ZINC06786506	Good	Good	Good	Good	NonInducer	Accepted
ZINC40521657	Good	Good	Good	Good	NonInducer	Accepted
ZINC59472609	Good	Good	Good	Good	NonInducer	Accepted
ZINC76937697	Good	Good	Good	Good	NonInducer	Accepted
ZINC94593912	Good	Good	Good	Good	NonInducer	Accepted
ZINC84606601	Good	Good	Good	Good	NonInducer	Accepted
ZINC94593831	Good	Good	Good	Warning	NonInducer	Accepted
ZINC93365350	Good	Good	Good	Good	NonInducer	Accepted
ZINC94263851	Good	Good	Good	Good	Inducer	Accepted
ZINC94593832	Good	Good	Good	Warning	NonInducer	Accepted
ZINC64025793	Good	Good	Good	Good	NonInducer	Accepted
ZINC95445378	Good	Good	Good	Good	NonInducer	Accepted
ZINC04062324	Good	Good	Good	Warning	NonInducer	Accepted
ZINC69704955	Good	Good	Good	Good	NonInducer	Accepted
ZINC04579041	Good	Good	Good	Good	NonInducer	Accepted
ZINC89269515	Good	Good	Good	Good	Inducer	Accepted
ZINC91444049	Good	Good	Good	Good	NonInducer	Accepted
ZINC06672415	Good	Good	Good	Good	NonInducer	Accepted
ZINC42232219	Good	Good	Good	Good	NonInducer	Accepted
ZINC04488161	Good	Good	Good	Bad	NonInducer	Accepted
ZINC47972375	Good	Good	Good	Good	NonInducer	Accepted
ZINC52794213	Good	Good	Good	Good	NonInducer	Accepted
ZINC67756223	Good	Good	Good	Good	NonInducer	Accepted
ZINC29434885	Good	Good	Good	Good	NonInducer	Accepted
ZINC29435548	Good	Good	Good	Good	NonInducer	Accepted
ZINC42322899	Good	Good	Good	Good	NonInducer	Accepted
ZINC69618255	Good	Good	Good	Good	NonInducer	Accepted
ZINC15732045	Good	Good	Good	Good	NonInducer	Accepted
ZINC77845816	Good	Good	Good	Good	NonInducer	Accepted
ZINC92421552	Good	Good	Good	Good	NonInducer	Accepted
ZINC47972369	Good	Good	Good	Good	NonInducer	Accepted
ZINC59381777	Good	Good	Good	Good	NonInducer	Accepted
ZINC06576259	Good	Good	Good	Good	NonInducer	Accepted
ZINC89953901	Good	Good	Good	Good	NonInducer	Accepted
ZINC04785895	Good	Good	Good	Good	NonInducer	Accepted
ZINC32617403	Good	Good	Good	Good	NonInducer	Accepted

Table 6 Results of physicochemicals properties to compounds calculated using FAF-Drugs3. (conclusion)

ID	Oral Bioavailability (VEBER)	Oral Bioavailability (EGAN)	4_400	3_75	Phospholipidosis	Result
ZINC94991865	Good	Good	Good	Good	NonInducer	Accepted
ZINC00517811	Good	Good	Good	Good	NonInducer	Accepted
ZINC04297058	Good	Good	Good	Bad	NonInducer	Accepted
ZINC12204753	Good	Good	Good	Good	NonInducer	Accepted
ZINC71081891	Good	Good	Good	Good	NonInducer	Accepted
ZINC93909314	Good	Good	Good	Good	NonInducer	Accepted
ZINC94263974	Good	Good	Good	Good	NonInducer	Accepted
ZINC59947565	Good	Good	Good	Good	NonInducer	Accepted
ZINC67157807	Good	Good	Good	Good	NonInducer	Accepted
ZINC72296120	Good	Good	Good	Good	NonInducer	Accepted
ZINC48533147	Good	Good	Good	Good	NonInducer	Accepted
ZINC38714907	Good	Good	Good	Good	NonInducer	Accepted
ZINC77888125	Good	Good	Good	Good	NonInducer	Accepted
ZINC55119488	Good	Good	Good	Good	NonInducer	Accepted
ZINC93909337	Good	Good	Good	Good	NonInducer	Accepted

Table 7 Analysis of the binders by lipinski's rule (Molar weight (MW) in Daltons (Da), number of hydrogen bond donors (HBD), number of hydrogen bond acceptors (HBA) and logarithm of partition coefficient (LogP). (continue)

ID	Prediction with FAF-Drugs3				
	MW (≤ 500)	HBD (≤ 5)	HBA (≤ 10)	logP (≤ 5)	Violation of Lipinski's rule
ZINC69138131	289.27	3	6	2.25	0
ZINC28047676	302.24	4	9	-0.34	0
ZINC92141766	220.18	4	5	0.69	0
ZINC28248286	342.30	2	7	2.96	0
ZINC36143324	341.24	3	10	2.60	0
ZINC89953875	296.21	2	7	1.67	0
ZINC33113820	338.29	2	6	2.85	0
ZINC78677180	318.26	2	7	2.02	0
ZINC67974743	309.21	1	6	1.33	0
ZINC81841136	298.21	2	7	1.73	0
ZINC89953900	308.22	2	6	2.63	0
ZINC47973221	329.29	3	7	2.26	0
ZINC04488159	327.24	1	4	4.24	0
ZINC72310844	405.15	3	8	3.39	0
ZINC72725050	334.26	2	8	0.74	0
ZINC72310843	405.15	3	8	3.39	0
ZINC74489165	307.24	3	7	1.83	0
ZINC89794093	278.24	2	6	1.66	0
ZINC81251469	307.23	3	5	2.20	0
ZINC69414439	330.28	2	8	2.06	0
ZINC78236323	349.27	2	6	1.80	0
ZINC68326065	323.24	3	7	0.73	0
ZINC79759898	320.24	2	7	1.68	0
ZINC34864608	354.31	2	7	3.32	0
ZINC78601901	293.21	1	5	1.73	0
ZINC08445929	283.22	3	6	1.92	0
ZINC76463896	333.25	3	7	3.64	0
ZINC92877478	310.26	4	8	-0.02	0
ZINC20467622	361.15	3	6	1.95	0
ZINC59158219	303.24	4	6	2.09	0
ZINC78235761	346.29	3	6	3.33	0
ZINC83411094	298.20	6	7	-1.56	1
ZINC73765427	325.23	3	8	1.70	0
ZINC94263938	268.23	4	6	0.92	0
ZINC94233008	247.19	3	7	0.61	0
ZINC15973895	277.2	5	8	2.36	0
ZINC72310845	405.15	3	8	3.39	0
ZINC13466561	339.10	3	6	1.81	0
ZINC17003701	330.10	3	6	2.38	0

Table 7 Analysis of the binders by lipinski's rule (Molar weight (MW) in Daltons (Da), number of hydrogen bond donors (HBD), number of hydrogen bond acceptors (HBA) and logarithm of partition coefficient (LogP). (continuation)

ID	Prediction with FAF-Drugs3				
	MW (≤ 500)	HBD (≤ 5)	HBA (≤ 10)	logP (≤ 5)	Violation of Lipinski's rule
ZINC07913920	317.27	3	6	1.47	0
ZINC14849722	340.24	2	9	1.23	0
ZINC56447933	369.69	2	6	3.09	0
ZINC78179327	322.23	2	6	1.81	0
ZINC06786506	330.25	4	9	1.82	0
ZINC40521657	310.22	2	7	1.57	0
ZINC59472609	287.20	3	7	1.09	0
ZINC76937697	294.24	2	6	0.50	0
ZINC94593912	259.17	1	6	0.61	0
ZINC84606601	359.29	3	9	1.47	0
ZINC94593831	257.18	1	5	2.09	0
ZINC93365350	294.20	0	7	1.11	0
ZINC94263851	243.22	5	5	1.18	0
ZINC94593832	257.18	1	5	2.09	0
ZINC64025793	328.25	4	9	-0.68	0
ZINC95445378	329.23	2	7	2.75	0
ZINC04062324	268.20	2	5	1.75	0
ZINC69704955	330.23	2	10	0.75	0
ZINC04579041	259.19	3	6	1.12	0
ZINC89269515	341.27	1	7	0.21	0
ZINC91444049	350.73	3	6	1.92	0
ZINC06672415	278.19	3	6	1.22	0
ZINC42232219	330.27	2	6	1.93	0
ZINC04488161	303.22	1	4	3.62	0
ZINC47972375	330.27	2	7	1.83	0
ZINC52794213	304.25	2	6	2.05	0
ZINC67756223	306.23	2	6	1.31	0
ZINC29434885	350.26	2	9	1.34	0
ZINC29435548	369.26	2	9	1.45	0
ZINC42322899	304.25	2	6	1.22	0
ZINC69618255	318.26	2	6	1.49	0
ZINC15732045	387.32	2	8	1.77	0
ZINC77845816	295.23	3	6	0.78	0
ZINC92421552	273.20	3	6	-0.22	0
ZINC47972369	337.33	3	7	1.78	0
ZINC04785895	306.07	4	8	1.0	0
ZINC32617403	344.30	2	8	1.17	0

Table 7 Analysis of the binders by lipinski's rule (Molar weight (MW) in Daltons (Da), number of hydrogen bond donors (HBD), number of hydrogen bond acceptors (HBA) and logarithm of partition coefficient (LogP). (conclusion)

ID	Prediction with FAF-Drugs3				
	MW (≤ 500)	HBD (≤ 5)	HBA (≤ 10)	logP (≤ 5)	Violation of Lipinski's rule
ZINC94291680	259.19	3	5	-0.99	0
ZINC40139487	309.23	3	7	1.89	0
ZINC71081891	295.25	3	7	0.6	0
ZINC93909314	350.28	3	7	1.75	0
ZINC94263974	254.22	4	5	1.3	0
ZINC59947565	299.22	3	7	1.46	0
ZINC67157807	297.22	3	7	1.91	0
ZINC72296120	328.26	2	6	2.78	0
ZINC48533147	332.26	2	7	0.61	0
ZINC38714907	280.23	2	6	0.22	0
ZINC77888125	342.30	2	8	2.28	0
ZINC55119488	309.23	3	6	2.01	0

Table 8 Results of prediction of toxic profiles to the compounds calculated using DataWarrior. (continue)

ID	Mutagenic	Tumorigenic	Irritant	DrugScore	Druglikeness
ZINC69138131	None	None	none	0.507	40.36
ZINC28047676	None	None	none	0.824	44.36
ZINC92141766	None	None	high	0.298	-29.49
ZINC28248286	None	None	none	0.688	0.745
ZINC36143324	None	None	none	0.461	-15.18
ZINC89953875	None	None	none	0.895	61.26
ZINC33113820	None	None	none	0.723	17.00
ZINC78677180	High	None	none	0.362	0.379
ZINC67974743	None	None	none	0.910	36.02
ZINC81841136	None	None	none	0.884	44.61
ZINC89953900	None	None	none	0.745	19.94
ZINC47973221	None	None	none	0.861	27.81
ZINC04488159	None	None	none	0.306	-53.14
ZINC72310844	None	None	none	0.359	-74.04
ZINC72725050	High	None	none	0.422	15.64
ZINC72310843	None	None	none	0.359	-74.01
ZINC89794093	None	None	none	0.762	0.730
ZINC81251469	None	None	none	0.629	-0.355
ZINC74489165	None	None	none	0.775	17.94
ZINC69414439	None	None	none	0.747	21.33
ZINC78236323	High	None	none	0.213	-41.20
ZINC68326065	None	None	none	0.380	0.188
ZINC79759898	None	None	none	0.606	-0.676
ZINC34864608	None	None	high	0.283	-31.10
ZINC78601901	None	None	none	0.499	-0.910
ZINC08445929	None	High	none	0.324	41.14
ZINC76463896	None	None	none	0.549	26.59
ZINC92877478	None	None	none	0.866	2.488
ZINC20467622	None	None	none	0.387	-38.71
ZINC59158219	high	None	none	0.438	11.02
ZINC78235761	none	None	none	0.671	-0.312
ZINC83411094	low	Low	none	0.483	0.404
ZINC73765427	none	High	none	0.222	-28.28
ZINC94263938	none	None	none	0.904	27.41
ZINC94233008	none	None	none	0.900	26.53
ZINC15973895	none	None	none	0.359	-74.01
ZINC72310845	none	None	low	0.477	-0.285
ZINC13466561	high	None	high	0.153	-23.39
ZINC17003701	none	High	low	0.236	44.42
ZINC54293756	none	High	none	0.301	26.33
ZINC07913920	none	None	high	0.289	-17.36
ZINC56447933	high	High	low	0.137	0.257

Table 8 Results of prediction of toxic profiles to the compounds calculated using DataWarrior. (continuation)

ID	Mutagenic	Tumorigenic	Irritant	DrugScore	Druglikeness
ZINC40521657	None	High	none	0.332	4.349
ZINC59472609	none	None	none	0.787	1.756
ZINC76937697	high	None	none	0.248	-74.09
ZINC94593912	none	None	none	0.957	44.18
ZINC84606601	none	None	none	0.796	58.45
ZINC94593831	none	None	none	0.895	24.26
ZINC93365350	none	None	none	0.925	46.81
ZINC94263851	none	None	none	0.743	0.563
ZINC94593832	none	None	none	0.895	24.26
ZINC64025793	high	None	high	0.142	-61.36
ZINC95445378	high	None	none	0.325	-11.36
ZINC04062324	none	High	none	0.221	-54.42
ZINC69704955	none	None	none	0.644	-0.365
ZINC04579041	none	High	none	0.336	44.23
ZINC89269515	none	None	none	0.650	59.50
ZINC91444049	none	None	none	0.921	74.13
ZINC06672415	none	High	none	0.324	30.83
ZINC42232219	none	None	none	0.433	-53.50
ZINC04488161	none	None	none	0.572	0.758
ZINC47972375	none	None	none	0.707	18.88
ZINC52794213	none	None	none	0.848	40.53
ZINC67756223	none	None	none	0.917	37.60
ZINC29434885	none	None	none	0.425	-35.43
ZINC29435548	none	None	none	0.426	-5.465
ZINC42322899	none	None	none	0.750	0.885
ZINC69618255	none	None	none	0.910	4.892
ZINC77845816	none	None	none	0.888	41.61
ZINC92421552	none	None	none	0.947	48.49
ZINC47972369	none	None	none	0.649	33.97
ZINC59381777	none	None	none	0.928	32.31
ZINC06576259	none	None	none	0.542	23.97
ZINC89953901	none	None	none	0.745	19.94
ZINC04785895	none	None	none	0.551	-0.875
ZINC32617403	none	None	none	0.652	14.64
ZINC59155358	none	None	none	0.471	-43.81
ZINC94291680	none	None	none	0.889	21.57
ZINC40139487	none	None	high	0.309	-10.96
ZINC04297058	high	None	none	0.548	32.54

Table 8 Results of prediction of toxic profiles to the compounds calculated using DataWarrior. (conclusion)

ID	Mutagenic	Tumorigenic	Irritant	DrugScore	Druglikeness
ZINC71081891	None	None	none	0.658	-0.145
ZINC93909314	None	None	high	0.359	0.111
ZINC94263974	None	None	none	0.799	11.95
ZINC59947565	None	None	none	0.228	-38.95
ZINC67157807	None	High	none	0.319	28.34
ZINC72296120	None	None	none	0.626	13.20
ZINC48533147	None	None	none	0.898	6.05
ZINC38714907	High	None	none	0.456	0.600
ZINC55119488	None	None	none	0.882	29.54
ZINC77888125	None	None	none	0.439	-1.951
ZINC15732045	None	None	high	0.202	-83.51
ZINC89510990	None	None	none	0.861	15.33

5. CONCLUSÃO

Neste presente trabalho foi construído e validado um modelo teórico para a prefenato desidratase, bem como a construção de bibliotecas de ligantes para busca de potenciais compostos candidatos a fármacos. Na análise dos cem ligantes cabe também destacar o ZINC0488161, ZINC004488159, ZINC04297058, ZINC04062324 e ZINC00517811 que demonstram bons resultados por não apresentarem nenhum efeito toxicológico, porém se diferem das outras moléculas em relação aos valores bem discrepantes da afinidade de ligação. De modo geral, nas análises para os cem ligantes, os valores de afinidade de ligação variaram de -12,45 a -10,52 kcal/mol em relação à fenilalanina (-7,8 kcal/mol), Drug-score de 0.13-0.95. e druglikeness de 74.1-93.5. Enquanto nas análises dos resíduos em comum entre (tabela 5) os dez melhores ligantes, houve presença de contatos hidrofóbicos nos resíduos Gly223, Gly534, Ile227, Ile232, Arg231 e Tyr565 que apresentaram estimativa de 9/10 e 10/10. Já para as ligações de hidrogênio se destacaram os resíduos Leu225 e Asn531 de 7/10. Estes valores indicam que estes resíduos têm grande probabilidade de fazer parte das interações necessárias para manter a ligação de um específico fármaco no sitio de ligação da proteína-alvo. Também o ZINC69138131 e ZINC28047676, compostos derivados do benzomidazol, têm valores bastante promissores e concordantes com os dados da literatura. Os resultados obtidos neste trabalho poderão ser úteis para uma maior compreensão da estrutura e da interação molecular da enzima bem como servir de base para futuras pesquisas *in vivo* e *in vitro* para o desenvolvimento de novos protótipos de fármacos. Outra perspectiva para este trabalho é a possibilidade de envolver a prefenato desidratase e os complexos destes ligantes em estudos de dinâmica molecular.

ANEXOS

ANEXO A – Normas do Journal molecular modelling

Instructions for Authors

EDITORIAL PROCEDURE

The Journal of Molecular Modeling is a high-quality journal with a high rejection rate. Authors are advised to consult the Aims and Scope before submitting a manuscript. Manuscripts that do not meet these criteria may be rejected directly by the Editor-in-Chief. Usually, manuscripts will be assessed by at least two expert referees. The final decision on acceptance and rejection rests with the responsible editor.

English language

In order to reduce the load on our referees, the editors reserve the right not to send manuscripts for refereeing before they are satisfied with the standard of English in the manuscript. Non native-English speakers are strongly encouraged to have their manuscripts corrected by a native speaker before submitting them, so that manuscripts can be judged on their scientific quality alone. See “Does Springer provide English language support?” below.

MANUSCRIPT SUBMISSION

Manuscript Submission

Submission of a manuscript implies: that the work described has not been published before; that it is not under consideration for publication anywhere else; that its publication has been approved by all co-authors, if any, as well as by the responsible authorities – tacitly or explicitly

– at the institute where the work has been carried out. The publisher will not be held legally responsible should there be any claims for compensation.

Permissions

Authors wishing to include figures, tables, or text passages that have already been published elsewhere are required to obtain permission from the copyright owner(s) for both the print and online format and to include evidence that such permission has been granted when submitting their papers. Any material received without such evidence will be assumed to originate from the authors.

Online Submission

Please follow the hyperlink “Submit online” on the right and upload all of your manuscript files following the instructions given on the screen.

TITLE PAGE

Title Page
The title page should include:
The name(s) of the author(s)
A concise and informative title
The affiliation(s) and address(es) of the author(s)
The e-mail address, telephone and fax numbers of the corresponding author
Abstract
Please provide an abstract of 150 to 250 words. The abstract should not contain any undefined abbreviations or unspecified references.
Keywords
Please provide 4 to 6 keywords which can be used for indexing purposes.

TEXT

Text Formatting
Manuscripts should be submitted in Word.
Use a normal, plain font (e.g., 10-point Times Roman) for text. Use italics for emphasis.
Use the automatic page numbering function to number the pages. Do not use field functions.
Use tab stops or other commands for indents, not the space bar. Use the table function, not spreadsheets, to make tables.
Use the equation editor or MathType for equations.
Save your file in docx format (Word 2007 or higher) or doc format (older Word versions).
Manuscripts with mathematical content can also be submitted in LaTeX.
LaTeX macro package (zip, 182 kB)
Headings
Please use no more than three levels of displayed headings.
Abbreviations
Abbreviations should be defined at first mention and used consistently thereafter.
Footnotes
Footnotes can be used to give additional information, which may include the citation of a reference included in the reference list. They should not consist solely of a reference citation, and they should never include the bibliographic details of a reference. They should also not contain any figures or tables.
Footnotes to the text are numbered consecutively; those to tables should be indicated by superscript lower-case letters (or asterisks for significance values and other statistical data). Footnotes to the title or the authors of the article are not given reference symbols.
Always use footnotes instead of endnotes.
Acknowledgments
Acknowledgments of people, grants, funds, etc. should be placed in a separate section on the title page. The names of funding organizations should be written in full.

LATEX AND ONLINE SUBMISSION

All source files you upload in the online submission system will be automatically compiled into a single PDF file to be approved by you at the end of the submission process. While the compiled PDF will be used for peer-review purposes, your uploaded source files will be transferred to the publisher for publication upon acceptance.
Please do not use subfolders for your LaTeX submission, e.g. for figures or bibliographic files. Further technical information on uploading and compiling your LaTeX submission can be found under
http://www.editorialmanager.de/pdf/latex/

SPECIFIC REMARKS

The Introduction should state the purpose of the investigation and give a short review of the pertinent literature.
The Methods section should follow the Introduction and should provide enough information to allow the work reported to be repeated.
The Results section should describe the outcome of the study. Data should be presented as concisely as possible, if appropriate in the form of tables or figures, although very large tables should be avoided.
The Discussion should be an interpretation of the results and their significance with reference to work by other authors.
The Summary should be concise and informative without repeating sections of the discussion.
Spectra. Submission of spectra as produced by a computer running a spectrometer or by a data station is encouraged. Routine infrared, electronic, NMR, and mass spectra of new compounds should be numerically summarized, as appropriate, in the Materials and methods section.
Crystallographic data. Manuscripts reporting determinations of molecular structure by Xray crystallography must be accompanied by supplementary material (see below) containing tables of positional and thermal parameters. Tables of bond lengths and angles may be published within the paper. If publication of more complete crystallographic details is planned, this should be stated in a footnote, with the authors' names and the journal of publication included, if possible. Chemical formulae and names as well as the names of organisms must be unambiguous and in accordance with the relevant international recommendations, cf. "IUPAC (1993) Quantities, Units and Symbols Trade, Blackwell Scientific, Oxford" and "ISO (1993) International Vocabulary of Basic and General Terms in
Metrology", Geneva. Trade names should be avoided: abbreviations and uncommon symbols should be explained at first mention.
Formulae and symbols. These must be written legibly and will be typeset in italics. They should be written or marked as such in the manuscript unless they require different styling. Please use correct designations for standardized DIN regulations.
Nomenclature. IUPAC rules must be used for designating chemical compounds. In some fields, e.g. pharmacology, generic or INN names may be used. The use of tradenames alone to identify such compounds as medicines or pesticides is not allowed.

Proprietary substances and materials, and instruments. The correct designation and the manufacturer's name should be given. Where the manufacturer is not well known, the address should also be included.

REFERENCES

Citation

Reference citations in the text should be identified by numbers in square brackets. Some examples:

1. Negotiation research spans many disciplines [3].
2. This result was later contradicted by Becker and Seligman [5].
3. This effect has been widely studied [1-3, 7].

Reference list

The list of references should only include works that are cited in the text and that have been published or accepted for publication. Personal communications and unpublished works should only be mentioned in the text. Do not use footnotes or endnotes as a substitute for a reference list.

The entries in the list should be numbered consecutively.

Journal article

Gamelin FX, Baquet G, Berthoin S, Thevenet D, Nourry C, Nottin S, Bosquet L (2009) Effect of high intensity intermittent training on heart rate variability in prepubescent children. Eur J Appl Physiol 105:731-738. doi: 10.1007/s00421-008-0955-8

Ideally, the names of all authors should be provided, but the usage of "et al" in long author lists will also be accepted:

Smith J, Jones M Jr, Houghton L et al (1999) Future of health insurance. N Engl J Med 965:325–329

Article by DOI

Slifka MK, Whitton JL (2000) Clinical implications of dysregulated cytokine production. J Mol Med. doi:10.1007/s001090000086

Book

South J, Blass B (2001) The future of modern genomics. Blackwell, London

Book chapter

Brown B, Aaron M (2001) The politics of nature. In: Smith J (ed) The rise of modern genomics, 3rd edn. Wiley, New York, pp 230-257

Online document

Cartwright J (2007) Big stars have weather too. IOP Publishing PhysicsWeb. http://physicsweb.org/articles/news/11/6/16/1. Accessed 26 June 2007

Dissertation

Trent JW (1975) Experimental acute renal failure. Dissertation, University of California

Always use the standard abbreviation of a journal's name according to the ISSN List of Title Word Abbreviations, see

ISSN.org LTWA

If you are unsure, please use the full journal title.

For authors using EndNote, Springer provides an output style that supports the formatting of in- text citations and reference list.

EndNote style (zip, 2 kB)

Authors preparing their manuscript in LaTeX can use the bibtex file spbasic.bst which is included in Springer's LaTeX macro package.

TABLES

All tables are to be numbered using Arabic numerals.
Tables should always be cited in text in consecutive numerical order.
For each table, please supply a table caption (title) explaining the components of the table.
Identify any previously published material by giving the original source in the form of a reference at the end of the table caption.
Footnotes to tables should be indicated by superscript lower-case letters (or asterisks for significance values and other statistical data) and included beneath the table body.

ARTWORK AND ILLUSTRATIONS GUIDELINES

Electronic Figure Submission
Supply all figures electronically.
Indicate what graphics program was used to create the artwork.
For vector graphics, the preferred format is EPS; for halftones, please use TIFF format. MSOffice files are also acceptable.
Vector graphics containing fonts must have the fonts embedded in the files. Name your figure files with "Fig" and the figure number, e.g., Fig1.eps.
Line Art
Definition: Black and white graphic with no shading.
Do not use faint lines and/or lettering and check that all lines and lettering within the figures are legible at final size.
All lines should be at least 0.1 mm (0.3 pt) wide.
Scanned line drawings and line drawings in bitmap format should have a minimum resolution of 1200 dpi.
Vector graphics containing fonts must have the fonts embedded in the files.
Halftone Art
Definition: Photographs, drawings, or paintings with fine shading, etc.
If any magnification is used in the photographs, indicate this by using scale bars within the figures themselves.
Halftones should have a minimum resolution of 300 dpi.
Combination Art
Definition: a combination of halftone and line art, e.g., halftones containing line drawing, extensive lettering, color diagrams, etc.
Combination artwork should have a minimum resolution of 600 dpi.
Color Art
Color art is free of charge for online publication.
If black and white will be shown in the print version, make sure that the main information will still be visible. Many colors are not distinguishable from one another when converted to black and white. A simple way to check this is to make a xerographic copy to see if the necessary distinctions between the different colors are still apparent.

If the figures will be printed in black and white, do not refer to color in the captions. Color illustrations should be submitted as RGB (8 bits per channel).

Figure Lettering

To add lettering, it is best to use Helvetica or Arial (sans serif fonts).

Keep lettering consistently sized throughout your final-sized artwork, usually about 2–3 mm (8–12 pt).

Variance of type size within an illustration should be minimal, e.g., do not use 8-pt type on an axis and 20-pt type for the axis label.

Avoid effects such as shading, outline letters, etc.

Do not include titles or captions within your illustrations.

Figure Numbering

All figures are to be numbered using Arabic numerals.

Figures should always be cited in text in consecutive numerical order. Figure parts should be denoted by lowercase letters (a, b, c, etc.).

If an appendix appears in your article and it contains one or more figures, continue the consecutive numbering of the main text. Do not number the appendix figures,

"A1, A2, A3, etc." Figures in online appendices (Electronic Supplementary Material) should, however, be numbered separately.

Figure Captions

Each figure should have a concise caption describing accurately what the figure depicts. Include the captions in the text file of the manuscript, not in the figure file. Figure captions begin with the term Fig. in bold type, followed by the figure number, also in bold type.

No punctuation is to be included after the number, nor is any punctuation to be placed at the end of the caption.

Identify all elements found in the figure in the figure caption; and use boxes, circles, etc., as coordinate points in graphs.

Identify previously published material by giving the original source in the form of a reference citation at the end of the figure caption.

Figure Placement and Size

Figures should be submitted separately from the text, if possible. When preparing your figures, size figures to fit in the column width.

For most journals the figures should be 39 mm, 84 mm, 129 mm, or 174 mm wide and not higher than 234 mm.

For books and book-sized journals, the figures should be 80 mm or 122 mm wide and not higher than 198 mm.

Permissions

If you include figures that have already been published elsewhere, you must obtain permission from the copyright owner(s) for both the print and online format. Please be aware that some publishers do not grant electronic rights for free and that Springer will not be able to refund any costs that may have occurred to receive these permissions. In such cases, material from other sources should be used.

Accessibility

In order to give people of all abilities and disabilities access to the content of your figures, please make sure that

All figures have descriptive captions (blind users could then use a text-to-speech software or a text-to-Braille hardware)

Patterns are used instead of or in addition to colors for conveying information (colorblind users would then be able to distinguish the visual elements)

Any figure lettering has a contrast ratio of at least 4.5:1

ELECTRONIC SUPPLEMENTARY MATERIAL

Springer accepts electronic multimedia files (animations, movies, audio, etc.) and other supplementary files to be published online along with an article or a book chapter. This feature can add dimension to the author's article, as certain information cannot be printed or is more convenient in electronic form.
Before submitting research datasets as electronic supplementary material, authors should read the journal's Research data policy. We encourage research data to be archived in data repositories wherever possible.
Submission
Supply all supplementary material in standard file formats.
Please include in each file the following information: article title, journal name, author names; affiliation and e-mail address of the corresponding author.
To accommodate user downloads, please keep in mind that larger-sized files may require very long download times and that some users may experience other problems during downloading.
Audio, Video, and Animations
Aspect ratio: 16:9 or 4:3 Maximum file size: 25 GB Minimum video duration: 1 sec
Supported file formats: avi, wmv, mp4, mov, m2p, mp2, mpg, mpeg, flv, mxf, mts, m4v, 3gp
Text and Presentations
Submit your material in PDF format; .doc or .ppt files are not suitable for long-term viability.
A collection of figures may also be combined in a PDF file.
Spreadsheets
Spreadsheets should be converted to PDF if no interaction with the data is intended.
If the readers should be encouraged to make their own calculations, spreadsheets should be submitted as .xls files (MS Excel).
Specialized Formats
Specialized format such as .pdb (chemical), .wrl (VRML), .nb (Mathematica notebook), and .tex can also be supplied.
Collecting Multiple Files
It is possible to collect multiple files in a .zip or .gz file.
Numbering
If supplying any supplementary material, the text must make specific mention of the material as a citation, similar to that of figures and tables.
Refer to the supplementary files as “Online Resource”, e.g., "... as shown in the animation (Online Resource 3)", “... additional data are given in Online Resource 4”.
Name the files consecutively, e.g. “ESM_3.mpg”, “ESM_4.pdf”.
Captions
For each supplementary material, please supply a concise caption describing the content of the file.
Processing of supplementary files
Electronic supplementary material will be published as received from the author without any conversion, editing, or reformatting.
Accessibility

In order to give people of all abilities and disabilities access to the content of your supplementary files, please make sure that
The manuscript contains a descriptive caption for each supplementary material Video files do not contain anything that flashes more than three times per second (so that users prone to seizures caused by such effects are not put at risk)

ENGLISH LANGUAGE EDITING

For editors and reviewers to accurately assess the work presented in your manuscript you need to ensure the English language is of sufficient quality to be understood. If you need help with writing in English you should consider:
Asking a colleague who is a native English speaker to review your manuscript for clarity.
Visiting the English language tutorial which covers the common mistakes when writing in English.
Using a professional language editing service where editors will improve the English to ensure that your meaning is clear and identify problems that require your review. Two such services are provided by our affiliates Nature Research Editing Service and American Journal Experts.
English language tutorial
Nature Research Editing Service
American Journal Experts
Please note that the use of a language editing service is not a requirement for publication in this journal and does not imply or guarantee that the article will be selected for peer review or accepted.
If your manuscript is accepted it will be checked by our copyeditors for spelling and formal style before publication.

ETHICAL RESPONSIBILITIES OF AUTHORS

This journal is committed to upholding the integrity of the scientific record. As a member of the Committee on Publication Ethics (COPE) the journal will follow the COPE guidelines on how to deal with potential acts of misconduct.
Authors should refrain from misrepresenting research results which could damage the trust in the journal, the professionalism of scientific authorship, and ultimately the entire scientific endeavour. Maintaining integrity of the research and its presentation can be achieved by following the rules of good scientific practice, which include:
The manuscript has not been submitted to more than one journal for simultaneous consideration.
The manuscript has not been published previously (partly or in full), unless the new work concerns an expansion of previous work (please provide transparency on the re-use of material to avoid the hint of text-recycling (“self-plagiarism”)).
A single study is not split up into several parts to increase the quantity of submissions and submitted to various journals or to one journal over time (e.g. “salami-publishing”).
No data have been fabricated or manipulated (including images) to support your conclusions
No data, text, or theories by others are presented as if they were the author’s own (“plagiarism”). Proper acknowledgements to other works must be given (this includes

material that is closely copied (near verbatim), summarized and/or paraphrased), quotation marks are used for verbatim copying of material, and permissions are secured for material that is copyrighted.
Important note: the journal may use software to screen for plagiarism.
Consent to submit has been received explicitly from all co-authors, as well as from the responsible authorities - tacitly or explicitly - at the institute/organization where the work has been carried out, before the work is submitted.
Authors whose names appear on the submission have contributed sufficiently to the scientific work and therefore share collective responsibility and accountability for the results.
In addition:
Changes in authorship, or in the order of authors, are not accepted after the acceptance for publication of a manuscript.
Requesting to add or delete authors at revision stage, proof stage, or after publication is a serious matter and may be considered when justifiably warranted. Justification for changes in authorship must be compelling and may be considered only after receipt of written approval from all authors and a convincing, detailed explanation about the role/deletion of the new/deleted author. In case of changes at revision stage, a letter must accompany the revised manuscript. In case of changes after acceptance for publication, the request and documentation must be sent via the Publisher to the Editor-in-Chief. In all cases, further documentation may be required to support your request. The decision on accepting the change rests with the Editor-in-Chief of the journal and may be turned down. Therefore authors are strongly advised to ensure the correct author group, corresponding author, and order of authors at submission.
Upon request authors should be prepared to send relevant documentation or data in order to verify the validity of the results. This could be in the form of raw data, samples, records, etc.
If there is a suspicion of misconduct, the journal will carry out an investigation following the COPE guidelines. If, after investigation, the allegation seems to raise valid concerns, the accused author will be contacted and given an opportunity to address the issue. If misconduct has been established beyond reasonable doubt, this may result in the Editor-in-Chief's implementation of the following measures, including, but not limited to:
If the article is still under consideration, it may be rejected and returned to the author.
If the article has already been published online, depending on the nature and severity of the infraction, either an erratum will be placed with the article or in severe cases complete retraction of the article will occur. The reason must be given in the published erratum or retraction note.
The author's institution may be informed.

COMPLIANCE WITH ETHICAL STANDARDS

To ensure objectivity and transparency in research and to ensure that accepted principles of ethical and professional conduct have been followed, authors should include information regarding sources of funding, potential conflicts of interest (financial or non-financial), informed consent if the research involved human participants, and a statement on welfare of animals if the research involved animals.

Authors should include the following statements (if applicable) in a separate section entitled “Compliance with Ethical Standards” when submitting a paper:
Disclosure of potential conflicts of interest
Research involving Human Participants and/or Animals
Informed consent
Please note that standards could vary slightly per journal dependent on their peer review policies (i.e. single or double blind peer review) as well as per journal subject discipline. Before submitting your article check the instructions following this section carefully.
The corresponding author should be prepared to collect documentation of compliance with ethical standards and send if requested during peer review or after publication.
The Editors reserve the right to reject manuscripts that do not comply with the above-mentioned guidelines. The author will be held responsible for false statements or failure to fulfill the above-mentioned guidelines.

DISCLOSURE OF POTENTIAL CONFLICTS OF INTEREST

Authors must disclose all relationships or interests that could have direct or potential influence or impart bias on the work. Although an author may not feel there is any conflict, disclosure of relationships and interests provides a more complete and transparent process, leading to an accurate and objective assessment of the work. Awareness of a real or perceived conflicts of interest is a perspective to which the readers are entitled. This is not meant to imply that a financial relationship with an organization that sponsored the research or compensation received for consultancy work is inappropriate. Examples of potential conflicts of interests that are directly or indirectly related to the research may include but are not limited to the following:

Research grants from funding agencies (please give the research funder and the grant number)
Honoraria for speaking at symposia Financial support for attending symposia Financial support for educational programs Employment or consultation
Support from a project sponsor
Position on advisory board or board of directors or other type of management relationships
Multiple affiliations
Financial relationships, for example equity ownership or investment interest Intellectual property rights (e.g. patents, copyrights and royalties from such rights) Holdings of spouse and/or children that may have financial interest in the work
In addition, interests that go beyond financial interests and compensation (non-financial interests) that may be important to readers should be disclosed. These may include but are not limited to personal relationships or competing interests directly or indirectly tied to this research, or professional interests or personal beliefs that may influence your research.
The corresponding author collects the conflict of interest disclosure forms from all authors. In author collaborations where formal agreements for representation allow it, it is sufficient for the corresponding author to sign the disclosure form on behalf of all authors. Examples of forms can be found
here:

The corresponding author will include a summary statement in the text of the manuscript in a separate section before the reference list, that reflects what is recorded in the potential conflict of interest disclosure form(s).
See below examples of disclosures:
Funding: This study was funded by X (grant number X).
Conflict of Interest: Author A has received research grants from Company A. Author B has received a speaker honorarium from Company X and owns stock in Company Y. Author C is a member of committee Z.
If no conflict exists, the authors should state:
Conflict of Interest: The authors declare that they have no conflict of interest.
AFTER ACCEPTANCE
Upon acceptance of your article you will receive a link to the special Author Query Application at Springer's web page where you can sign the Copyright Transfer Statement online and indicate whether you wish to order OpenChoice and offprints.

Once the Author Query Application has been completed, your article will be processed and you will receive the proofs.
Copyright transfer
Authors will be asked to transfer copyright of the article to the Publisher (or grant the Publisher exclusive publication and dissemination rights). This will ensure the widest possible protection and dissemination of information under copyright laws.
Creative Commons Attribution-NonCommercial 4.0 International License
Offprints
Offprints can be ordered by the corresponding author.
Color illustrations
Publication of color illustrations is free of charge.
Proof reading
The purpose of the proof is to check for typesetting or conversion errors and the completeness and accuracy of the text, tables and figures. Substantial changes in content, e.g., new results, corrected values, title and authorship, are not allowed without the approval of the Editor.
After online publication, further changes can only be made in the form of an Erratum, which will be hyperlinked to the article.
Online First
The article will be published online after receipt of the corrected proofs. This is the official first publication citable with the DOI. After release of the printed version, the paper can also be cited by issue and page numbers.
OPEN CHOICE
In addition to the normal publication process (whereby an article is submitted to the journal and access to that article is granted to customers who have purchased a subscription), Springer provides an alternative publishing option: Springer Open Choice. A Springer Open Choice article receives all the benefits of a regular subscription-based article, but in addition is made available publicly through Springer's online platform SpringerLink.
Open Choice Copyright and license term – CC BY
Open Choice articles do not require transfer of copyright as the copyright remains with the author. In opting for open access, the author(s) agree to publish the article under the Creative Commons Attribution License.
Find more about the lice

ANEXO B – Registro da Comissão de Pesquisa da UFCSPA (ComPesq)

REPÚBLICA FEDERATIVA DO BRASIL
MINISTÉRIO DA EDUCAÇÃO

UFCSPA
UNIVERSIDADE FEDERAL DE CIÊNCIAS DA SAÚDE DE PORTO ALEGRE
COMISSÃO DE PESQUISA

Certificado

Certificamos que o projeto de pesquisa intitulado *"Estudo estrutural e planejamento de novos inibidores para a enzima prefanato desidratase (E. C 4. 2. 1. 51) de Mycobacterium tuberculosis"*, de Rafael Andrade Caceres, está registrado na Comissão de Pesquisa da Universidade Federal de Ciências da Saúde de Porto Alegre sob o número 079/2015. Salientamos que este registro **não autoriza o pesquisador a coletar ou analisar dados oriundos de sujeitos de pesquisa**.

Salientamos ainda que tal registro **não garante** a concessão de recursos financeiros por parte da UFCSPA a este projeto de pesquisa.

Porto Alegre, 20 de junho de 2016.

Paulo Ricardo Gazzola Zen
Coordenador Geral da Pesquisa
UFCSPA